UNIVERSITY
OF TASMANIA

Geometallurgical Mapping and Mine Modelling - Comminution Studies: La Colosa Case Study, AMIRA P843A

by

Paula Andrea Montoya Lopera

CODES – ARC Centre of Excellence in Ore Deposit

Submitted in fulfilment of the requirements for the Master of Science in Geology

University of Tasmania February, 2014

Declaration of originality

This thesis contains no material which has been accepted for a degree or diploma by the University or any other institution, except by way of background information and duly acknowledged in the thesis, and to the best of my knowledge and belief no material previously published or written by another person except where due acknowledgement is made in the text of the thesis, nor does the thesis contain any material that infringes copyright.

Paula A Montoya L

_____
Paula Andrea Montoya Lopera
February 2014

Statement of authority of access

This thesis is not to be made available for loan for 24 months from the date this statement was signed. Copying and communication of any part of this thesis is prohibited for 24 months from the date this statement was signed; after that time limited copying and communication is permitted in accordance with Copyright Act 1968.

Paula A Montoya L

_____
Paula Andrea Montoya Lopera
February 2014

Statement of Ethical Conduct

The research associated with this thesis abides by the international and Australian codes on human and animal experimentation, the guidelines by the Australian Government's Office of the Gene Technology Regulator and the rulings of the Safety, Ethics and Institutional Biosafety Committees of the University.

Paula A Montoya L

_____
Paula Andrea Montoya Lopera
February 2014

Acknowledgements

This research is part of a major collaborative geometallurgical project of AMIRA P843 and P843A GEM^{III} Project being undertaken at CODES (University of Tasmania), JKMRC, BRC and CMLR (Sustainable Minerals Institute, University of Queensland) and Parker Centre (CSIRO).

I would like to express my sincere gratitude to La Colosa Project, in particular Rudolf Jahoda Geology Manager of Colosa, Vaughan Chamberlain Senior Vice President of geology and metallurgy, who have provided financial support and permission to publish. Udo Drews Metallurgy Manager of Colosa, Paul Linton Geometallurgy Manager of Anglogold Ashanti, Stacey Leichliter Senior Geologist of CC&V and all the staff at La Colosa Project. Without your help and assistance, the work in this project would not have been possible.

I would like to say many thanks to: Dr. Ron Berry and Dr Julie Hunt my principal advisors, whose encouragement, guidance and support from the initial to the final level enabled me to develop an understanding of the subject. I would also like to thank Dr. Luke Keeney, Dr. Toni Kojovic, Dr. Simon Michaux, Dr Steve Walters for their assistance and willingness to help and explain geometallurgical concepts, and Dr. Khoi Ngyuen for his programming assistance over the duration of the project.

Finally, the four pillars of my life: God, my husband and my parents, they have always supported and encouraged me to do my best in all matters of life.

Abstract

La Colosa is a world-class porphyry gold (Au) project located in Colombia, currently undergoing pre-feasibility analysis. As part of collaboration between AngloGold Ashanti and the AMIRA P843A GeM^{III} Project, the application of emerging geometallurgical characterisation testing and modelling tools has been incorporated into the early stages of project development.

The aim of the geometallurgical study is to map inherent comminution variability across the La Colosa deposit providing information critical for mine/mill design and optimisation. In this study, site-based data incorporating 17,505 multi-element assays, 275 QXRD bulk mineralogy measurements, 15,195 EQUOtip rebound hardness values, 9015 sonic velocity measurements, 16,676 density measurements and routine geological logging information from 92 diamond drill holes has been integrated with a range of geometallurgical comminution tests (i.e. 155 A*b values and 151 BMWi values).

The thesis demonstrates the integration techniques used at La Colosa to link routine data acquisition methods with comminution test results through the development of proxy support models. The integration incorporates a range of statistical techniques including principal component analysis, regression modelling and geostatistics. By creating proxy models, comminution index estimates can be propagated into the geological database enabling comminution processing domains to be defined. These domains provide the first spatial representation of comminution performance and variability at La Colosa and these can be compared with traditional geological domains.

In general, the comminution hardness of the rocks is related to proximity to structural corridors (trending 350), to topographic surface and the western contact between intramineral diorite and hornfels. The study shows that, overall, La Colosa rocks are intermediate to hard in terms of crushing and grinding. Seven hardness domains were identified for crushing and seven for grinding.

This study will provide the foundation for ongoing comminution characterisation as the La Colosa project evolves through project cycles into an operational mine.

Keywords

Geometallurgy, Comminution Modelling, Comminution Mapping, Orebody Knowledge, La Colosa

Australian and New Zealand Standard Research Classifications (ANZSRC)

091414: Mineral Processing/Beneficiation (50%)
0403: Geology (50%)

Table of Contents

List of Figures

List of Tables

Abbreviations Contained in this Thesis

AMIRA: Australian Minerals Industry Research Association

CODES: Centre of Excellence in Ore Deposit Studies (University of Tasmania)

JKMRC: Julius Kruttschnitt Mineral Research Centre

GeM^{III}: Geometallurgical Mapping and Mine Modelling, the parent project of this thesis

GML: Geometallurgical Matrix level

JKRBT: Julius Kruttschnitt Rotary Breakage Tester

BMWi: Bond Ball Mill Work index

kWh/t: Kilowatt Hours per Tonne

GeMCi: GeM Comminution Index

ICP: Inductively Coupled Plasma

QAQC: Quality Assurance/Quality Control

PCA: Principal Component Analysis

Chapter 1: Introduction

1.0 Introduction

The key functions of project evaluation are to assess potential profitability and to develop an effective operational design. For mining projects, design aspects include mining methodology, ore treatment methodology and production rates. All of these characteristics affect the project economics and overall value (Dunham and Vann, 2007).

Resource models, which form the ultimate basis of project evaluation, typically consist of tonnes above cut-off, grade above cut-off and the spatial distribution (connectivity) of tonnes/grade above cut-off, for one or more variables. Dilution, ore loss and metallurgical recovery are all modifying factors applied to the resource model during evaluation and determination of profitability. A key issue is: how is the value determined? In addition to the traditional combination of in situ tonnes/grade, the following merit serious consideration: the concentration of deleterious elements, throughput rates, mining/processing costs and – importantly – metallurgical recovery.

Geometallurgy is an emerging field targeted at integrating the above issues by identifying either direct measurements or proxies for throughput (crushing and grinding hardness), recovery (liberation, mineral shape/texture, etc) and concentrate quality from easily collected macro-, meso- and microscopic data. Geometallurgy involves a quantified and spatially constrained understanding of ore characterisation in terms of critical processing performance behaviour (Hunt, et al. 2008).

The primary aim of geometallurgy is to provide constrained inputs that reflect inherent geological variability and its impact on metallurgical performance. This requires quantification of ore deposits in terms of machine-based process parameters such as hardness, comminution energy, size reduction, liberation potential and product recovery (Walters, 2008).

These parameters are used to populate deposit-scale block models typically through the application of geostatistics. Incorporation of geometallurgical parameters into resource modelling supplements traditional geology and grade-based attributes, enabling a more holistic approach to economic optimization of mineral production. Sophisticated geometallurgical block models can be used to predict and optimize economic attributes such as throughput, grade, grind size and recovery.

The La Colosa gold porphyry deposit, which is currently undergoing feasibility, represented an opportunity to apply emerging GeM testing and modelling tools at an early stage of project development and is the focus of this study.

1.1 Research Aim

The aim of this geometallurgical study is to understand and map inherent comminution variability across the La Colosa deposit providing information critical for mine/mill design and optimisation.

1.2 Research Scope

The La Colosa project area is subdivided into 6 different zones by structural controls. The focus of this research was zone 2 where the main porphyry gold deposit (La Colosa North) is located. The thesis concentrates on predictive comminution modeling based on 92 drill holes located in La Colosa North. The work involved integration of geometallurgical proxies and methodologies with measured comminution values in order to improve ore characterization and allow predictive modelling of processing behaviour. Figure 1.1 displays a simplified schematic representation of the methodology used in this thesis.

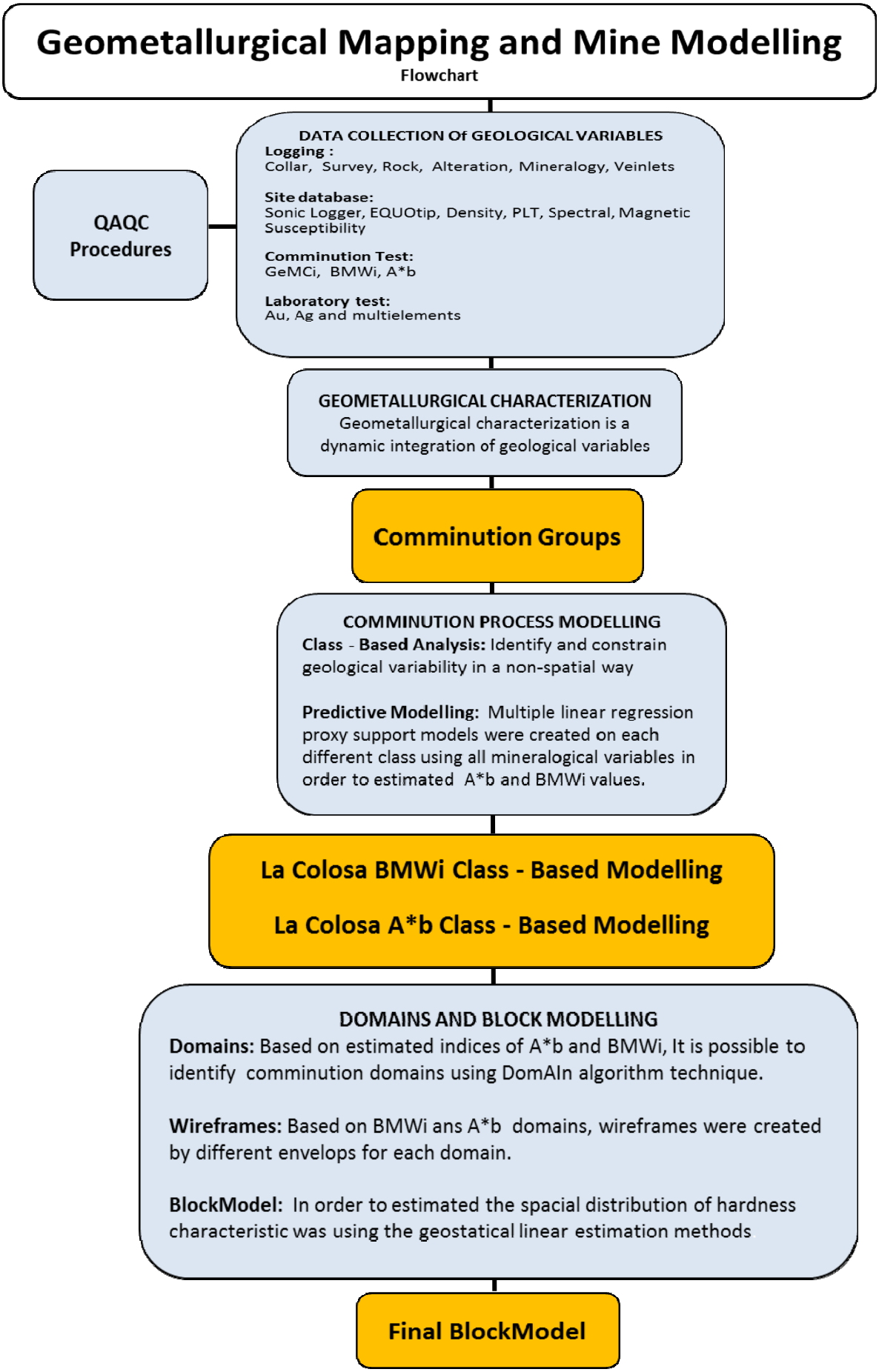

Figure 1.1 Geometallurgical Mapping and Mine Modelling Methodology.

1.3 Project Background

The La Colosa project was discovered by AngloGold Ashanti's Colombian greenfields exploration team in 2006. In 2007 the La Colosa deposit was defined, based on 57 drill holes, as a low-grade porphyry-style Au system. Currently, the La Colosa project is in the pre – feasibility stage. This is the major technical reporting stage on which the decision to proceed to production will be based and the search for financing will be started (Shillabeer and Gypton, 2003). Common problems of pre-feasibility projects are related to mill design. A fault in any of the technical fundamentals can have a devastating effect on project outcome. For this reason, in 2010, AngloGold Ashanti decided to start fundamental studies related to resources, reserves, development, process metallurgy, product quality and capacity. The focus of this thesis is related to metallurgical processing and to comminution in particular.

Chapter 2: Literature Review

2.0 Introduction

Geometallurgy involves a quantified and spatially constrained ore characterisation relevant to processing performance (Walters, 2008). One of the more significant problems is the link between geological understanding of mineral systems, typically expressed in terms of fundamental origin and biased towards an exploration perspective, with the mineral processing characteristics, which generally involves mechanical size reduction leading to liberation. The physical nature of mineral processing requires a material-based understanding of what the rock feed is, rather than a genetic model of how the deposit formed.

While many geological techniques and concepts can be modified to create engineering-based solutions, this is not a common approach, is rarely taught effectively at the undergraduate geology level, and has received minimal research attention. The critical link of geology to mineral processing and the significant gaps in current practice were recognised by industry as major constraints to advancing geometallurgy (Hunt, et al. 2008).

This chapter describes the geology of the La Colosa district and various parameters that are used to predict the comminution behaviour of the resource. This chapter represents a review of previous work by the La Colosa geology department and comes from a variety of internal company reports and the logging database. Various types of data are considered to mirror the spatial varability in processing performance. A specific aim is to identify primary geological controls on the comminution behaviour.

2.1 Geology of the La Colosa Deposit

The La Colosa gold porphyry deposit is 100% owned by AngloGold Ashanti and is located 150 km west of Colombia's capital city, Bogota, and 30km west of the major town of Ibague, which falls within the department of Tolima (Figure 2.1). La Colosa is genetically linked to a Miocene (8 Ma) porphyritic intrusive centres intruded into Paleozoic schists (Valencia, 2012, Lodder, et al., 2010). The highest grade gold mineralization is associated with a suite of early porphyry intrusions and related breccias with potassic and sodic-calcic alteration. These typically contain ~5% pyrite and have traces of chalcopyrite and molybdenite. The intrusions have been emplaced within the structural framework created by Andean deformation during Middle/Late Miocene (Sillitoe, 2007). Brittle post-mineralisation deformation is evident along normal/left

lateral NE-SW striking faults. Late stage alteration, commonly causing removal of gold, is rare (Jahoda, 2012). The reported mineral resource for the La Colosa project is 516 million tonnes at 0.98 g/t gold (506 tonnes or 16.3 million ounces Au, AngloGold Ashanti, 2011).

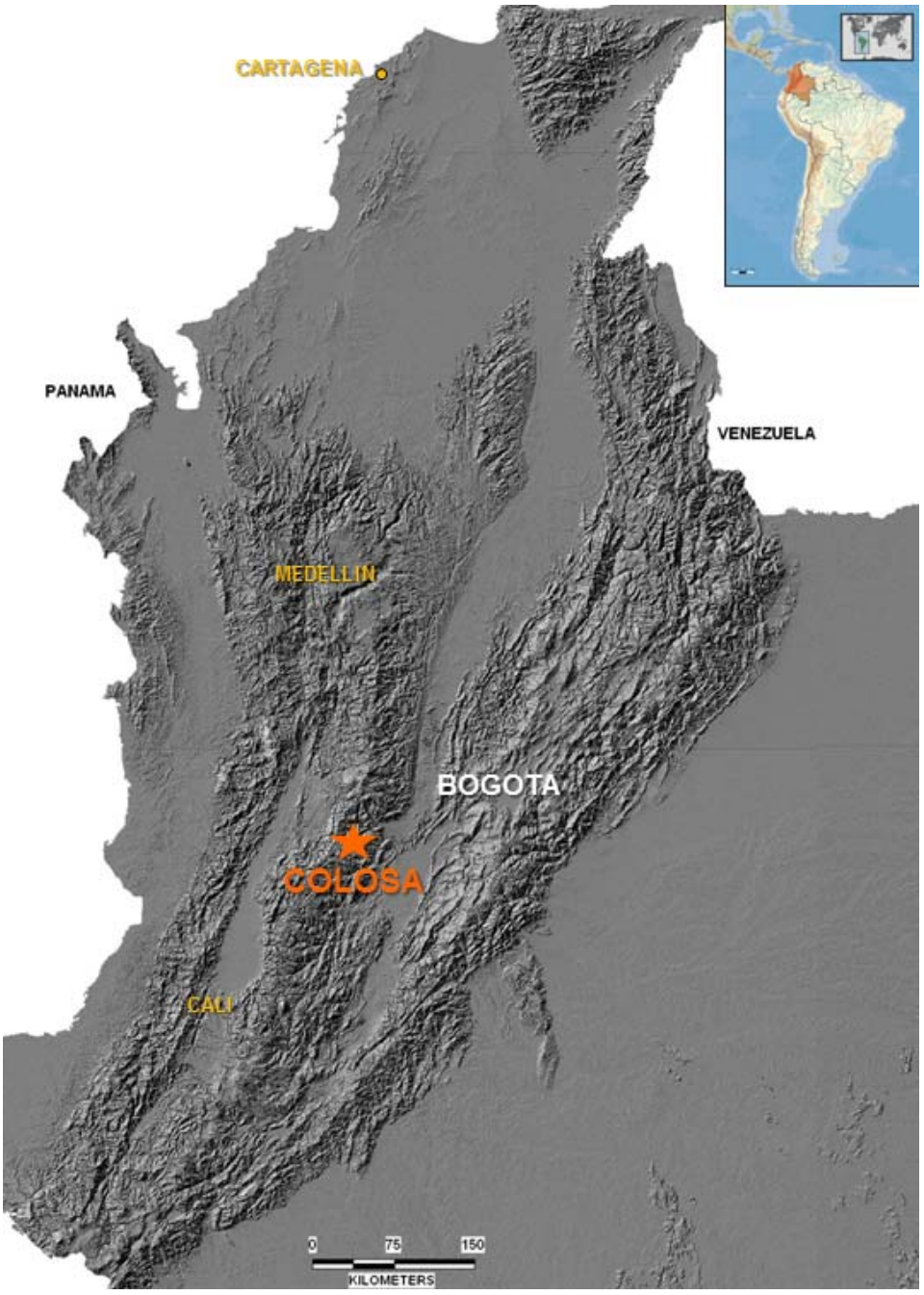

Figure 2.1. Location of the La Colosa deposit within Colombia. Inset shows the position of Colombia within South America.

2.2 Lithologies of the La Colosa Deposit

The La Colosa porphyry gold mineralization is located along a N-S ridge crest located between the La Arenosa and the La Colosa drainages. The Colosa porphyry stock is subdivided into early porphyries that are intruded by inter-mineral (syn-mineralisation) and late mineral (late syn- to post-mineralisation) intrusive bodies. The early porphyry stage is divided into three phases (phase 1 E0 + E1, phase 2 E2, phase three E3). The earliest, volumetrically minor, intrusions are composed of medium grained, diorite porphyry (E0, E1). The two early diorite porphyry types, are coarse grained (E2), and fine-grained (E3) varieties. The inter-mineral-stage diorite porphyry intrusions are divided into two phases: coarse-grained (I1) and fine-grained (I2), both of which are texturally similar to E2 and E3 respectively (Jahoda, 2012).

The early and inter-mineral, coarse-grained porphyries are difficult to distinguish from one another because of their textural similarity, even where they are in direct contact with one another. The main criteria used for distinguishing the inter-mineral phases are lower alteration and veinlet intensities and markedly lower gold content. Narrow, fine-grained chilled contacts have been mapped but are not common.

The late-mineral intrusions (DA) are composed of dacite/granodiorite porphyry with round quartz phenocrysts, locally up to 1 cm across, and by fine grained dacite (Jahoda, 2012).

Contacts between porphyry phases are commonly characterised by broad zones of intrusion breccia. The clast boundaries of the breccias are commonly diffuse implying varying degrees of reaction of the clasts of the earlier igneous rocks with the matrix which represents the later intrusions.

The most common intrusion breccia contains clasts of the early, coarse-grained porphyry (E2) in a matrix of fine-grained porphyry (E3) and is called EBX2. EBX1 is an intrusion breccia that contains clasts of E1 in a matrix of E2. The intrusion breccia occurs as vertically continuous bodies along the contacts between the two porphyry phases and internally within the E3 porphyry (Jahoda, 2012).

A similar intrusion breccia (IBX) was formed at the inter-mineral porphyry stage, where the fine-grained phase (I2) contains clasts of the coarse-grained phase (I1). A distinctive intrusion breccia occurs as a 5 to >15m wide rind to the porphyry stock, where it consists of variously orientated schist (S), hornfels (H) and intrusive clasts in an early or intermineral, fine-grained porphyry matrix (SBX breccias). Figure 2.2 shows the relative abundance of rock types at the La Colosa deposit.

The late-mineral granodiorite/dacite porphyry occurs as a prominent stock occupying the northeast corner of the composite Colosa stock and as a series of dykes. The following histogram (Figure 2.2) displays the main La Colosa lithologies. Ash (ASH), colluvium (COLLV), and saprolite (SAPR) are only reported from the first few metres of surface drill holes. Core loss is classified as SGNCRLSS.

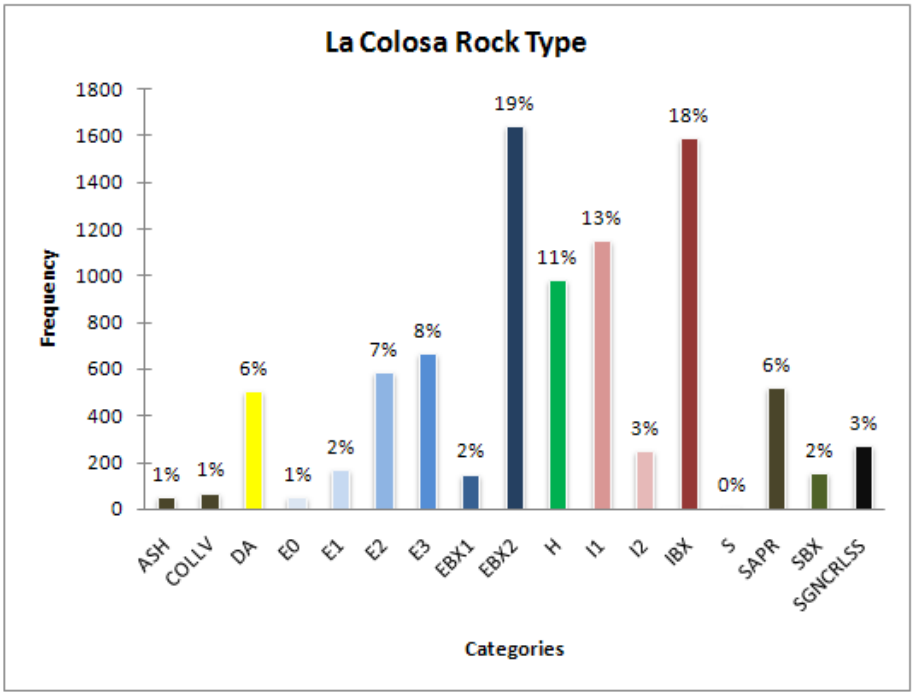

Figure 2.2. Relative abundance of rock types at La Colosa. Classification based on drill core logs in the La Colosa deposit database.

Alteration types associated with La Colosa have been subdivided into: potassic, calcic-sodic, actinolite, albitization, epidotization, chlorite, propylite, quartz-sericite, sericite, silicification, intermediate argillic, supergene argillic and oxidation. Figure 2.3 shows the frequency of these alteration types at the La Colosa deposit.

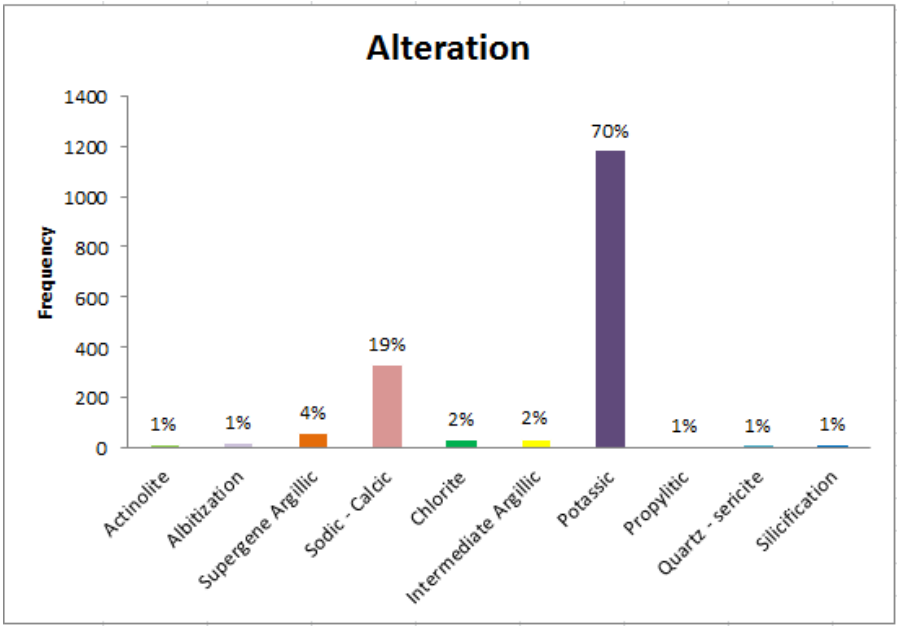

Figure 2.3 Relative abundance of alteration types in the drill core logs of the La Colosa North deposit. (From deposit geology logs.)

Potassic alteration occurs mainly as a pervasive replacement of the early and intramineral diorite porphyry phases. The sodic-calcic mineral assemblage is mainly confined to irregular, centimetre-scale patches and well-defined veinlets., Sodic – calcic alteration overprints the potassic alteration in the early porphyry phases. Intermediate argillic, sericitic, and propylitic alteration is only weakly developed, mainly in the late intermineral granodiorite porphyry, and no mappable zones have been recognised (Lodder, et al. 2010) Figure 2.4 shows examples of the dominant alteration types at La Colosa.

Diorite with strong potassic alteration

Diorite with patch of of sodic-calcic alteration

Figure 2.4 Most common alteration types at the La Colosa deposit

The veinlets at the La Colosa deposit (Figure 2.5) have been divided into the following sequence: The earliest event produces biotite veinlets (EB), that are cut by early quartz and quartz-pyrite veinlets (A and B veinlets, respectively, of Gustafson and Hunt, 1975), magnetite occurs in M veinlets (as defined by Clark and Arancibia, 1995). Actinolite (ACT) -chlorite sulphide and chlorite sulphide veins (CHL) follow the A-B veinlets. Pyrite or Pyrrhotite veins (S) with or without quartz-sericite (D) halos follow the chlorite veinlets, sodic calcic (N), albite (AB) and quartz carbonate (CCQZ) veinlets. In the early, well-mineralized diorites vein density is > 50 veinlets per meter, whereas in the intermineral porphyry phases, densities on the order of 5 to 10 veinlets per meter are reported in the geological logs. Veinlets are mostly <2 mm wide.

The La Colosa ore mineral assemblage (Sillitoe, 2007), in paragenetic order, includes magnetite-pyrite-pyrrhotite, with traces of chalcopyrite and molybdenite, which is followed by traces of arsenopyrite and marcasite Figure 2.5 shows examples of veinlets found at La Colosa.

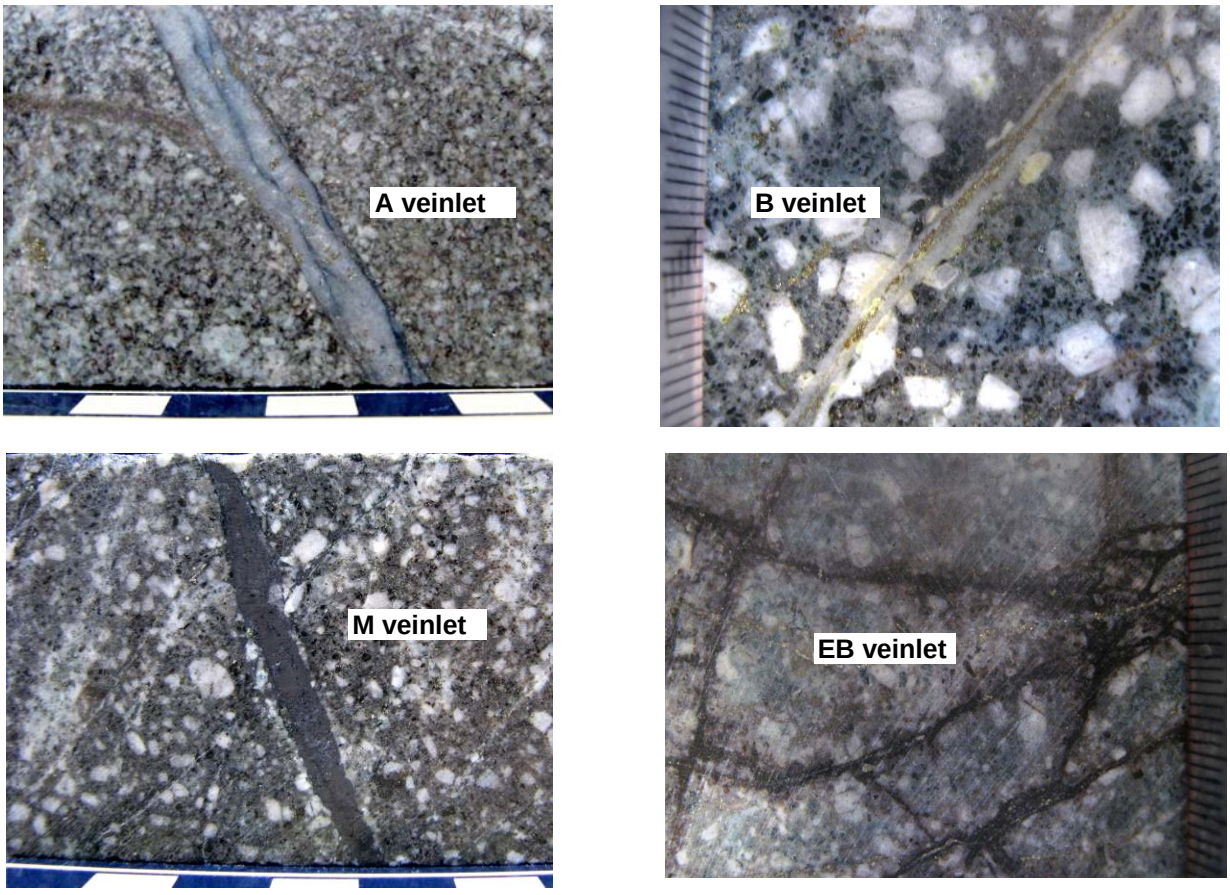

Figure 2.5 continues on the next page

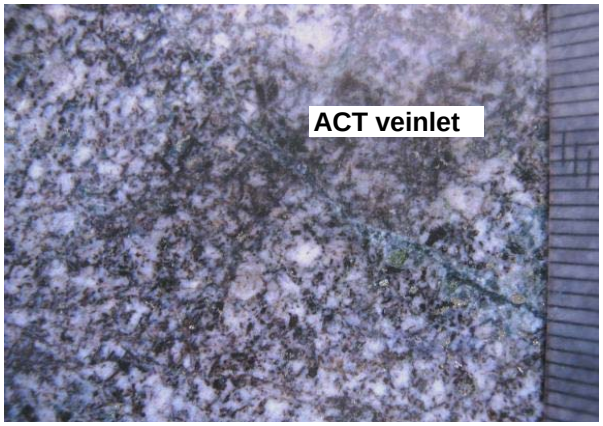

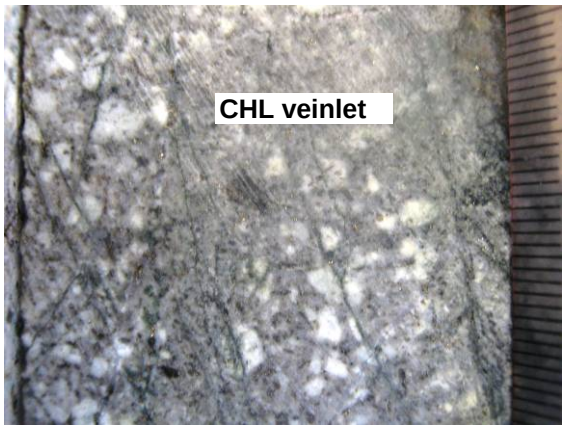

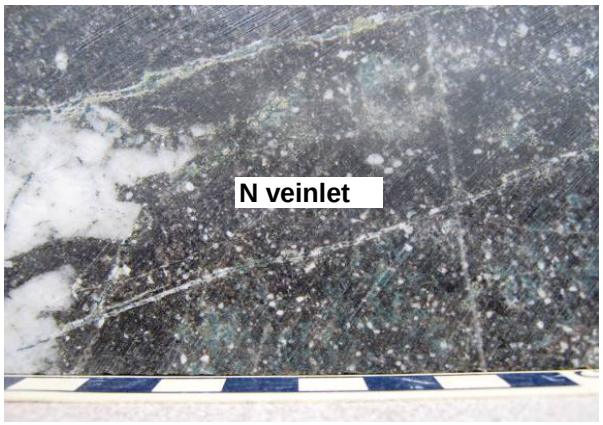

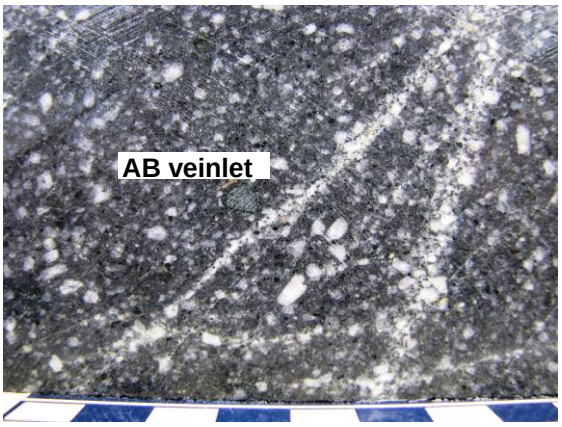

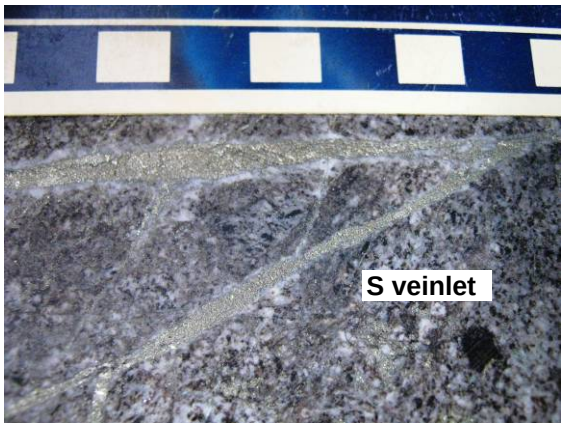

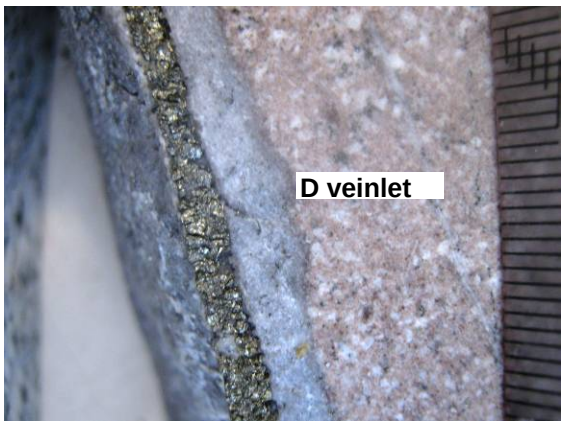

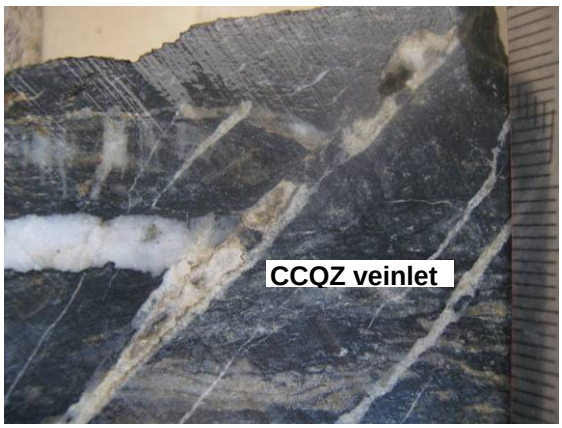

Figure 2.5 caption is on the next page

Figure 2.5 Examples of veinlets types at La Colosa: A- early quartz, B- quartz pyrite, M- magnetite, EB-very early biotite, ACT- actinolite chlorite sulphide, CHL- chlorite, N- sodic-calcic , AB- albite, S- pyrite and/or pyrrhotite, D- quartz sericite, CCQZ- quartz carbonate.

2.3 Structural Geology

The following summary of the structural geology of the La Colosa deposits is based on confidential consultant reports available at the mine site (e.g. IC Consulten, 2011). The La Colosa deposit is cut by NE-SW and NNW-SSE striking faults. Movement along regional NE-SW striking left-lateral strike-slip faults favoured the formation of a steep pull-apart basin which is controlled by E-W and approximately NNW-SSE striking normal faults.

The orientation of the intermineral dikes (predominantly NNW-SSE) is interpreted as evidence for extension towards ENE. There is also strong control by pre-existing weak zones in the metamorphic rocks. The major boundary faults of the pull-apart basin were still active after emplacement of the intermineral magmatic phase and caused further deepening of the basin. The last magmatic phase is represented by the Dacite body as well as the Late Dikes that cross-cut all previous described structures.

Mineralization, though intrusion-related, has a structural component. This is expressed in the predominance of veinlets in exposures of intrusive rocks dipping towards ENE, and veinlets following inherited anisotropies in schist/hornfels such as sub-parallel to foliation (S_1) or perpendicular to the fold axis (E-W strike with varying dips). Figure 2.6 shows a simplified map of the geology and main faults at La Colosa.

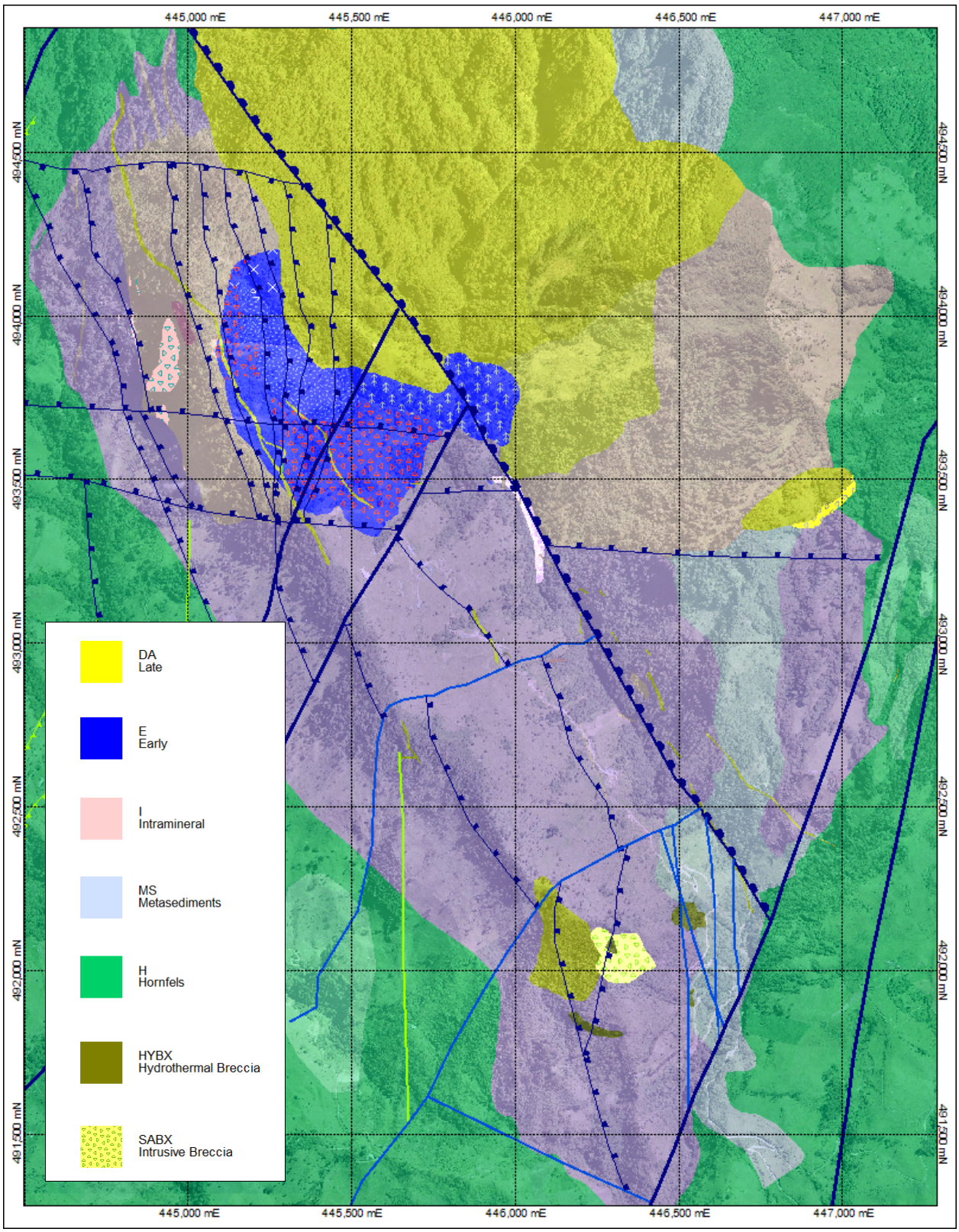

Figure 2.6 La Colosa geology map. Modified from IC Consulten (2011). Faults shown as blue lines.

2.4 Traditional Comminution Tests

There are a number of medium to large scale metallurgical tests that are traditionally used to measure crushing and grinding hardness (e.g. Keeney, 2010). Measures of impact hardness and grindability are suitable for comminution modelling and mill design. Traditionally, comminution performance is estimated using large-scale tests that require a significant amount of sample material (5–200 kg) and are time consuming to carry out. Examples include the Drop Weight Test (DWT), Rotary Breakage Test (RBT), and the Bond Mill Work Index (BMWi). Typically only a small number of tests are completed due to sample size requirements and the high cost of the tests.

In comminution, it is important to predict product size distribution based on a given feed size as well as obtaining the energy required to generate that product size (Napier-Munn et. al., 1996). Energy to size reduction relationship is the focus of laboratory testing to assist in comminution circuit design and optimization. Inherent rock strength parameters (UCS, Young's Modulus, and Poisson ratio) and microfracture patterns influence how a rock material behaves during comminution (e.g. Keeney, 2010).

2.4.1 Drop Weight Test

The Drop Weight Test (DWT) (Figure 2.7) measures the resistance of an ore to size reduction by impact breakage at controlled input energy levels (Kojovic, 2008). Individual breakage events (points on the energy breakage curve) represent a product size distribution at a specific comminution energy level, Ecs (kWh/t). The resulting size reduction versus energy relationship is parameterised using the following expression:

$$t_{10} = A\,(1 - e\,(-b\,Ecs)) \qquad \text{(Equation 1)}$$

(Napier-Munn et al 1996)

The output parameters of the DWT are A, b and A*b values.

Where t_{10} is the percent passing 1/10th of the initial mean particle size (Figure 2.8). Ecs is the specific comminution energy (kWh/t) and A, b are the ore impact breakage parameters, "A" is the asymptote of the t_{10} – Ecs curve at high Ecs. A*b is the slope of the curve at zero input energy (Figure 2.9).

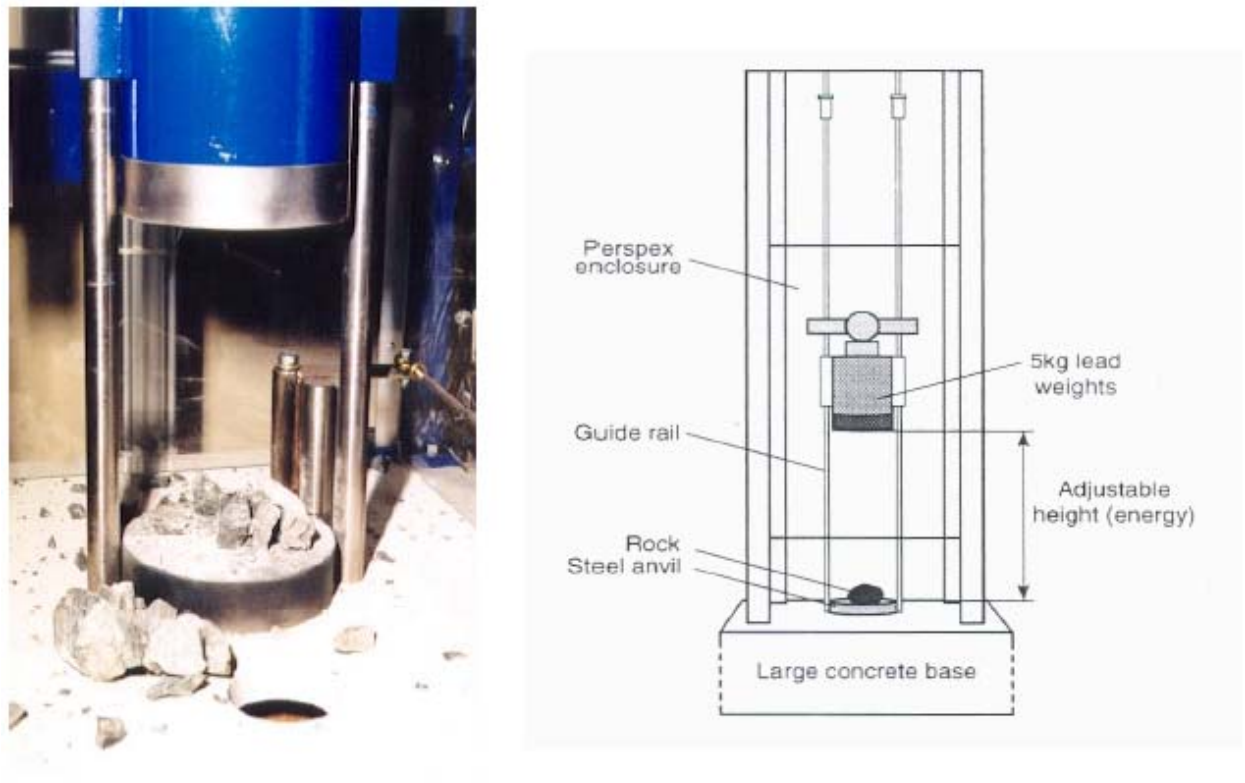

Figure 2.7 JKMRC Drop Weight Tester (from Napier-Munn et al 1996)

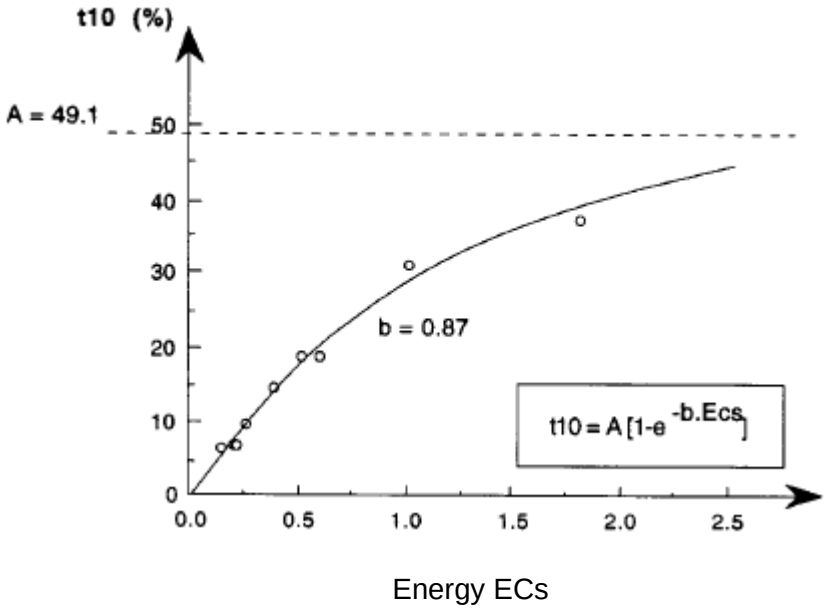

Figure 2.8 Specific comminution energy Ecs (kWh/t) (from Michaux, 2005)

The breakage index has been developed for studying breakage phenomena and for designing and predicting the performance of industrial comminution equipment.

2.4.2 Bond Ball Mill Work Index

The Bond Ball Mill work index (BMWi) was defined by Bond (1952) as the comminution parameter which expresses the resistance of a material to crushing and grinding; numerically it is the kilowatt hours per tonne required to reduce the material from theoretically infinite feed size to 80% passing 100 μm. In practice BMWi has to be determined from plant data or by conducting laboratory grinding tests in which the P_{80} and F_{80} (see below) are measured.

For ball mills, Equation (2) is used to calculate the specific power required to reduce a given F_{80} to the required P_{80} in an 8 ft diameter wet overflow ball mill. For a given throughput (t/h) the specific power (kWh/t) is converted to power draw (kW).

$$BMWi = \frac{49.1}{P^{0.23}\, Gbp^{0.82} \left(\frac{10}{\sqrt{P_{80}}} - \frac{10}{\sqrt{F_{80}}} \right)} \qquad \text{(Equation 2)}$$

(Bond 1961)

BMWi = Work Index (kWh/t)

P = closing sieve size (μm)

Gbp = Grams per revolution averaged over the last three cycles (μm)

P_{80} = size at which 80% of the product passes (μm)

F_{80} = size at which 80% of the feed passes (μm)

2.5 Non – Traditional Measurements of Hardness

Within the AMIRA P843 and P843A geometallurgy project non - traditional tests have been tested on volumes of rock that are much smaller than traditional comminution sampling practice. Ideally the sample size should match the site assay interval (e.g. 2m of ½ drill core). This would provide comminution samples that are well defined geologically and whose spatial context is clear (e.g. Michaux and Kojovic, 2008).

To characterise blocks of ore for comminution purposes, the output of the small-scale tests has been compared to that of large scale-tests (e.g. Michaux and Kojovic, 2008). The results indicate that the outcomes of the small-scale tests can be used as proxies for the behaviour represented by the large-scale tests. The output of the small-scale tests is most suitable to define

variability between samples, rather than absolute values. This allows an orebody to be divided into domains based on comminution data.

2.5.1 GeM Comminution Test (GeMCi)

The GeM Comminution Index test (GeMCi) has been designed to provide information rapidly on comparative size reduction characteristics through application of a standard jaw crusher with a power meter attached. Through the use of constrained protocols, size distributions resulting from this crushing can be used to calculate both a grinding index (GeMCi-GRD) and a crushing index (GeMCi-CRU). These are direct proxies. They can be used to predict metallurgical comminution indices such as the A*b parameter for crushing or BMWi for grinding if there is sufficient calibration data available for the specific deposit (e.g. Michaux and Kojovic, 2008). However they are not fundamental measurements and must be calibrated against all lithotypes included in the study.

The GeMCi test has been designed to be inserted as part of routine sample preparation for assay with sized material returned to the sample. The GeMCi was developed as an outgrowth of work by Michaux (2006) and is described in detail in Michaux (2013). It provides a new approach that allows rapid and low cost comminution testing, the results of which show promise as an ore body domaining tool. In addition, samples that have been through the GeMCi test can be used as potential feed for further metallurgical tests, thus allowing each assay sample to be equally well characterised in terms of comminution (Michaux and Kojovic, 2008).

2.5.2 JKRBT Lite Test

In the JKRBT test a number of fragments are broken in the JKMRC RBT Impact Breakage Device to calculate an approximate A*b value (Figure. 2.10). Two hundred particles from the 11.2+9.5mm size fraction of the crushed product of the GeMCi test are used. These particles are broken by high energy impact in groups of 50, at four different energies as shown in Table 2.1 The broken products from each sample are sized at 1 mm using a Rotap mechanical shaker for 5 minutes to determine the T10 parameter. The data from this test work are then used to calculate the impact breakage parameters A, b and A*b using the JKMRC JKRBT data treatment procedure (Kojovic 2007). The –11.2+9.5mm A*b values can be scaled-up to estimate the A*b expected from a full Drop Weight Test (which is based on 13.2–63 mm particle sizes). The scale up requires mine site specific calibration but is based on the typical ratio of the A*b values between the smaller (-11.2+9.5 mm) and the larger (13.2-63 mm) size, derived from the existing DWT database.

Figure 2.9 JKRBT Device (From JKRMC Laboratory 2011)

Target	*Specific Breakage Energy Ecs (kWh/t)*			
Size Fraction (mm)	0.2	0.5	1	2
-11.2 + 9.5	50	50	50	50

Table 2.1 JKRBT Breakage experimental conditions. Fify fragments in the size range -11.2+9.5 mm are broken at four energy levels from 0.2 kWh/t to 2 kWh/t.

2.5.3 JK Bond Ball Lite Test - JKBBL

A comparative grinding test was adopted to rank the grinding behaviour of the small volume samples (Walters, 2012). The JK Bond Ball Lite (JKBBL) test provides a comparative measurement that can be correlated with Full Bond Ball Mill work index (BMWi) in a given ore body, as shown in Figure 2.11. In contrast to a full Bond Ball test which requires about 5 kg of starting material the JKBBL test requires only 700 gm of material as a feed sample.

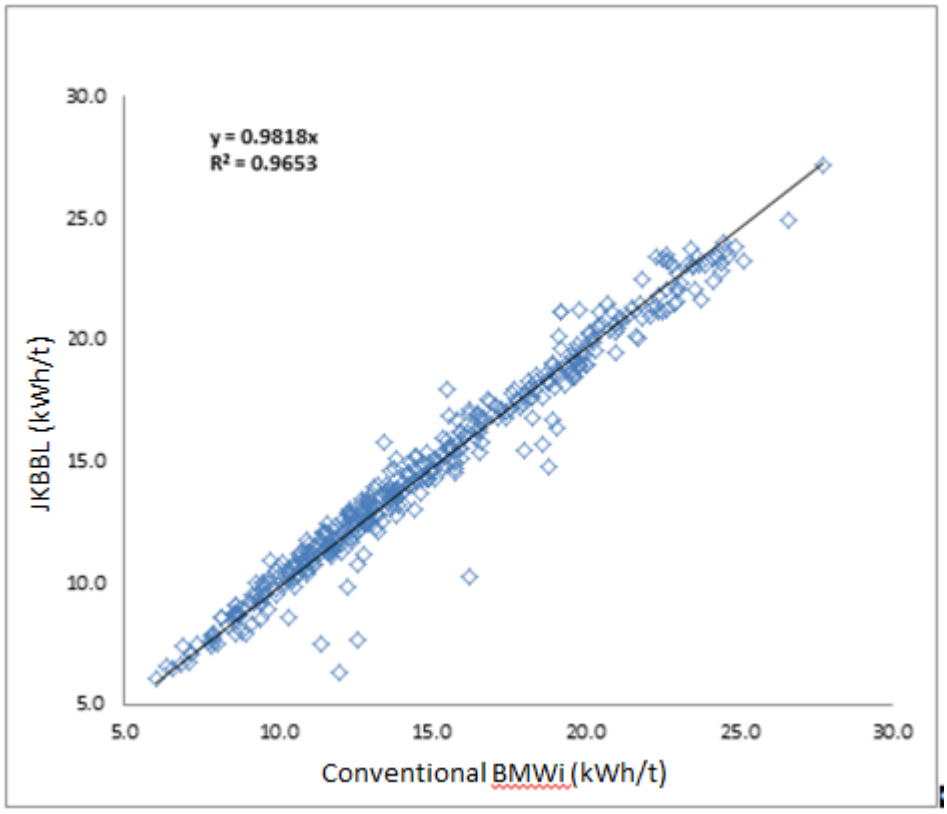

Figure 2.10 JKBBL test results compared to those of conventional Bond testing (Walters 2012).

The procedure of JKBBL test is similar to that of the Full Bond test, but uses a smaller amount of sample and only three cycles in order to obtain the final results. Details about this procedure are in Walters (2012).

2.5.4 EQUOtip Hardness Measurements

The EQUOtip device is a portable electronically-controlled velocity rebound hardness tester designed for testing metallic materials (Verwaal and Mulder, 1993). It provides a direct proxy for comminution hardness. It provides similar information to point load testing without the destruction of the core associated with the point load test.

The EQUOtip unit consists of an impact device and a control/logging box (Figure 2.12). The impact device is a 3mm diameter spherical tungsten carbide test tip that is spring mounted in an impact body. During a hardness test, the tungsten carbide test tip impacts under spring force against the test surface with an impact energy of approximately 11Nm and then rebounds. Impact and rebound velocities are measured in a contactless manner when the test tip is located 1mm from the test surface. The measurement is obtained by a permanent magnet built into the impact body which passes through a wire coil. During movement of the magnet through the

coil, electrical voltages are generated that are proportional to the velocity of the impact tip. Measurements take only a few seconds to record.

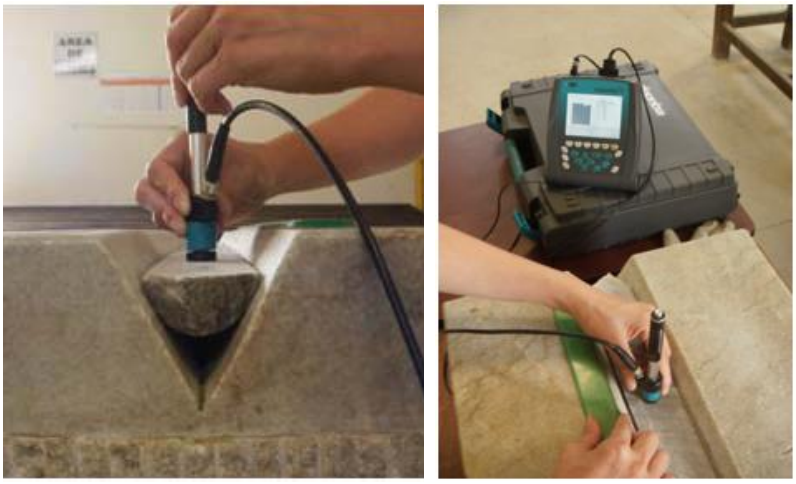

Figure 2.11 EQUOtip hardness measuring device in normal application. It is important to support the core with a massive block to prevent low values being recorded. (From AngloGold Ashanti La Colosa Laboratory)

2.5.5 Sonic Velocity Measurements

The Sonic Logger measures P wave sonic velocity (Figure 2.13). The results of testing can be interpreted to detect and estimate the solidity and homogeneity of material and identify structural damage.

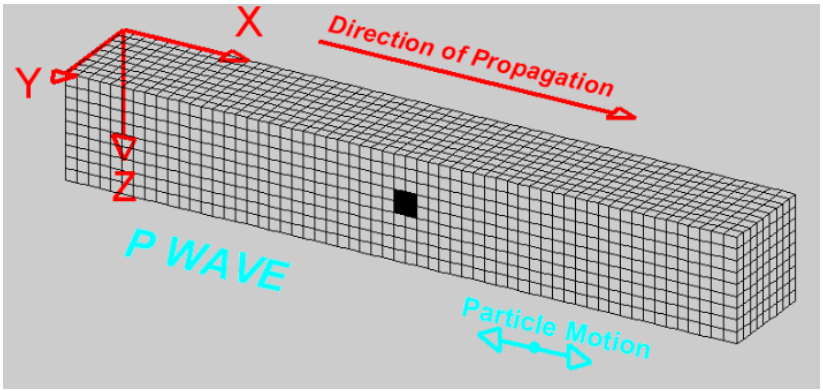

Figure 2.12 P-wave propagation as a compressional wave where the particle movement is in the direction of wave propagation. (Michaux and Walters, 2011)

Sonic Logger measurements form part of core logging data of the La Colosa project. The measurements were averaged over each 2 meters assay interval in order to link the P wave velocity with comminution response (see Appendix B, Sonic Logger – La Colosa Project).

2.5.6 Density Measurements

Density measurement is based on the principle that the weight of the displaced fluid is directly proportional to the volume of the displaced fluid (if the surrounding fluid is of uniform density). In simple terms, the principle states that the buoyant force on an object equal to the weight of the fluid displaced by the object, or the density of the fluid multiplied by the submerged volume times the gravitational constant, g. Thus, among completely submerged objects with equal masses, objects with greater volume have greater buoyancy. (Netz and Noel, 2007)

Density measurements as well as sonic velocity and EQUOtip hardness are carried out routinely during the core logging process at the La Colosa Project. Density values are also required for resource estimation and validation (See Appendix C).

2.6 Methodology for Geometallurgical Characterization

Geometallurgy is the dynamic integration of geology with small scale physical measurements to define the spatial variability of a deposit and aid prediction of metallurgical performance (Dobby et al., 2006). It provides the basis for an informed selection of metallurgical test samples to determine metallurgical behaviour of an orebody. Regression equations built from the larger scale tests can be used to populate the drill core database with processing relevant parameters. These parameters can be modelled using conventional geostatistical techniques to support a metallurgical process model (e.g. Walters and Keeney, 2008)

The methodology used in this thesis has four discrete steps. QAQC procedures were developed to ensure the highest quality information was collected. The four steps are also shown in Figure 2.14 and are summarised here:

- 1st step is data collection. There are three types of data collection, classified as direct measurements, direct proxies and indirect proxies. The indirect proxies are routine drill core-based data sets dominated by assays and geological observations typically used to define geological and grade domains (rock type, alteration, mineralogy estimated by assays). The direct proxies include additional core-based data that can be calibrated against relative processing performance (EQUOtip, Sonic Logger Velocity and density). The direct measures (e.g. A*b, BMWi) are carried out on sub-set of samples systematically selected in order to provide a calibration data set for the proxy data.

- 2nd step involves the integration of geological variables and comminution indices, investigation of data to identify different populations and relationships and identification of preliminary controls on geometallurgical parameters. Based on these controls class-based analysis was used to identify groups that constrain geologic variability in a non-spatial way.

- 3rd step is comminution process modelling using the classes defined in step 2. The purpose of this step is to estimate comminution indices from the proxy data. An analysis of samples in each class is used to identify characteristics of the classes include mineralogical information, assay data, and geological/geotechnical logging information that relate to the comminution attribute being investigated. Parameters were selected through an iterative process using Principle Component Analysis (PCA). A general description of the application of Principle Component Analysis is provided by Walters and Keeney (2008). Multiple linear regression was used to develop proxy models for each class. In this way, each assay interval in the La Colosa database can be assigned a calculated (estimate of) A*b and BMWi.

- 4th step is domaining and block modelling. Domaining is the operation that consists of separating an ore body into zones of similar characteristics so that blocks inside any of the zones are estimated from measured values of samples within the same zone (Dagbert and Bennet, 2006). Geostatistical analysis is used to quantitatively define the spatial variability (variography) of the data within each domain. In addition to estimating the variography within each domain, the nature of the contacts between the domains should be examined to determine whether changes are transitional or abrupt across the contact. Then the point data is converted into a volumetric estimate through the use of interpolation techniques that calculate weighted averages of the analytical data on a block-by-block basis. The material characteristics thus estimated are supplied to the appropriate process model for conversion to metallurgical outcomes.

Finally estimated values are reconciled against “actual” values obtained from production data and reports, and reasons determined for any variances. This forms a feed-back loop back into the four steps which can be used to obtain improvements of the estimates.

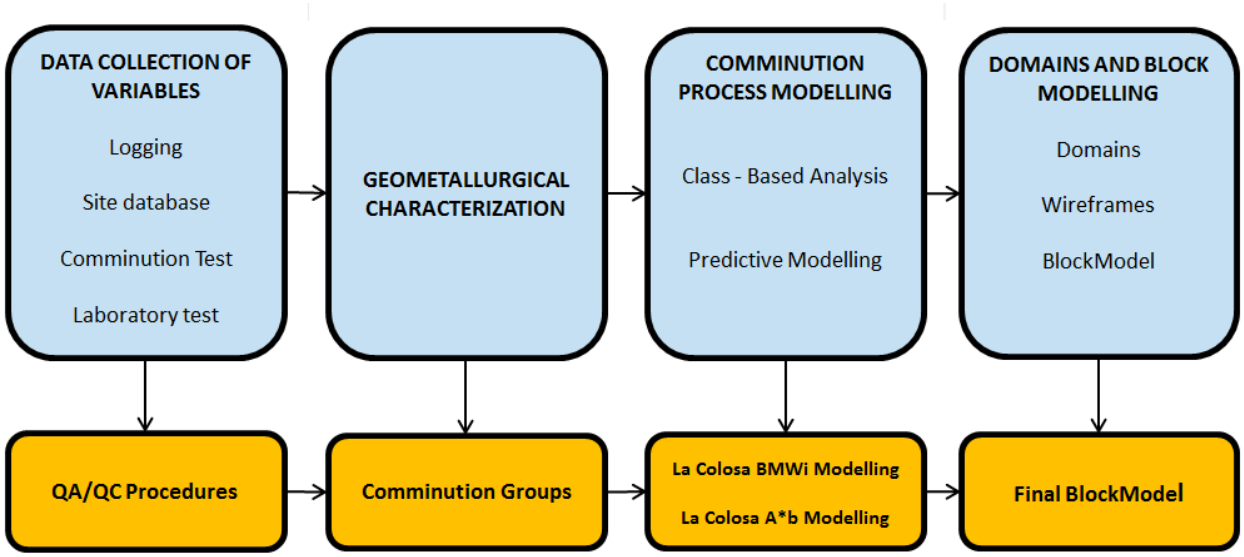

Figure 2.13 La Colosa geometallurgy methodology

Chapter 3: Data Acquisition and Interpretation

3.0 Introduction

One of the key underlying themes behind the current emergence of geometallurgy is a move towards low-cost physical testing which can be applied to small samples that are suitable for defining natural variability.

For geometallurgical modelling, large data sets based on small samples are required to define natural variability. The metallurgical concept of "representative" samples can only be applied when the variability is known. The end result of this type of approach is a multi-tiered sampling and testing strategy, with large numbers of relatively low-cost 'comparative' tests used to define variability followed by small numbers of high precision 'bankable' tests selected to include all the ore types (in terms of processing characteristics) (Walters, 2008). "Bankable" tests meet the guidelines for JORC compliant resource assessment (http://www.jorc.org/).

For the La Colosa Project, quantitative and qualitative continuous data available for analysis included multi-element assays, EQUOtip hardness results, Sonic Logger velocity measurement, density measurements, geological logging information, and QXRD mineralogy estimates. The measurements were taken on half core of HTW, NTW, NQ and HQ size for each 2m assay interval. Table 3.1 provides a summary of the number of samples used in this thesis.

Linear programming, calibrated on the QXRD data, was used to convert multi-element assay results into estimated mineralogy (Berry and Hunt, 2011). This calibration model enabled continuous down holes mineralogical information to be estimated for all 92 diamond drill holes at assay scale.

QA/QC procedures (Appendix A.3, B.3, C) for EQUOtip hardness, density and sonic velocity measurements were developed and were routinely applied to all data acquisition. An appropriate format for data storage and reporting has been implemented.

Small-scale comminution tests were conducted in 3 different phases of sampling. The first phase was from 2009 covering a range of geological units (AngloGold Ashanti, 2009). This testing incorporated 25 samples for full Bond tests and, 55 RBT lite tests. The second phase of sampling (Appendix E), which was part of this study, was conducted on 90 samples of drill core

on which EQUOtip, sonic velocity and density measurements had already been recorded. The aim was to validate the comminution model developed based on phase 1 sampling. Phase 2 samples were taken to cover different ranges of BMWi and A*b values in the deposit. The spatial distribution of the sampling was also important in order to avoid leaving gaps without samples in the deposit. The third phase of sampling (AngloGold Ashanti, 2011) was undertaken by Anglogold Ashanti in 2011 to provide full core material of adequate size for specific comminution test work and also for high pressure grinding roll (HPGR) test work. This testing program consisted of 46 samples covering a range of BMWi and A*b domains in La Colosa.

ITEM	Data Source	# Samples
Qualitative Logging	COLLAR	92 Holes
	SURVEY	92 Holes
	ROCK	92 Holes
	ALTERATION	92 Holes
	VEINLETS	92 Holes
Quantitative Logging	EQUOtip	15195
	SONIC LOGGER	9015
	DENSITY	16676
Mineralogical and Element Data	ASSAYS (AU + ICP)	17505
	QXRD	275
	MLA	11
Comminution Test Work	A*b	155
	BMWi	151

Table 3.1 La Colosa quantitative and qualitative continuous data

3.1 Site Geological and Geotechnical Logging

Much of the non-grade information derived from drill core is the result of visual inspection as part of geological and geotechnical logging. Many of the geological observations collected in routine logging have been collected but not previously been used for geometallurgical analysis. They were not calibrated with or validated against processing performance. However, many of the lithologies recognised during routine geological logging can contribute to the definition of processing 'ore types' (Walters, 2008).

In this study geological logging information provided by site was used in order to understand the relationship between geological variables and the behaviour of comminution parameters in the La Colosa deposit. Figure 3.1 and 3.2 show the variation of BMWi and A*b comminution index by rock type and alteration types.

A*b and BMWi probability plots overall show two different behaviours between rock types from drill logs and comminution parameters. “hard grinding” samples (i.e. high BMWi values) are related to intramineral intrusive rocks (I1, I2, IBX) while “soft grinding” (i.e. low BMWi values) samples are common in the schist (S), hornfels (H) and early diorite lithologies (E0, E1, E2, E3, EBX1, EBX2, EDM). This agrees with the geological knowledge of La Colosa where early diorites and hornfels have the highest sulphide content in the deposit which is related to veinlets, faults or contact zones which produce soft areas in terms of grinding. On the other hand, hard crushing areas, i.e. low A*b values, are related to intrusive rocks (I, E) and soft crushing is related to hornfels and schist (H, S).

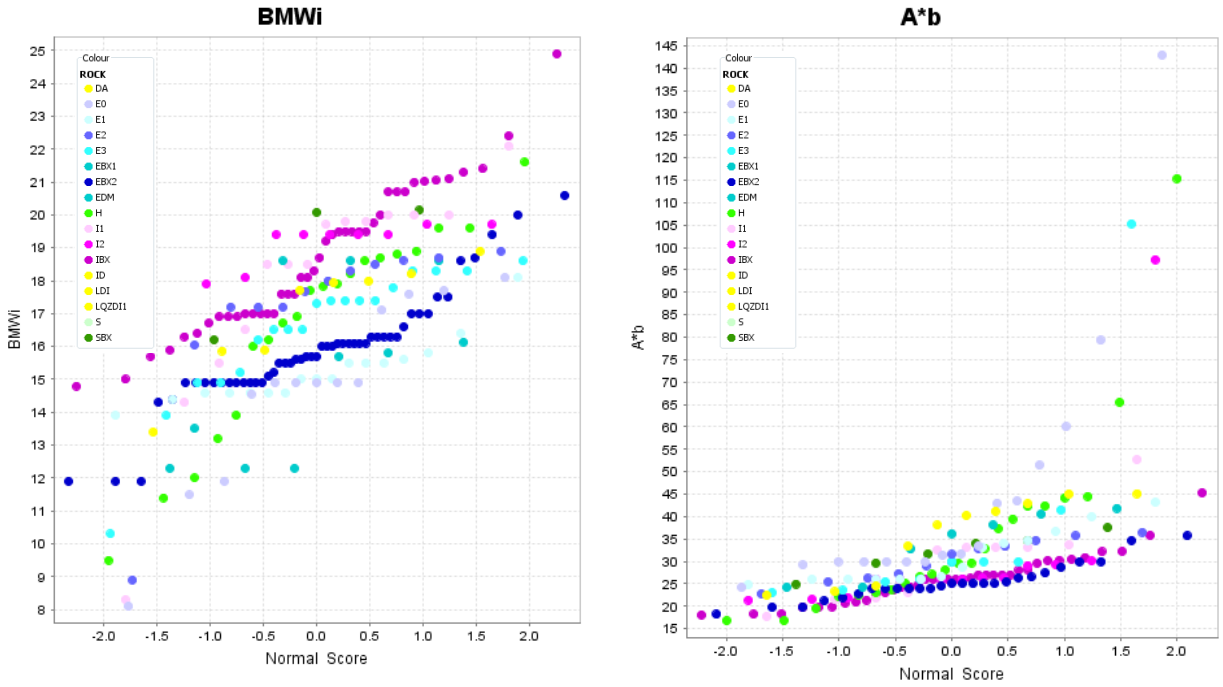

Figure 3.1 A*b and BMWi probability plots by rock logging type. Lithology codes as described in section 2.2. E0, E1, E2, E3, EBX1, EBX2, EDM are early diorites. I1, I2, IBX are intramineral intrusive rocks. DA is late dacite/granodiorite. S is schist. H is hornfels. SBX is breccia with S and H clasts. LD1 is late diorite. LQZDI1 is quartz diorite.

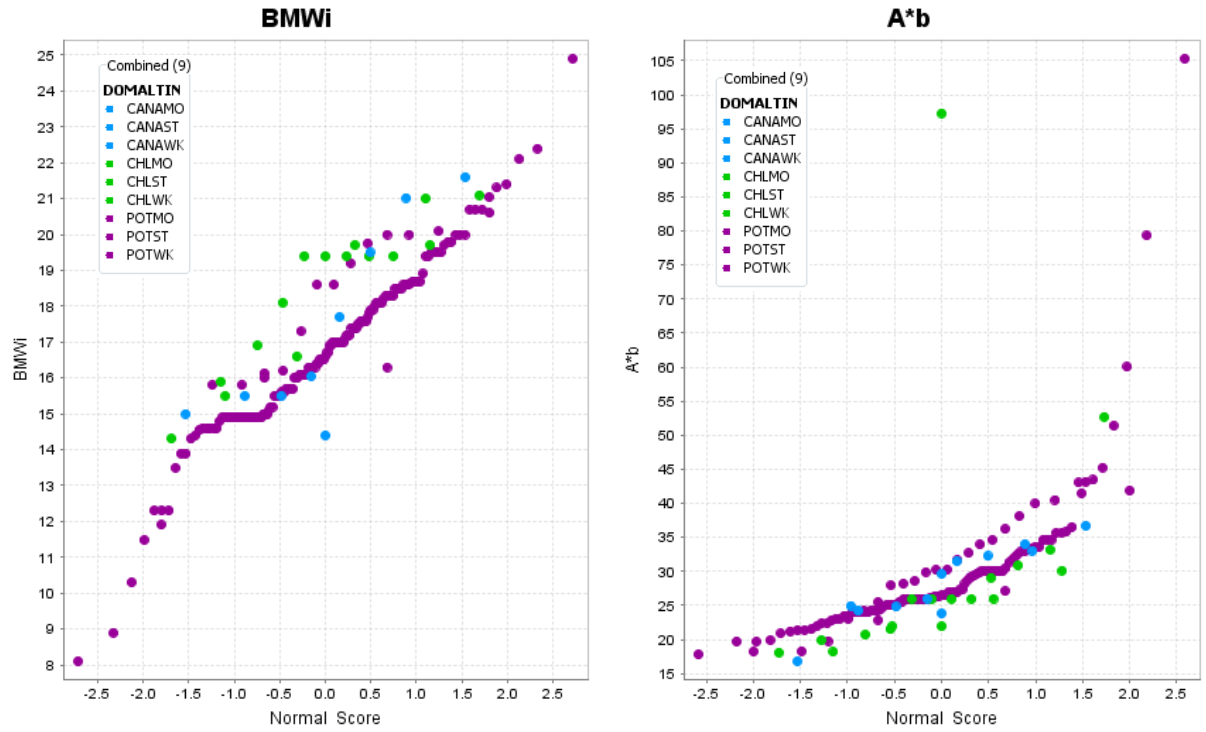

Figure 3.2 A*b and BMWi probability plots divided by alteration logging type and alteration intensities, sodic calcic (CANA), chlorite (CHL) and potassic (POT). - showing the crushing and grinding behaviour of the different alteration types are similar. MO is moderated alteration. ST is strong alteration. WK is weak alteration.

3.2 Site Database

The aim of petrophysical core logging is to provide systematic and continuous profiles of physical parameters such as density, EQUOtip rebound velocity hardness and sonic logger velocity. The raw data was measured at spacing ranging from of 2.5 cm to 2 meters. For comparison purposes all data was averaged over the assay intervals. This information can be compared against more subjective information such as geological logging to see if they display similar trends and boundaries. All of these parameters provide information on trends that are related to bulk rock parameters that can influence comminution behaviour (e.g. Walters, 2008). Appendix C, D and E describe the sample measurement methodologies.

QA/QC activities are essential to the development of comprehensive, high-quality information for any purpose. Furthermore, a well-developed and well-implemented QA/QC procedure fosters a high confidence level in the data.

3.2.1 EQUOtip results

During EQUOtip test work for La Colosa, half core from 92 drill holes underwent EQUOtip hardness testing. EQUOtip data was collected each 2.5 centimetres, continuously down hole, and was converted to produce an average hardness value for each assay interval (2 meters) (see Appendix A.1, A.2). Five numbers derived from EQUOtip measurements are potentially important as proxies for comminution modelling: Mean (Ls), standard deviation (s), and 90th, 50th, and 20th percentiles. The mean provides a standardized hardness value for the interval over which data were collected. The standard deviation provides a measure of hardness variability over the same interval, and the percentile values provide hardness information for hard, medium, and soft components of the rock being measured. The reason for the use of five derived numbers is that a single value does not fully describe the distribution of EQUOtip data (Walters and Keeney, 2008).

The EQUOtip range for Ls at La Colosa is between 200 and 890. Ls mean for the deposit is 773 with a standard deviation of 60 across the 92 holes tested (15195 individual measurements). There is a complex distribution with a strong skew to low Ls values (Figure 3A). Figure 3.3B shows the relationship between EQUOtip values with BMWi and A*b values. The probability plot is subdivided into EQUOtip quartiles in order to see BMWi and A*b variations related to EQUOtip. Overall, It is clear that higher (i.e. harder) BMWi values are related to higher EQUOtip values, while high (i.e. softer) A*b values correlate with low EQUOtip values. Therefore, hard rock values in terms of comminution are related to high EQUOtip values.

A)

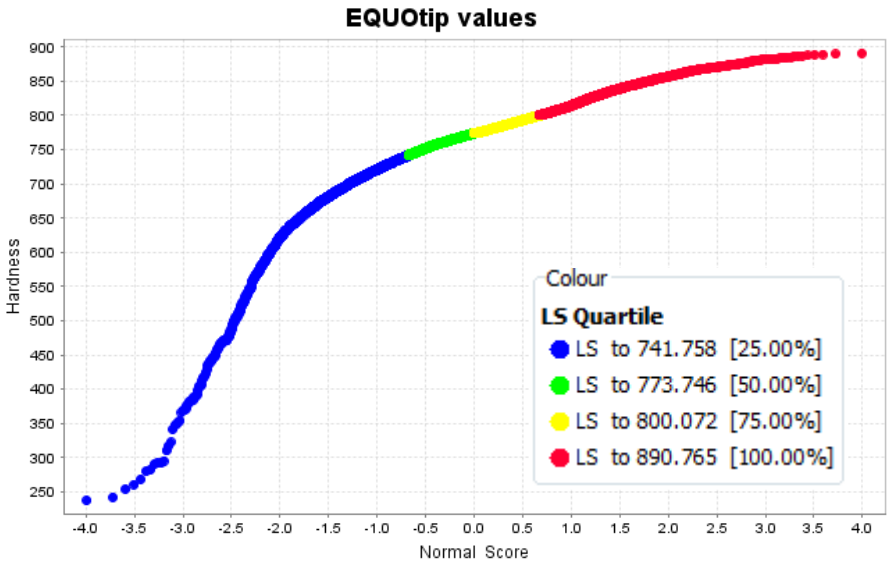

B)

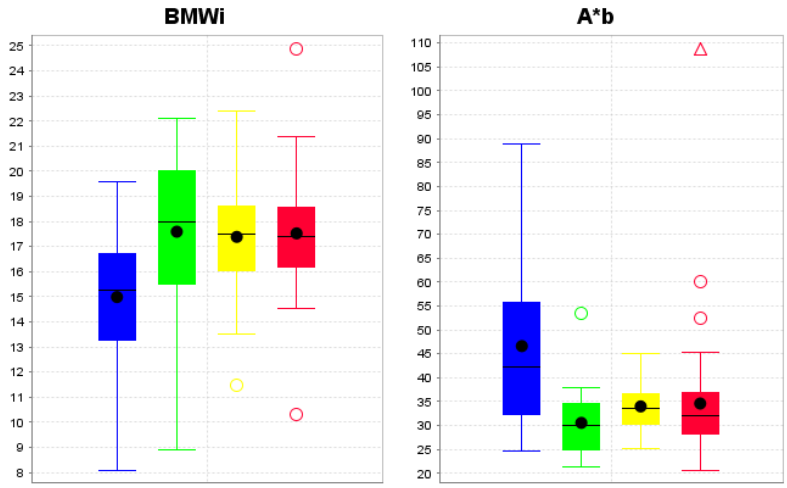

Figure 3.3. A. Ls on normal probability graph showing skew to low Ls values. B. BMWi and A*b values classified by EQUOtip hardness values. Colours are defined by Ls quartile as shown in Fig 3.3A. The low Ls quartile is low in BMWi and high in A*b.

In order to explain the EQUOtip variation within the deposit, diagrams and figures divided by rock types were developed. Examples of these are shown in figures 3.4 and 3.5 which show the EQUOtip values divided by rock types. The difference of EQUOtip value ranges for intrusive rocks (yellow, blue and rose colours) and hornfels (green colour) is clear. Overall, Ls values taken in intrusives rocks (blues and pinks) are between 750 and 850 Ls in contrast with metamorphic rocks (schist, hornfels or intrusive – metamorphic breccias in various greens) where the Ls values range between 450 and 750.

In general, EQUOtip values higher than 750 in hornfels are related to silica or potassic alteration, while values below 750 Ls in intrusives are related to supergene argillic alteration. High Ls variability in hornfels reflects the variability in hornfels composition (green schist, black schist, breccias and variation in alteration).

This work demonstrates that EQUOtip non-destructive hardness testing does differentiate zones of different hardness. The results from the 92 holes tested indicate that La Colosa has BMWi values in the range 14-19 kWh/t and A*b from 25 to 50. A number of the down-hole profiles (e.g. Figure 3.4) display zones of weakness in the lowest quartile of Ls and that there are coherent trends in hardness. The zones of weakening are commonly related to contact zones. No difference was found between different intrusive rock types. See appendix A for more details.

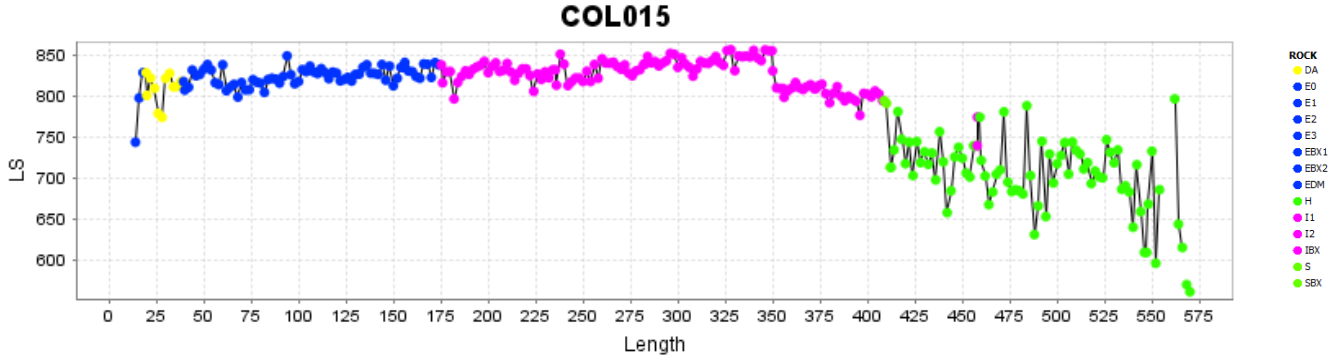

Figure 3.4 Down hole profile of drill hole number 15 and EQUOtip results by rock type. Lithology codes as described in section 2.2. E0, E1, E2, E3, EBX1, EBX2, EDM are early diorites. I1, I2, IBX are intramineral intrusive rocks. DA is late dacite/granodiorite. S is schist. H is hornfels. SBX is breccia.

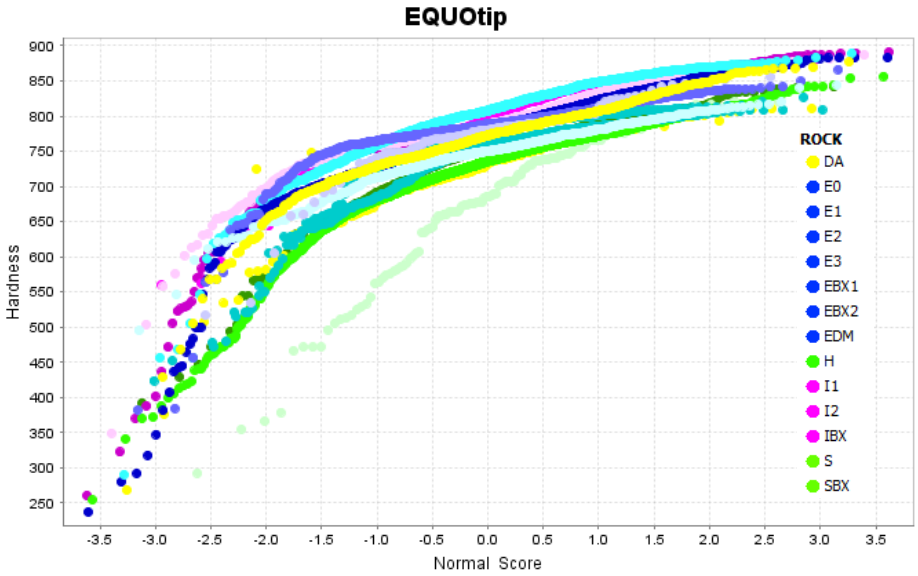

Figure 3.5 EQUOtip probability plot by rock type. Lithology codes as described in section 2.2. E0, E1, E2, E3, EBX1, EBX2, EDM are early diorites. I1, I2, IBX are intramineral intrusive rocks. DA is late dacite/granodiorite. S is schist. H is hornfels. SBX is breccia.

3.2.2 Sonic Velocity results

During sonic velocity test work, half core from 92 drill holes underwent P – wave velocity measurements. Data was collected continuously in the half core samples and was converted to produce an average value for each assay interval (2 meters). The method is described in Appendix B. The sonic velocity range for La Colosa is between 1890 and 6600 m/sec, with a mean of 5080 m/sec and standard deviation 390 m/s across the 92 holes tested (9015 measurements). Figure 3.6 shows the relationship between sonic velocity values with BMWi and A*b values. The probability plot is subdivided into sonic velocity quartiles in order to see BMWi and A*b variations related to sonic velocity values. Overall, It is clear that high BMWi values are related to high sonic velocity values, while high A*b values correlate with low sonic velocity values. Therefore, hard rock values in terms of comminution are correlated with high sonic velocity values.

A)

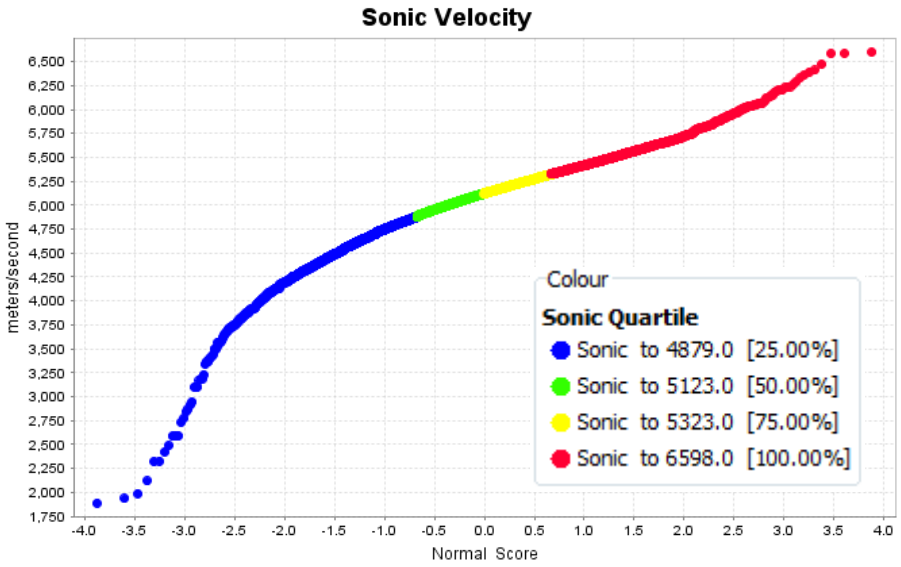

B)

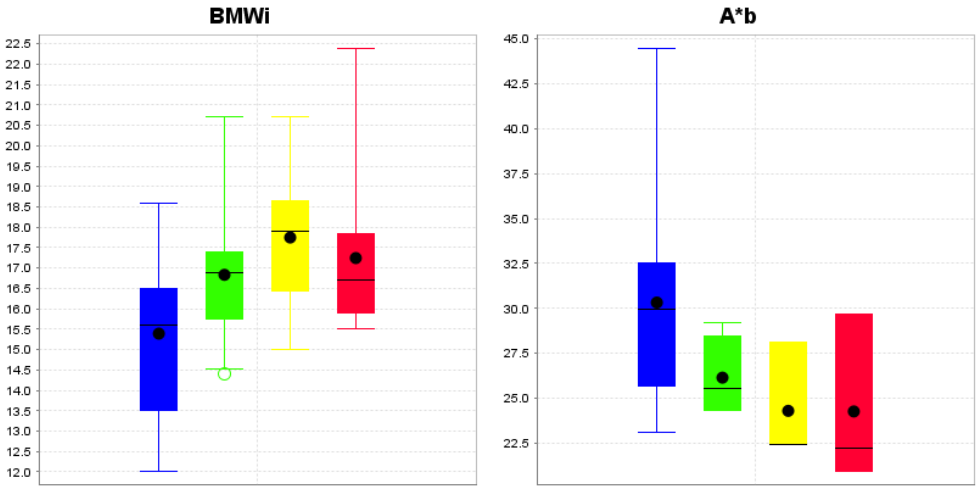

Figure 3.6 A. Sonic velocity on normal probability graph showing skew to low velocity values B. A*b and BMWi box and whisker plots for four quartiles of sonic velocity defined in A.

The following figure shows that the sonic velocity is similar in the sedimentary rock types to the intrusive rocks, in contrast with EQUOtip hardness. All the rock types show a similar velocity distribution. The main control on sonic velocity is not mineralogy but may be porosity or microfracture density (e.g. Schon 2004).

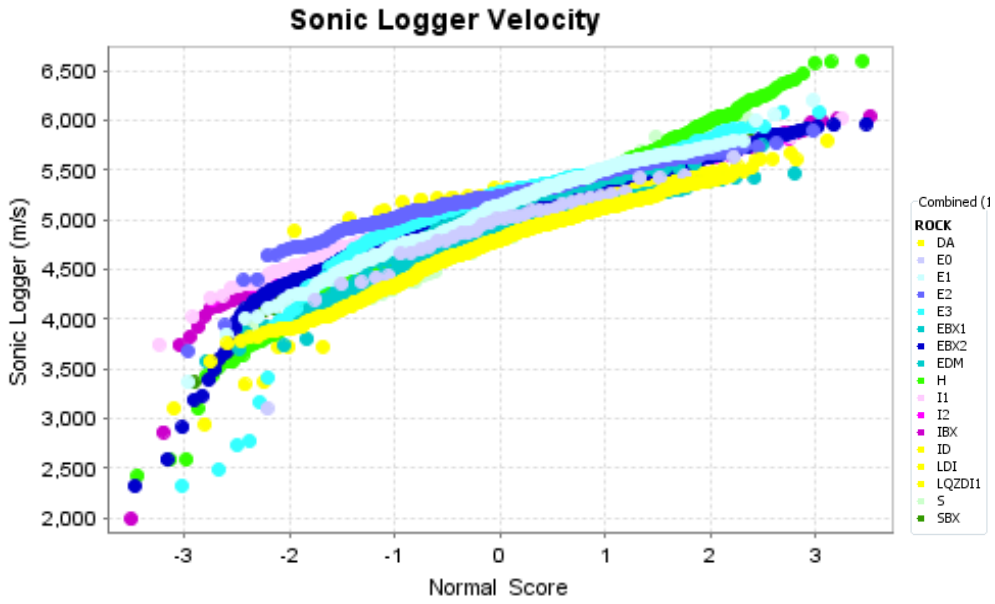

Figure 3.7 Sonic velocity probability curves by rock type. Lithology codes as described in section 2.2. E0, E1, E2, E3, EBX1, EBX2, EDM are early diorites. I1, I2, IBX are intramineral intrusive rocks. DA is late dacite/granodiorite. S is schist. H is hornfels. SBX is breccia. LD1 is late diorite. LQZDI1 is quartz diorite.

Figure 3.8 shows a sonic velocity probability plot divided by alteration types. Again there is no difference in sonic velocity between alteration types.

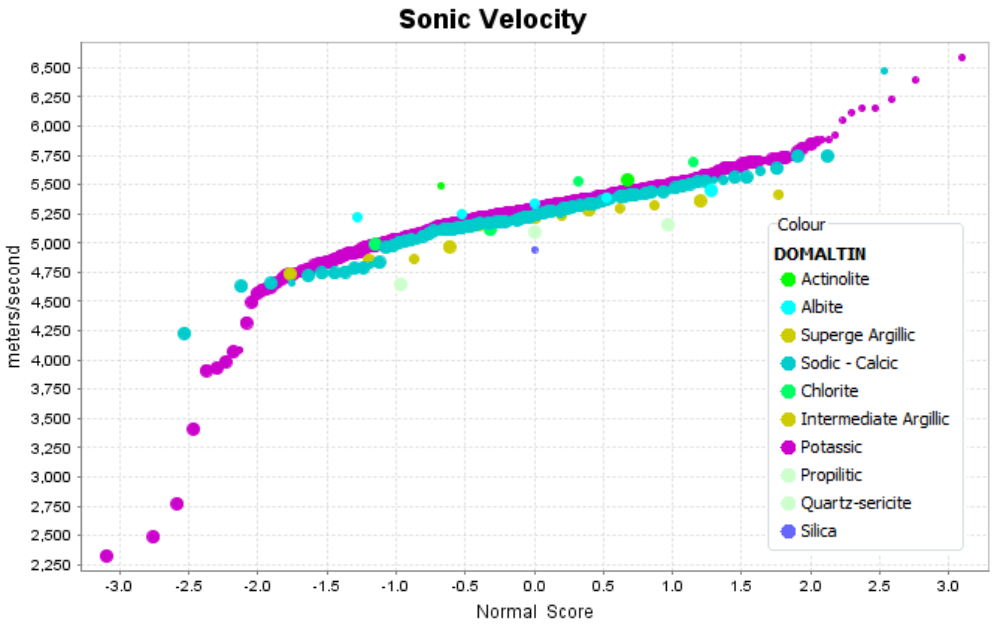

Figure 3.8 Sonic velocity probability plot by alteration types.

Sonic velocity is a non-destructive test which is correlated with comminution parameters. It does not correlate with other logged data and therefore is providing additional constraints on

processing behaviour. The results from the 92 holes tested indicate that La Colosa has variable P-wave velocity. There are contiguous zones of similar sonic logger values that are controlled by structural or physical features in the rock. Possible interpretations are discussed in section 3.3.

3.3 Rock Mineralogy

Rock mineralogy can be a key parameter in predicting performance characteristics such as mill throughput, concentrator efficiency, loss to tailings and acid generation/neutralisation potential. In this thesis bulk mineralogy of the rocks was estimated from assays. The technique used is linear programming (Berry and Hunt, 2011). From 92 drill holes, the mineralogy was calculated for 17,152 assays. In order to determine the accuracy of the calculated mineralogy, 922 QXRD values were used to validate the results; details are given in Appendix F. In this study calculated mineralogy was used as one of the key proxies to estimate A*b and BMWi parameters.

Correlations between assay mineralogy and other variables such as EQUOtip, sonic velocity were examined in order to understand the relationships between mineralogy and hardness, and between mineralogy and P wave velocity in the deposit.

Figure 3.9 compares mineralogical parameters (calculated mineralogy from assays) to EQUOtip hardness values: low EQUOtip values correspond to high mica content. This may reflect a contribution from the argillic alteration.

On the other hand, high EQUOtip values correlate with higher feldspar, carbonates, amphibole and magnetite abundance. Linking this with a geology relationship, areas in Colosa with high feldspar, magnetite and amphiboles are commonly intramineral diorites (at deeper areas of the deposit) and hornfels. Therefore, in terms of comminution, we will expect the intermineral diorite and hornfels to have higher BMWi and A*b than other rock types.

Figure 3.10 shows assay mineralogy abundance versus sonic velocity. Overall the mineralogy has very little correlation with sonic velocity. Amphibole and magnetite show a very weak correlation with high sonic velocities. This is limited to rocks with sonic velocity over 5000 m/sec. The mineralogy of rocks at La Colosa could be used to calculate the sonic velocity for intact rocks assuming no porosity (cf. Hacker and Abers 2004). In this case, all rock compositions recorded from La Colosa have predicted velocities over 6000 m/sec (Table 3.2).

However 75% of rocks measured have velocities below 5340 m/sec. The only explanation for this velocity range is that the rocks have extensive porosity or microfracture contents. For example, sandstone with 15% porosity has a sonic velocity of 3800 m/sec (Mavko et al 2009). The dominant cause of variation in the sonic velocity is independent of the composition and related to microfractures and/or porosity. In most rocks the sonic velocity correlates with the unconfined uniaxial strength (Mavko et al 2009) and therefore a correlation with processing performance is expected.

.

Minerals	*Vp*	*Minerals*	*Vp*
	km/s		*km/s*
Quartz	*6.2*	*Actinolite*	*6.3-7.1*
Albite	*6.5*	*Hornblende*	*6.7-7.3*
Anorthite	*7.3*	*Biotite*	*5.2-5.7*
Orthoclase	*6.3*	*Muscovite*	*5.7*
Garnet	*8.4*	*Chlorite*	*6.6-7.4*
Clinopyroxene	*7.9*	*Magnetite*	*7.7*
Calcite	*6.7*	*Pyrite*	*8*

Table 3.2. Typical sonic velocity for minerals common at La Colosa (from Hacker and Abers, 2004)

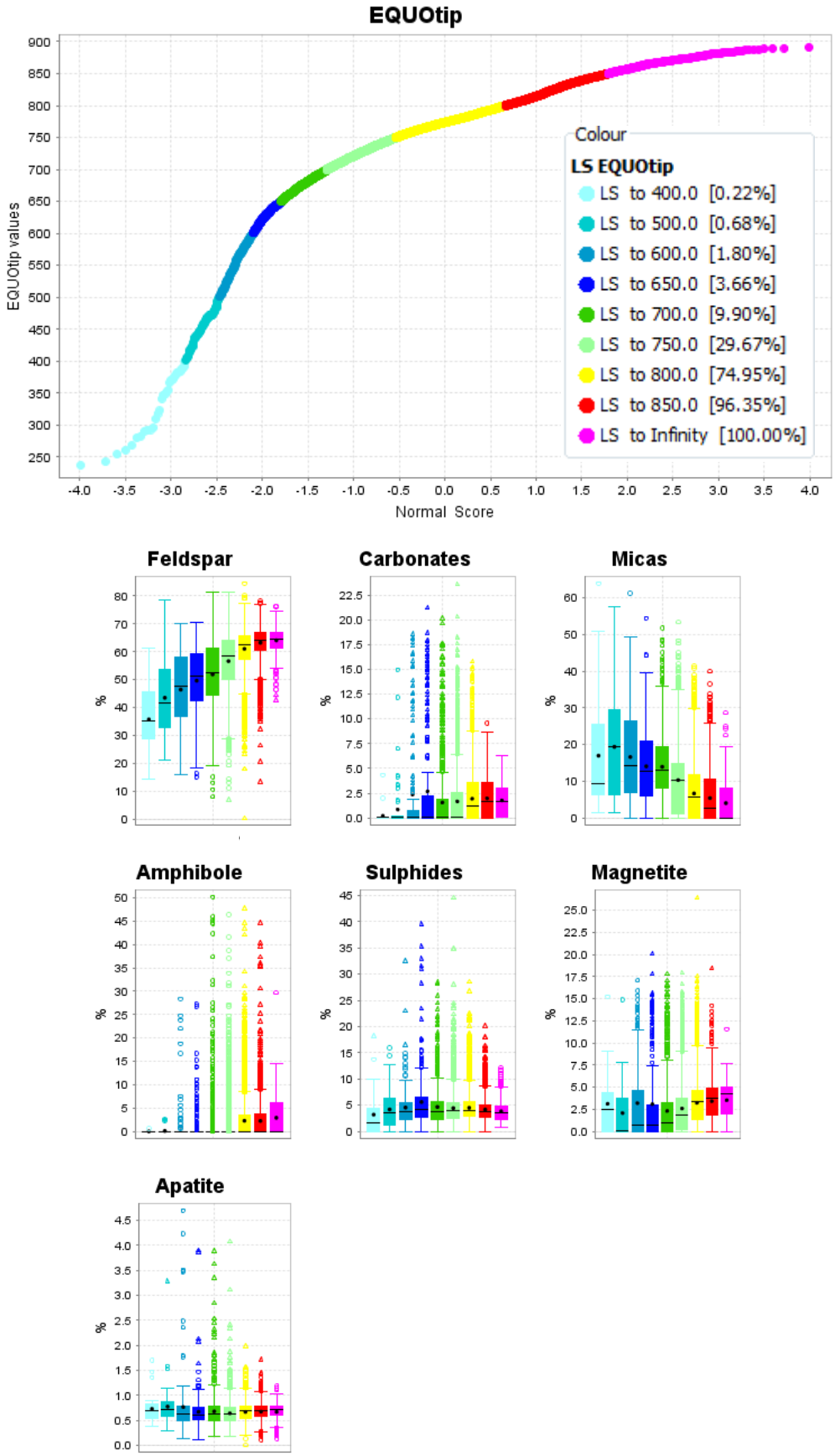

Figure 3.9 EQUOtip probability plot and box and whisker plot for mineralogy by decile defined on Equotip. Lowest decile on Equotip curve is low in feldspar, carbonate and amphibole, and high in mica.

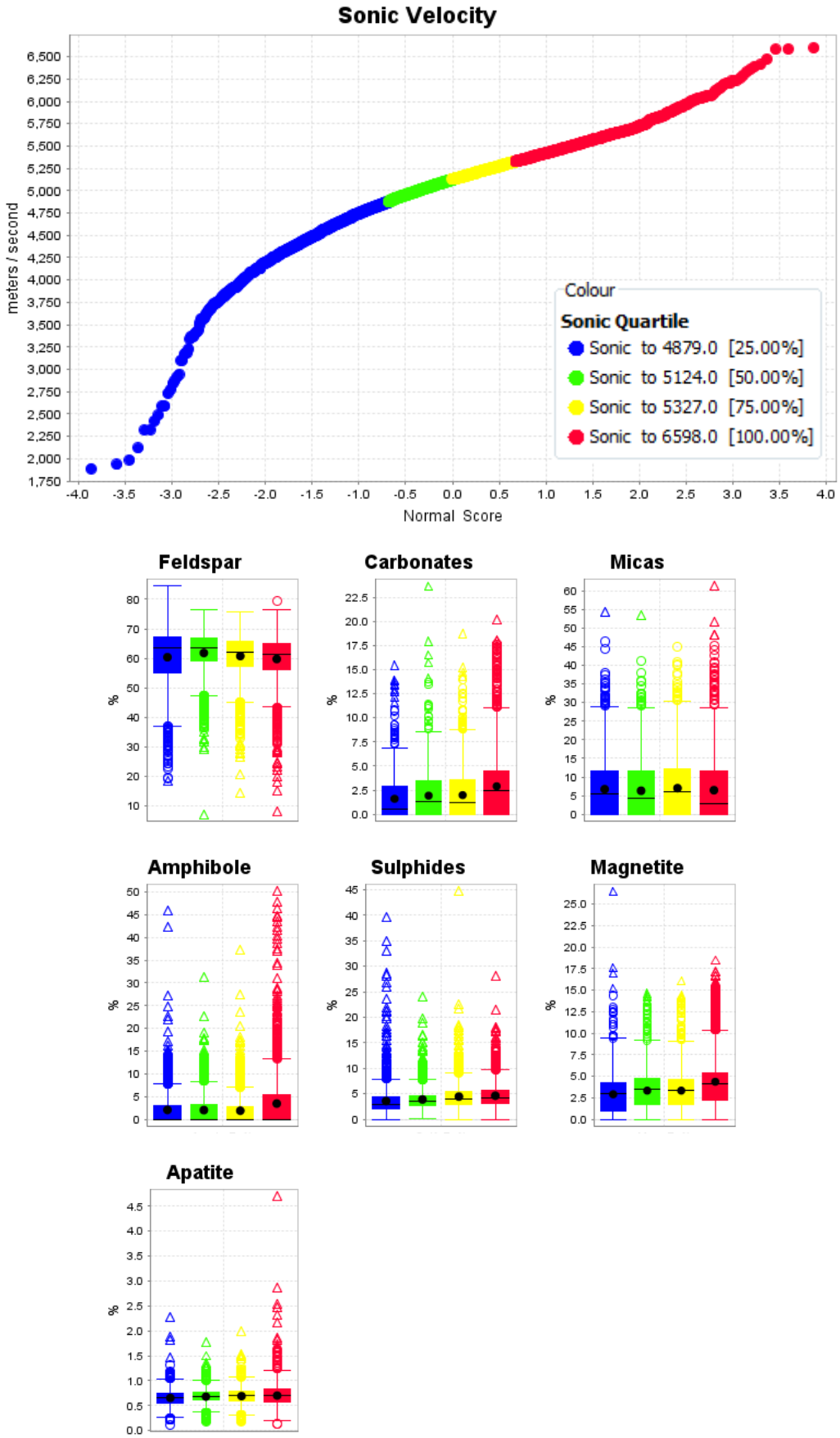

Figure 3.10 Sonic velocity probability plot and box and whisker plots of mineralogy for each quartile of the sonic velocity distribution. There is no systematic trend in mineralogy by quartile.

3.4 Sampling Strategy for Direct Measurements (Calibration Data)

The La Colosa comminution test program consisted of three main phases of sampling as listed in Table 3.3 (details are provided in Appendix D):

Phase 1 was conducted in late 2009 by Anglogold Ashanti. The primary aim was to obtain the comminution data for application in class-bases modelling initiatives. The testing program consisted of 80 drill hole samples covering a range of geological units. Twenty five samples were submitted for full bond tests, and 55 samples for RBT lite tests.

Samples for Phase 2, which were a part of this study, were selected from individual drill holes in different A*b and BMWi domains as predicted by the initial calibration in order to cover the range of known comminution variability of the deposit, taking in to account the spatial distribution and covering a range of lithologies. The 90 drill core samples in phase 2 (Table 3.3) were selected from the north part of the deposit called La Colosa North. Table 3.4 shows the sample selection by rock types. Forty samples were taken of early diorites because of the fact these rock types have the highest gold values in the deposit. Five samples were taken of dacite, reflecting the fact that this rock type only represents 5% of the rock in the deposit. Figure 3.11 shows the spatial distribution of each phase of sampling in La Colosa.

The Phase 3 testing program was undertaken in 2011 by Anglogold Ashanti. This phase consisted of 46 samples covering a range of BMWi and A*b domains. Comminution testing incorporated 36 samples for JKBBL testing and 10 samples for JKRBT tests.

Test Work		
Sampling Phase	*JKRBT*	*JKBBL*
1	*55*	*25*
2	*90*	*90*
3	*10*	*36*

Table 3.3 La Colosa comminution test program

PHASE 2			
Number of samples	*Rock type*	*Total samples per group*	*Overall rock type*
5	DA	5	Late dacite
5	E0	40	Early diorite
4	E1		
8	E2		
6	E3		
2	EBX1		
14	EBX2		
1	EDM		
4	I1	25	Intramineral diorite
3	I2		
18	IBX		
19	H	20	Metamorphic rocks
1	SBX		

Table 3.4 Phase 2 sample selection

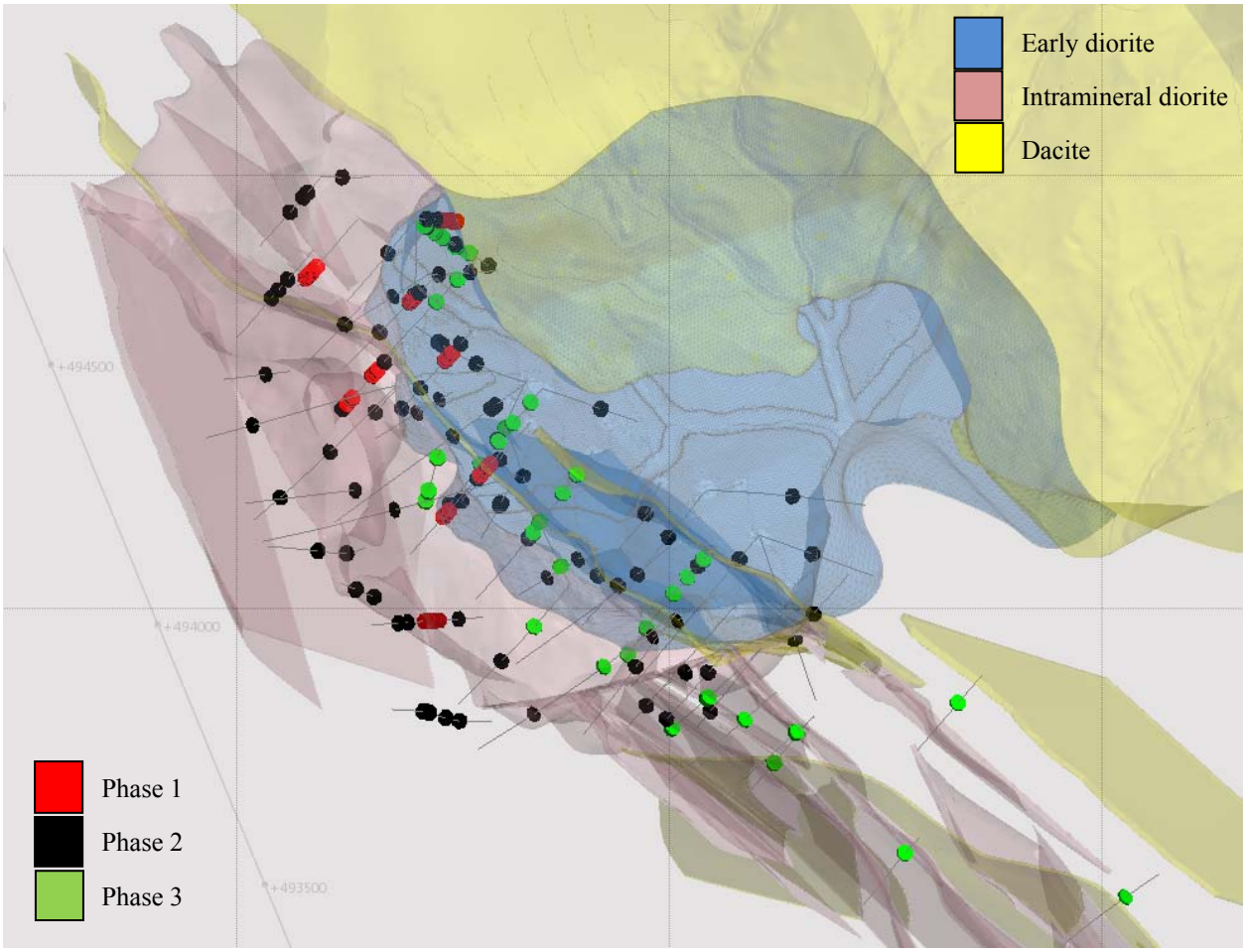

Figure 3.11 Spatial distribution of comminution samples in La Colosa

The following chapter shows an integration of geological variables with comminution indexes in order to investigate preliminary geometallurgical controls on comminution behaviour.

Chapter 4: Geometallurgical Characterization and Integration Modelling

4.0 Introduction

Geometallurgical characterization and integration modelling are processes that link geology variables, such as non-destructive continuous core logging with small scale comminution tests (e.g. A*b, BMWi) in order to understand, identify and quantify controls that can help to explain the orebody hardness variability.

4.1 Geometallurgical Characterization

Geometallurgical characterization is a dynamic integration of geological variables, such as rock type, alteration, assays, mineralogy calculated from assay, EQUOtip hardness, sonic velocity and density with comminution indices (e.g. BMWi and A*b). The aim is to gain an understanding of correlations and relationships between the geological drivers and processing performance so as to enable robust predictive models to be developed. The comminution footprint diagram (Figure 4.1) was arbitrarily divided into fields defining ten groups to cover the range of comminution responses observed. These groups were used to search for correlations between mineralogy and comminution performance.

The following box and whisker plots (Figure 4.1) show the relationship of mineralogy and the physical measurements with processing performance. Colours were assigned based on the hardness of each group: hot colours represent hard rock, and cold colours for soft rock. Calculated mineralogy and site test results were plotted as box plots per variable in order to identify comminution trends. Clay, sulphides and micas are more abundant in the soft rock; whereas EQUOtip hardness, sonic velocity, feldspar, carbonate, magnetite content and density are positively correlated with hard rock (hot colours).

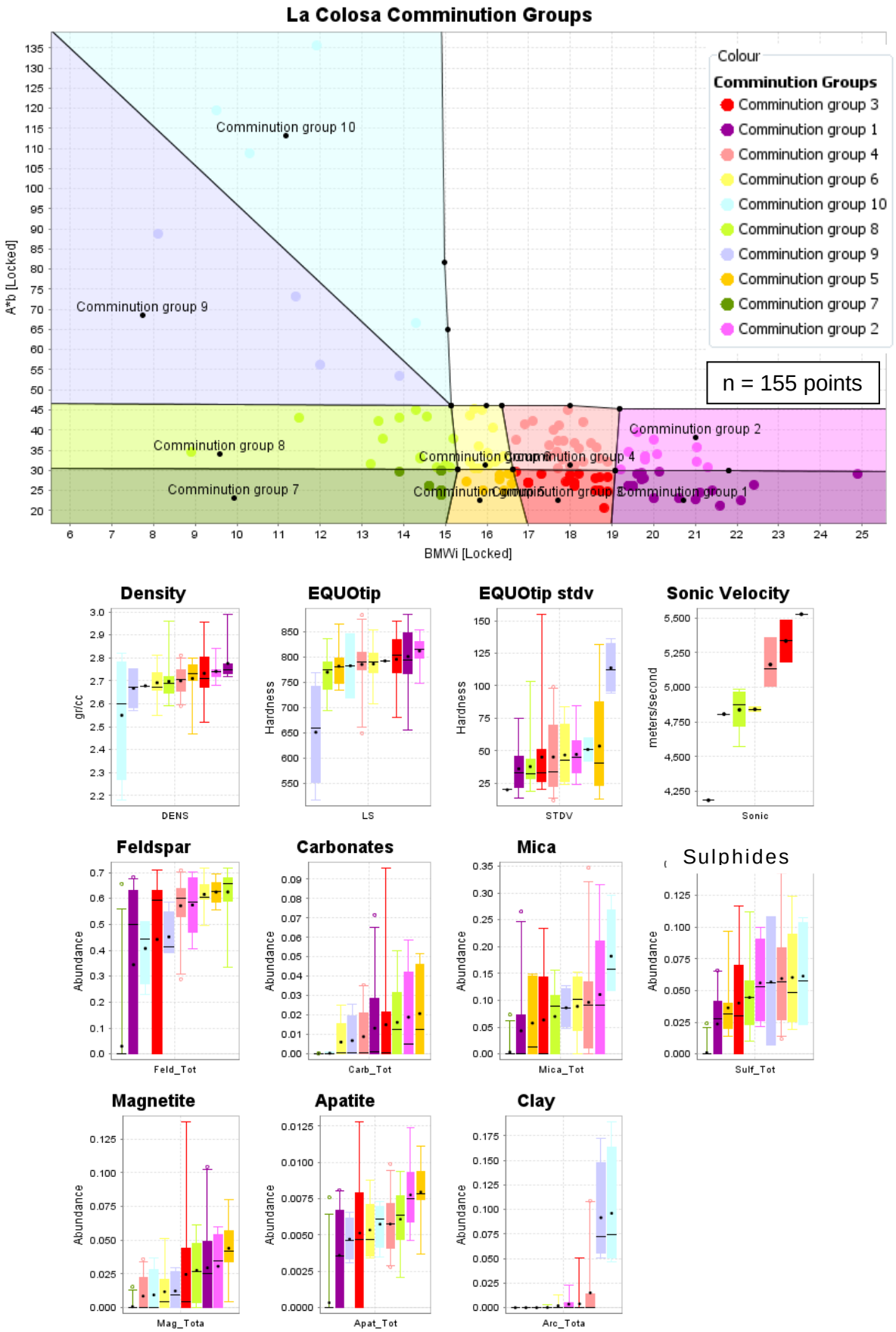

Figure 4.1 La Colosa Comminution Groups. Plot of measured A*b against BMWi has been manually separated into 10 groups. Box and whisker plots of 11 parameters are shown with data classified into these 10 groups. Colours based on operator selected groups.

4.2 Multivariate Class – Based Analysis

The purpose of multivariate class – based analysis, as recommended by Walters and Keeney (2008), is to identify and group samples that have similar characteristics. These characteristics include mineralogical, site test and geological logging information. The characteristics selected are specific to the attribute being investigated and are selected through an iterative process using Principle Component Analysis (PCA)

The generation of principal components is the first step in an interactive iterative process achieved by adding and removing inputs into the analysis based on statistical output, with the primary objective of obtaining the largest spread in the data with the fewest number of input parameters, and accounting for the maximum amount of variation in the data set with the first two principal components.

. The input variables used were:

- Mineralogy calculated from assay
- Density
- EQUOtip Hardness parameters
- Sonic Velocity

These input variables formed the initial parameters incorporated into the PCA. Through a process of iteration where redundant parameters were removed based on eigenvector results (Keeney and Walters, 2011), the final set of input parameters were feldspar, micas, magnetite, carbonate, sulphides, clay and density (Table 4.1). Eigenvalues record the data variability along each principle component. The eigenvalues indicate principal component 1 (41%) and 2 (23%) capture 64% of the data variability (Table 4.2).

Input Columns	Term
Feldspar	V0
Micas	V1
Magnetite	V2
Carbonate	V3
Sulphides	V4
Clay	V5
Other minerals	V6
Density	V7

Table 4.1 La Colosa – final set of PCA input variables

Eigenvalues			Eigenvector			
	Values	Variance Proportion (%)	Input Terms	Data Source	Eigenvector 1	Eigenvector 2
Eigenvalues 1	3.2923	41.1531	Feldspar	Assays Mineralogy	-0.4516	0.1383
Eigenvalues 2	1.8199	22.7493	Mica		0.3742	0.2503
Eigenvalues 3	0.9658	12.0731	Magnetite		-0.2736	-0.5545
Eigenvalues 4	0.8326	10.4071	Carbonate		-0.3905	-0.3323
Eigenvalues 5	0.5865	7.3315	Sulphides		-0.1127	0.4257
Eigenvalues 6	0.2469	3.0856	Clay		0.3704	-0.4114
Eigenvalues 7	0.2193	2.7417	Other Mineral		0.3905	0.06021
Eigenvalues 8	0.03668	0.4585	Density	Site Database	-0.3554	0.3823

Table 4.2 Principal component analysis results. Eigenvalues show how much population variability is modelled by each PCA vector. The eigenvectors show the component contribution to the specified PCA vector 1 and 2.

A scatterplot of data in the field of principal components 1 and 2 (Figure 4.2) shows the major trends in the data in a simple two dimensional representation. It is important to note that this diagram does not indicate spatial distribution but rather, the compositional (mineralogical and density) distribution. Through a process of interactive examination of this diagram, an understanding of why data points plot in a particular region of the graph is obtained. The class boundaries were defined manually.

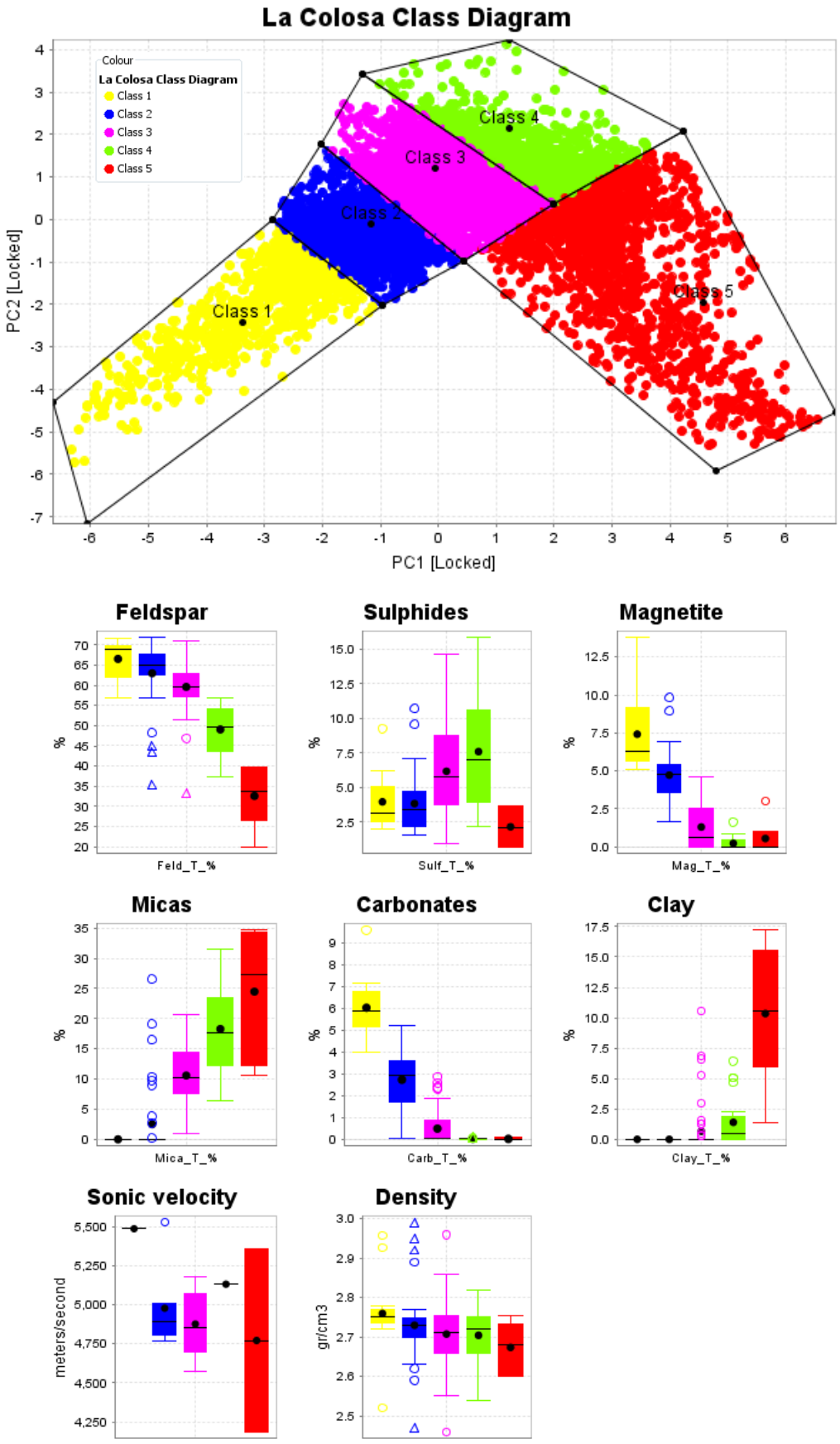

Figure 4.2 La Colosa sample variation in principle components 1 and 2. Compositional classes were defined based on the diagram to cover the range of compositions found. Box and whisker plots are shown for all 8 input variables included in the analysis and coloured by class.

The contribution of each input variable to the principal components is shown in the eigenvector columns of Table 4.2. For principle component 1 (eigenvector 1), mica, clay and other mineral are positive while feldspar, carbonate and density are negative For principal component 2, sulphide and density are strongly positive (increasing to right on Fig 4.2) and magnetite, carbonate and clay are negative. The class boundaries were constructed manually around clusters of high data point densities. The 5 defined classes contain discrete hardness, density and mineralogy characteristics, which can be seen in the box and whisker plots of Figure 4.2. For example class 5 is high in clay and mica. Class 1 is high in carbonate and magnetite. Assessing the mineralogical variability discrimination diagram in this way allows mineralogy to be associated with different regions of the graph, which is critical to obtaining a geometallurgical understanding of the sample set. The mineralogical trends associated with this diagram are shown in in figures 4.3 to 4.6. The regression equations used to predict comminution parameters across the deposit were calculated for each of these classes separately.

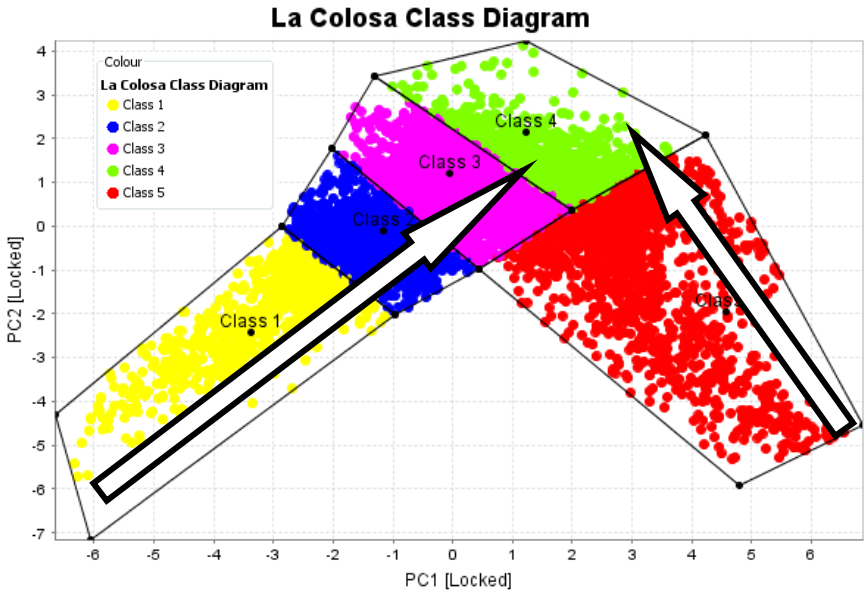

Figure 4.3 La Colosa class diagram, showing sulphide trend. Classes 1 and 2 are low in sulphide which increases through class 3 to class 4. There is very little sulphide in class 5. (See Figure 4.2 for supporting detail.)

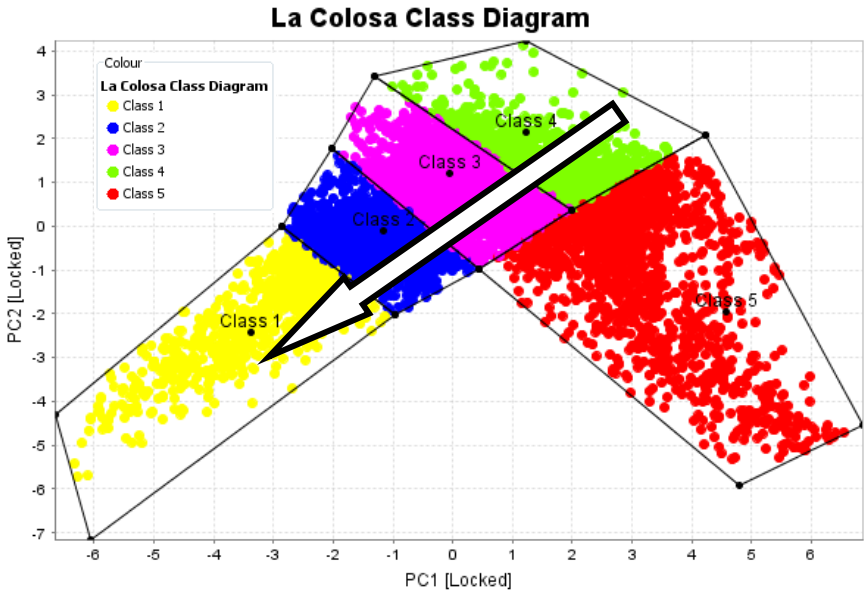

Figure 4.4 La Colosa class diagram showing direction of increasing magnetite and density across the classes.

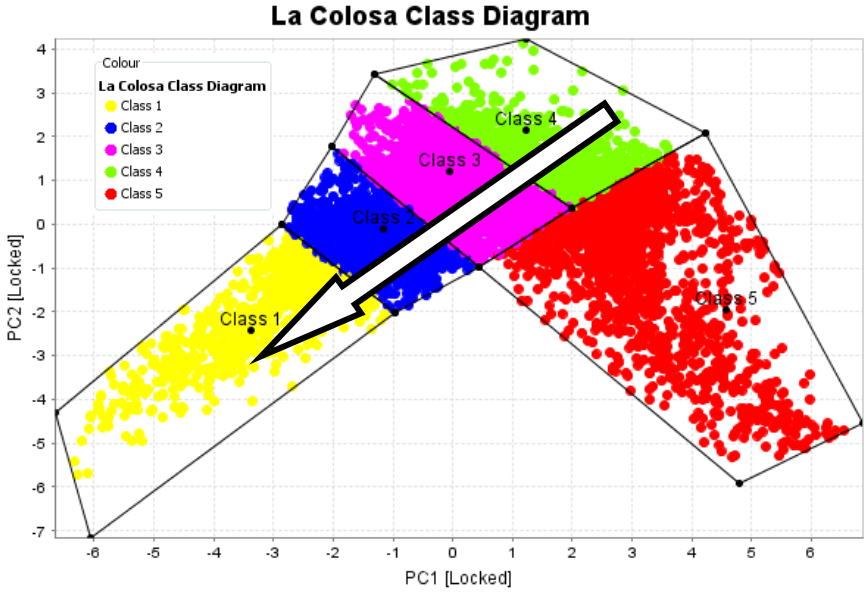

Figure 4.5 La Colosa class diagram showing direction of increasing carbonate across the diagram.

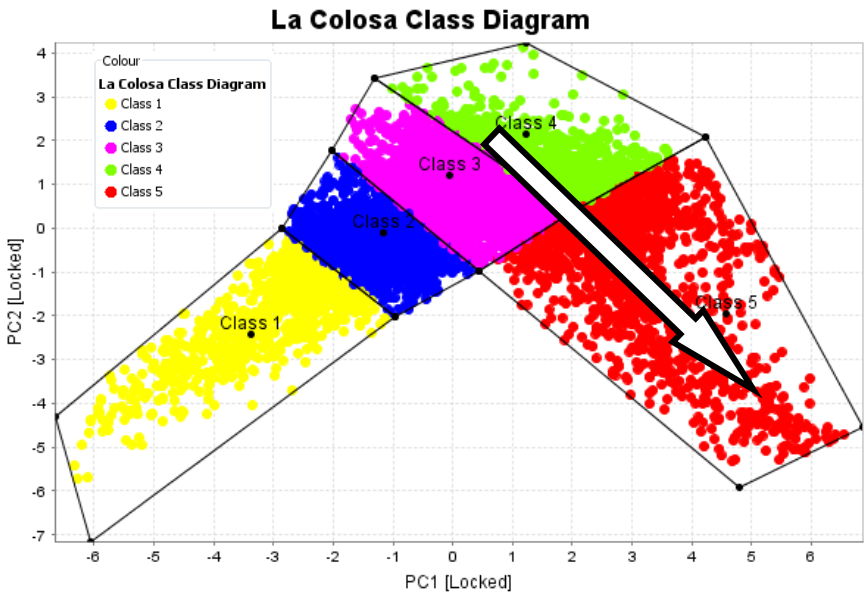

Figure 4.6 La Colosa class diagram showing direction of increasing micas and clay across the diagram.

4.3 Predictive Modelling

Mineral processing data currently available for comminution modelling consists of the comminution parameters A*b and BMWi. The samples for which this data are available were plotted within the polygons on the principal component analysis diagram to identify the class of each sample. Multiple linear regression models were created using ioGas® for each class shown in Figure 4.3 using inputs such us mineralogy, EQUOtip hardness, velocity and density. Figure 4.7 shows BMWi and A*b estimation results class by class. Classes 1 and 5 have only a small number of BMWi and A*b test values. As a result these regression equations need to be improved by obtaining more samples for these classes in order to map the real variability. Figure 4.8 shows the relative error for all the calibration samples (number of BMWi test values = 149, number of A*b test values = 136).

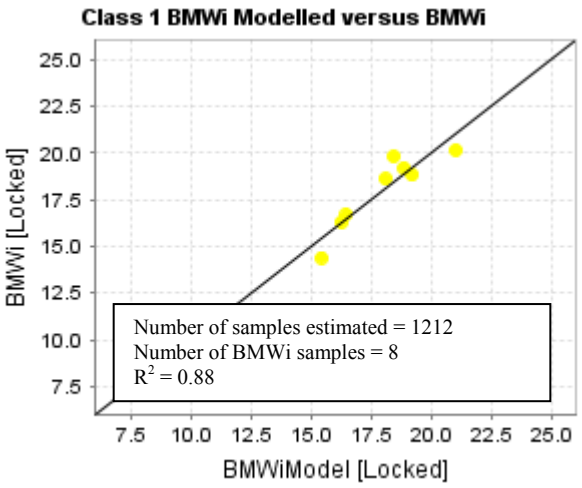

BMWi = 14.174 density + 0.729 * EQUOtip + 0.2176*

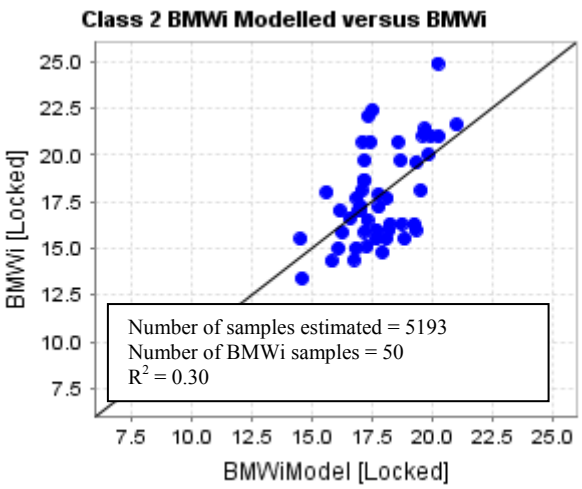

*BMWi = 16.817 * density + 0.05026 * EQUOtip stdv + 0.02743 * EQUOtip 20th - 51*

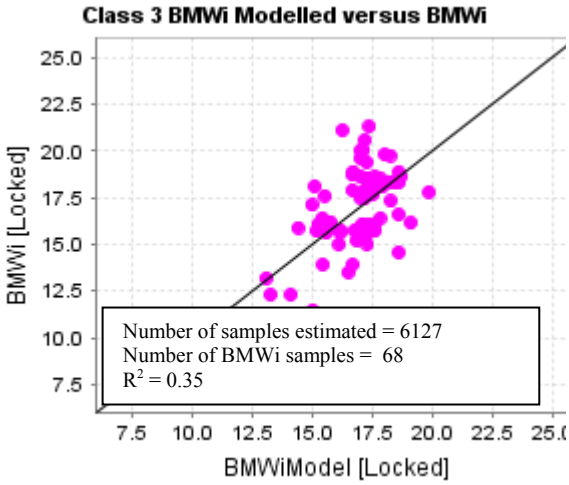

*BMWi = 0.02037 * EQUOtip + 140.2 * carbonate + 24.85 * sulphur*

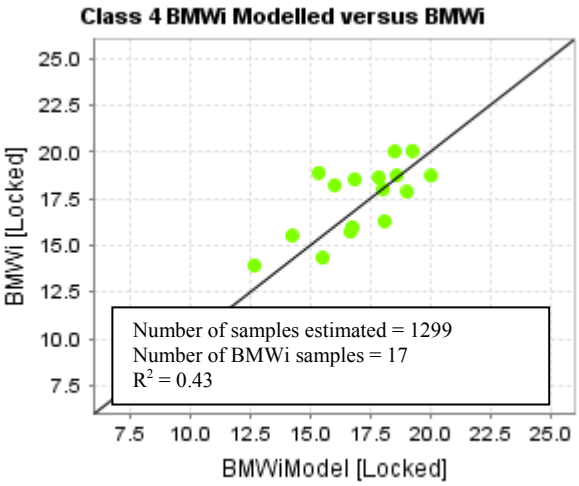

*BMWi = 25.89 * feldspar + 25.35 * micas*

Figure 4.7 continues on the next page

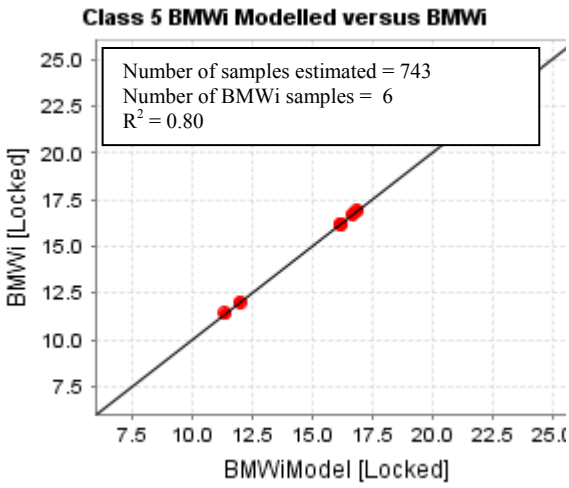

*BMWi = - 50.44 * density + 0.02459 * EQUOtip + 133.2*

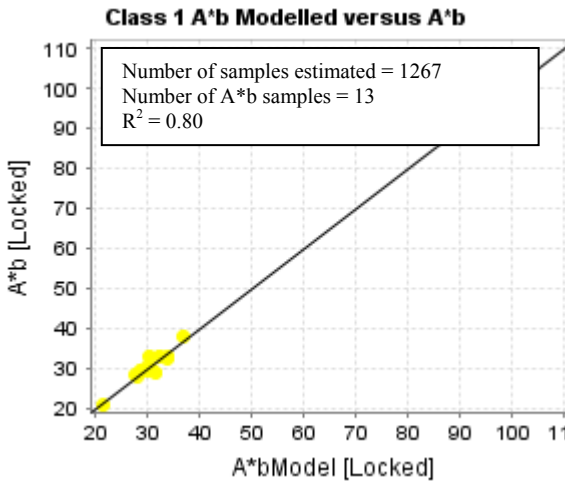

*A*b = -189.1 * carbonate + 118.3 * sulphur + 37.1*

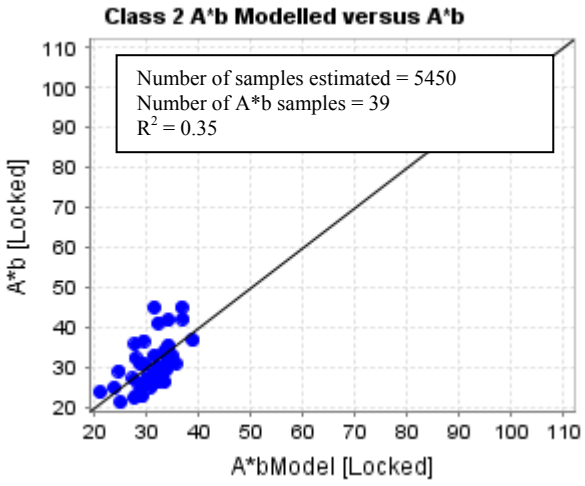

*A*b = 15.32 * density - 0.03326 * EQUOtip + 36.6 * feldspar -154.6 * magnetite*

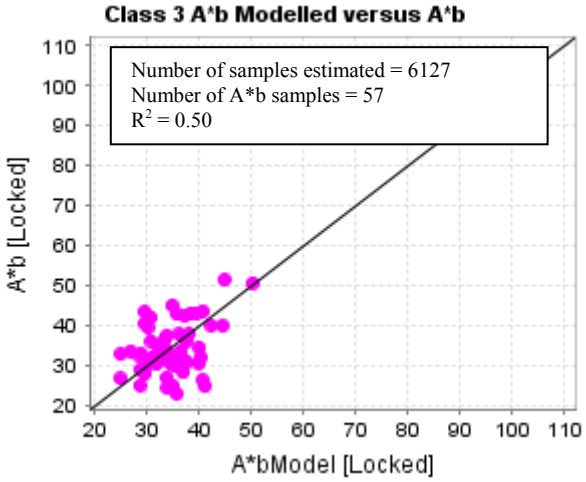

*A*b = - 30.75 * density + 0.1 * EQUOtip 50th +197.3*

Figure 4.7 Continues on the next page

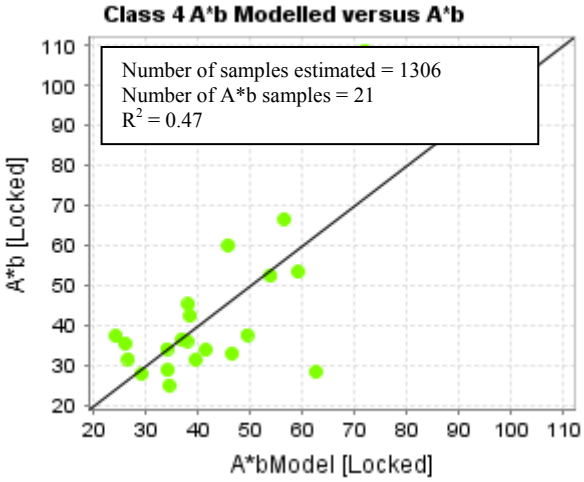

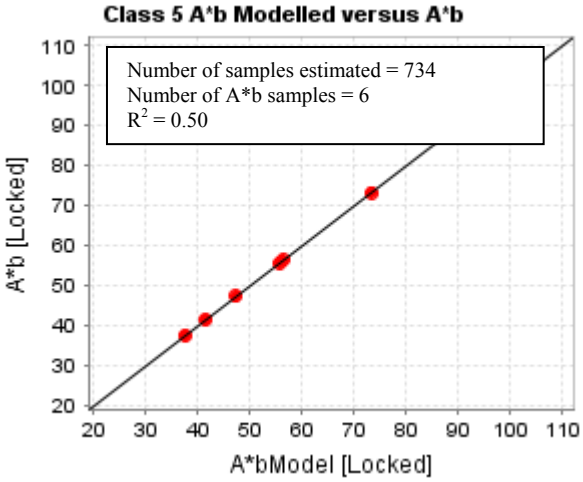

*A*b = 0.1987 * EQUOtip + 563.2 * Clay - 122.38*

*A*b = 262.6 * density + 0.763 * EQUOtip - 320.29*

Figure 4.7 Results of class-based multiple linear regression models for BMWi and A*b. The samples in each class for which A*b and BMWi have been measured were used to build a regression equation. The calculated equations are shown for each class along with a plot of the measured value against the estimated value.

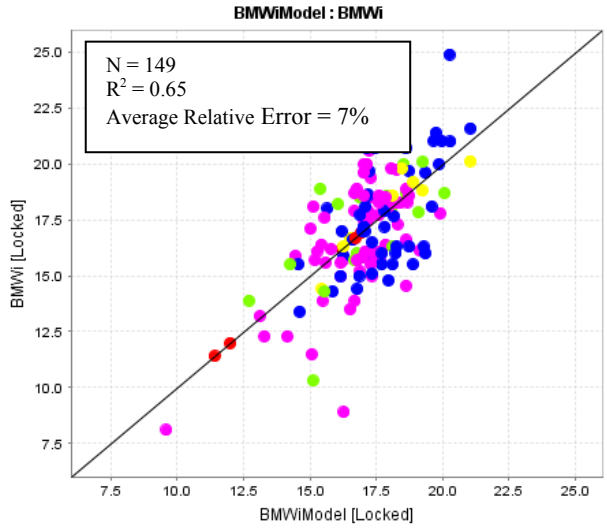

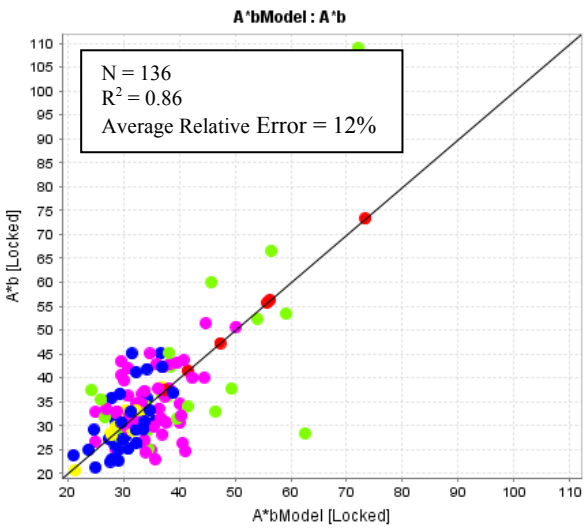

Figure 4.8 Estimated BMWi (BMWi Model and A*b Model) plotted against measured BMWi and A*b values. Colours represent different classes as in Figure 4.2. The quoted relative error provides a first order estimate of the likely precision of the prediction generally.

Using the predictive models created, each assay interval in the La Colosa database was assigned estimated A*b (14259) and BMWi (14461) values (e.g. Figure 4.9, 4.10). This dataset was then used to evaluate the global response and undertake population modelling. Results indicate that La Colosa contains a unimodal variation in both crushing and grinding response. There was no obvious separation into discrete clusters of significantly different comminution performance (Figure 4.10). However this may reflect the low resolution associated with the errors in the predictive equations. Also with this very large data set there may be a large number of modes that cannot be resolved without adding the spatial modelling to this analysis.

At La Colosa, the initial modelling suggests that within the deposit A*b is in the range of 20 to 60 and BMWi is in the range of 12 to 23 kWh/t. It is important to note that the comminution footprint does not provide a spatial representation of comminution variability, but rather a signature of inherent variability. It is important to convert this information into a spatial representation to investigate the spatial distribution and variability of comminution indices (see Chapter 5).

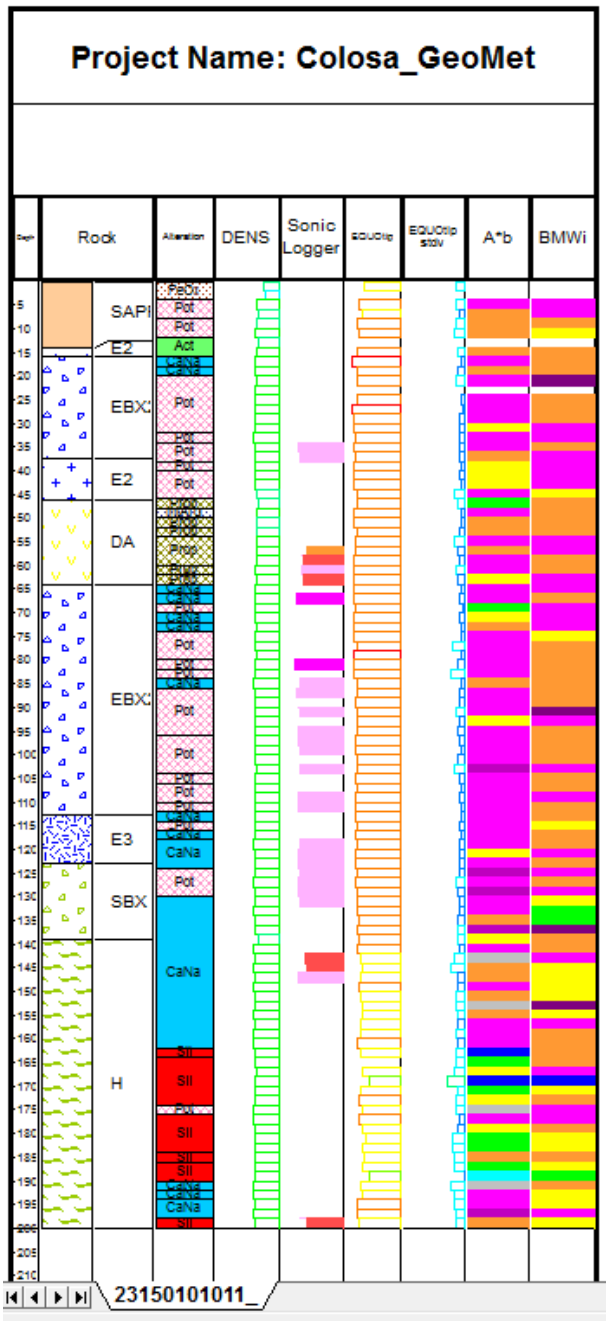

Figure 4.9 An example of BMWi and A*b estimated for each assay interval in drill hole 11. Colours for BMWi and A*b match colours for classes as in figure 4.2

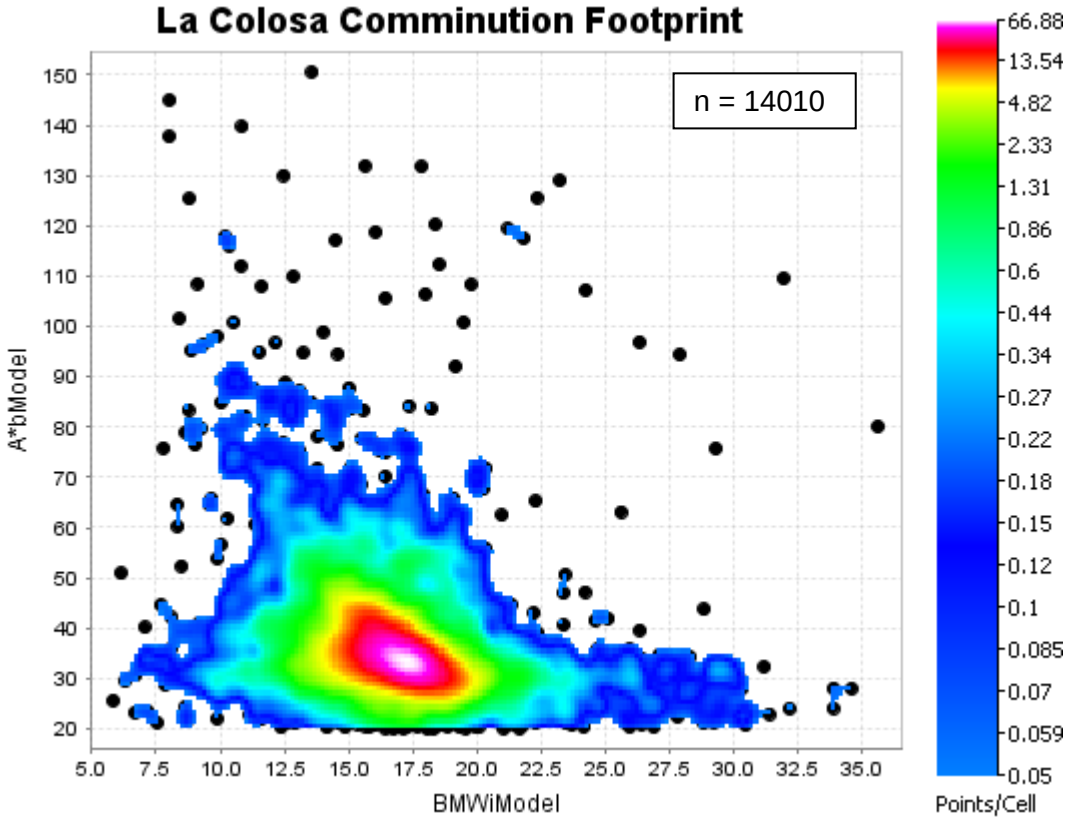

Figure 4.10 Data density plot drawn in ioGas® showing the predicted A*b and BMWi for the 14010 samples in the database of this study.

Chapter 5: Spatial Analysis

5 Introduction

The application of spatial analysis to constrain the estimation of grade is a well-established and essential process in ore reserve modelling. Defining the geometallurgical domains for an ore deposit is an equally important process in developing a fully attributed geometallurgical block model. It should be noted that ore domains and geometallurgical domains are normally not directly related (Bye and Newton, 2009).

Traditional approaches have focussed on using the geology or grade to define 'ore types'. This is an important step but depending on the complexity of the deposit, it may not always capture the process performance of the ore types in terms of comminution and throughput.

In this study for the La Colosa deposit a mineralogy model (non-spatial) has been derived from Principal Components Analysis (PCA) and linear regression techniques (Chapter 4). In this chapter spatial modelling is carried out using Leapfrog® interpolations, which is related to the mineralogy model.

5.1 Domains

The goal of domaining is to propagate geometallurgical characteristics into large volumes. In the previous example, each assay interval was assigned comminution parameters using the class-based models as displayed in the comminution footprints (Figure 4.6). While the number of estimated results (~14000) was high, it is still small compared to the La Colosa deposit size so all the models must be considered provisional.

In order to understand the comminution variability of the deposit, variograms of the calculated A*b and BMWi were developed. These variograms provide information required to map the inherent comminution response and variability across the La Colosa deposit.

5.1.1 Descriptive Statistics

Before calculating a variogram, descriptive statistical analyses should be done in order to identify data set issues and multiple populations. Descriptive statistics include calculated means, ranges, standard deviations, coefficients of variation and the creation of cumulative

frequency distribution plots and histograms of data as necessary to gain an understanding of the nature of the data.

For example, a histogram of calculated BMWi values for La Colosa shows approximately Gaussian behaviour which means that the variography process will not have problems with outliers values (Figure 5.1). On the other hand a histogram of calculated A*b values shows a skewed distribution (Figure 5.2). This means that the variography process could have problems with outliers. Therefore outlier values should be masked before developing the variogram. This is a common feature of A*b distributions. Other possible options are to log transform A*b or use 1/A*b for the modelling. For simplicity, outliers were masked in this example.

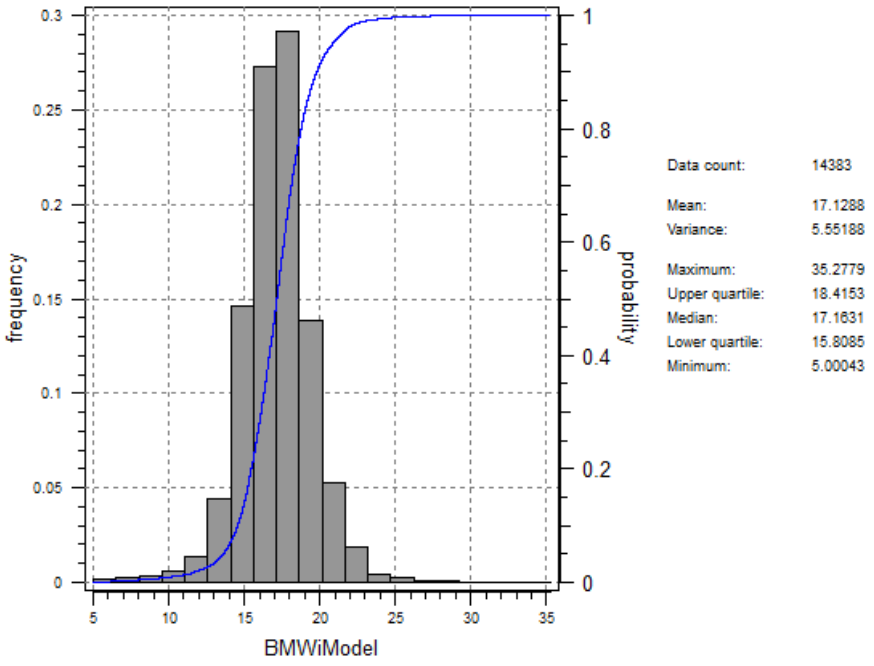

Figure 5.1 Histogram of La Colosa BMWi values

.

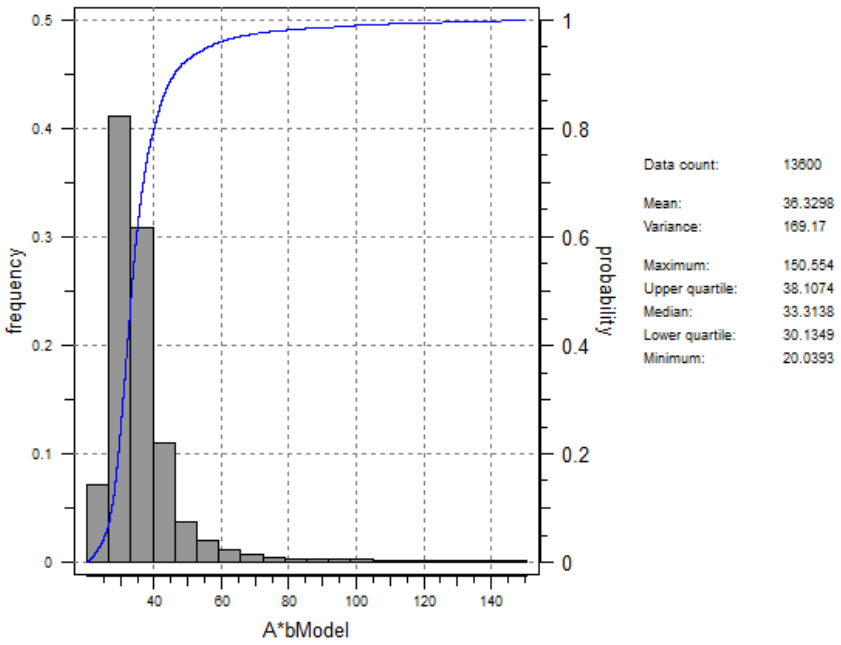

Figure 5.2 Histogram of La Colosa A*b values.

5.1.2 Experimental Variograms

The geostatistical analysis presented in this section firstly describes how the spatial correlation of the A*b and BMWi index are characterised through the fitting of a variogram model, and secondly, describes the use of the spherical model which provides a means of deriving the distribution of comminution parameters from the available support.

An important first step of a variogram analysis is to model and review the omnidirectional variogram to infer the sill of the anisotropic variograms (Isaaks and Srivastava, 1989). The total sill of an omnidirectional variogram provides an approximation of the total sill of specific directional variograms. The total sill of the directional variogram should be less than or equal to the sample (population) variance (V).

Variogram (semi-variance) values above the global variance (V) were not included in the variogram model. The slope at the beginning of the variogram model (at $0 < h < R$) represents the structural part of the variogram (Figure 5.3). The tangent drawn to this part of the variogram meets the sill at approximately 95 percent of the range. This property is helpful in estimating the range from the first few experimental-variogram points at the beginning of the process of variogram analysis.

The nugget-effect represents the randomness of the variables at $h \rightarrow 0$, which is a characteristic of the variable, hence should remain constant in all directions. A nugget-effect for a variable

can be calculated by using the omnidirectional variogram. The nugget-effect can preferably be calculated by modelling down-the-hole variograms. This normally provides the closest pairs for interpretations close to the zero distance. (Figure 5.3)

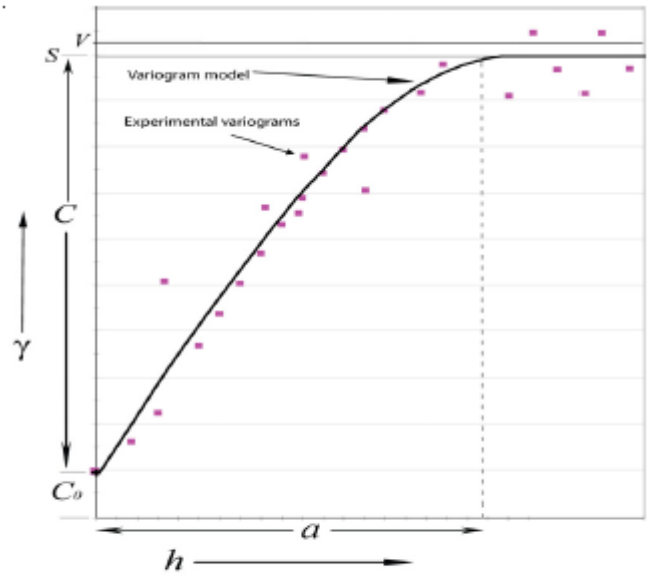

$$\gamma = C_0 + C^* \left(1.5 * \left(\frac{h}{a}\right) - 0.5 * \left(\frac{h}{a}\right)^3\right)$$

Figure 5.3 Spherical variogram model fitted to the experimental variograms points. C_o is nugget effect, V is variance, "a" is the variogram range, S is called sill (C_0 + C), γ is the model variogram, h is sample distance. (Isaaks and Srivastava, 1989).

In the second step, variogram maps were developed to search for evidence of anisotropy using the estimated A*b and BMWi values in the La Colosa data. The principle is to define a set of regular directions in space for which there are sufficient samples to define the variogram. Experimental variograms are calculated for each direction. Figures 5.4 and 5.5 show the variogram calculation parameters for BMWi and A*b per plane respectively (UV = azimuth, VW = dip), where N is the number of directions to be calculated in the reference plane. The first direction coincides with the reference direction and the other directions are regularly rotated by an angle of 180/N (in other words, the size of each angular sector in the fan representation will equal 180/N degrees). The number of Lags is the minimum number of samples between drill holes. The Lag value is the average distance between drill holes in order to see a pattern. The tolerance on lags refers to the proportions between lags to be calculated. The tolerance of direction is the proportion by angle (e.g. 1 = 100%) and slice thickness.

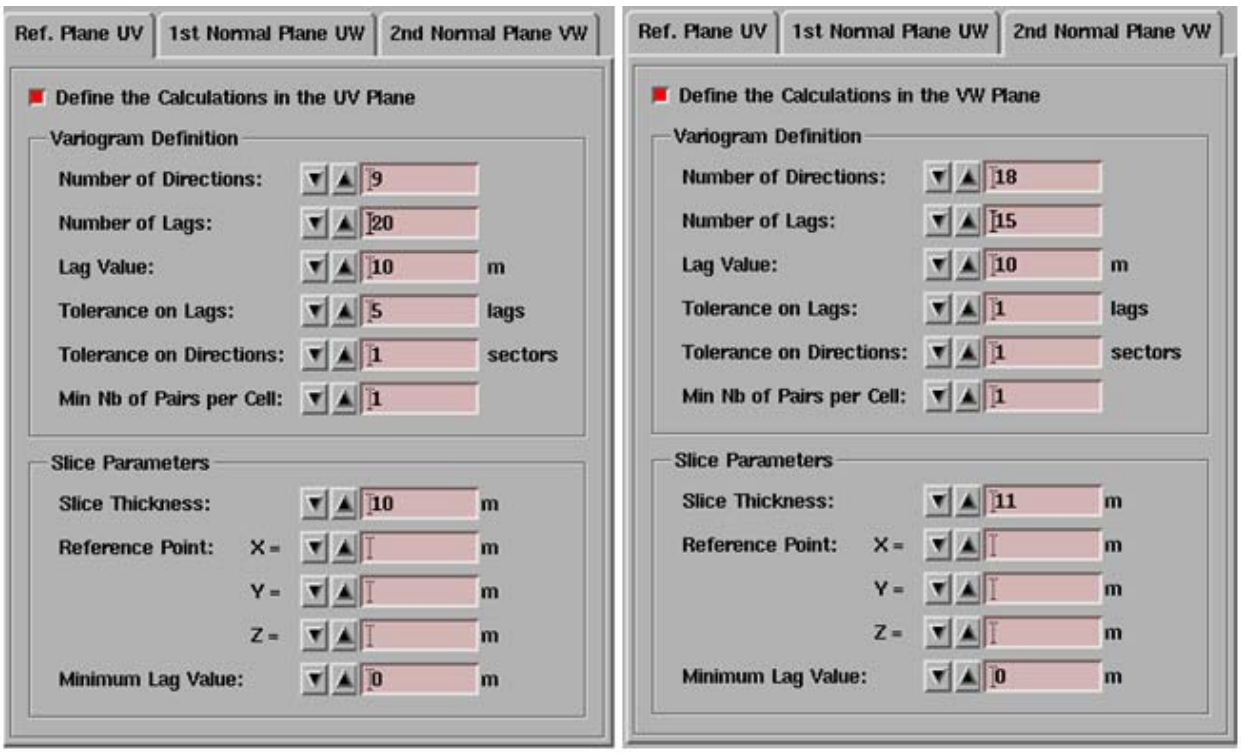

Figure 5.4 Anisotropy parameters per direction plane (azimuth, dip) for BMWi (Variography analysis was developed using ISATIS®)

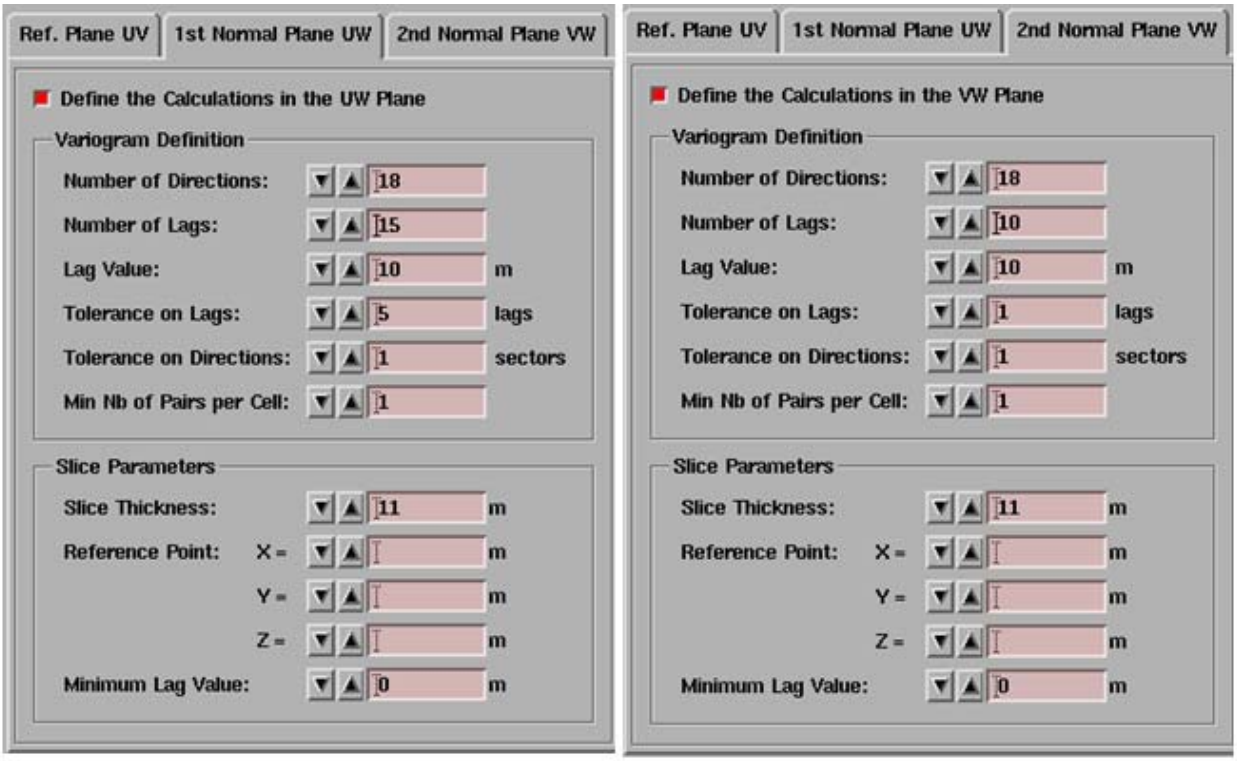

Figure 5.5 Anisotropy parameters per direction plane (azimuth, dip) for A*b (Variography analysis was developed using ISATIS®)

The variogram map is calculated on two orthogonal planes, UV = azimuth, VW = dip. The space is cut in slices of constant thickness per plane, the final variogram being the mean of all the calculated variabilities for each direction. Variograms can directly be selected from this variogram map in order to extract and display the corresponding experimental variogram. Variogram map colours represent the spatial continuity, cold colours mean high continuity and hot colours low continuity (Figure 5.6, 5.7)

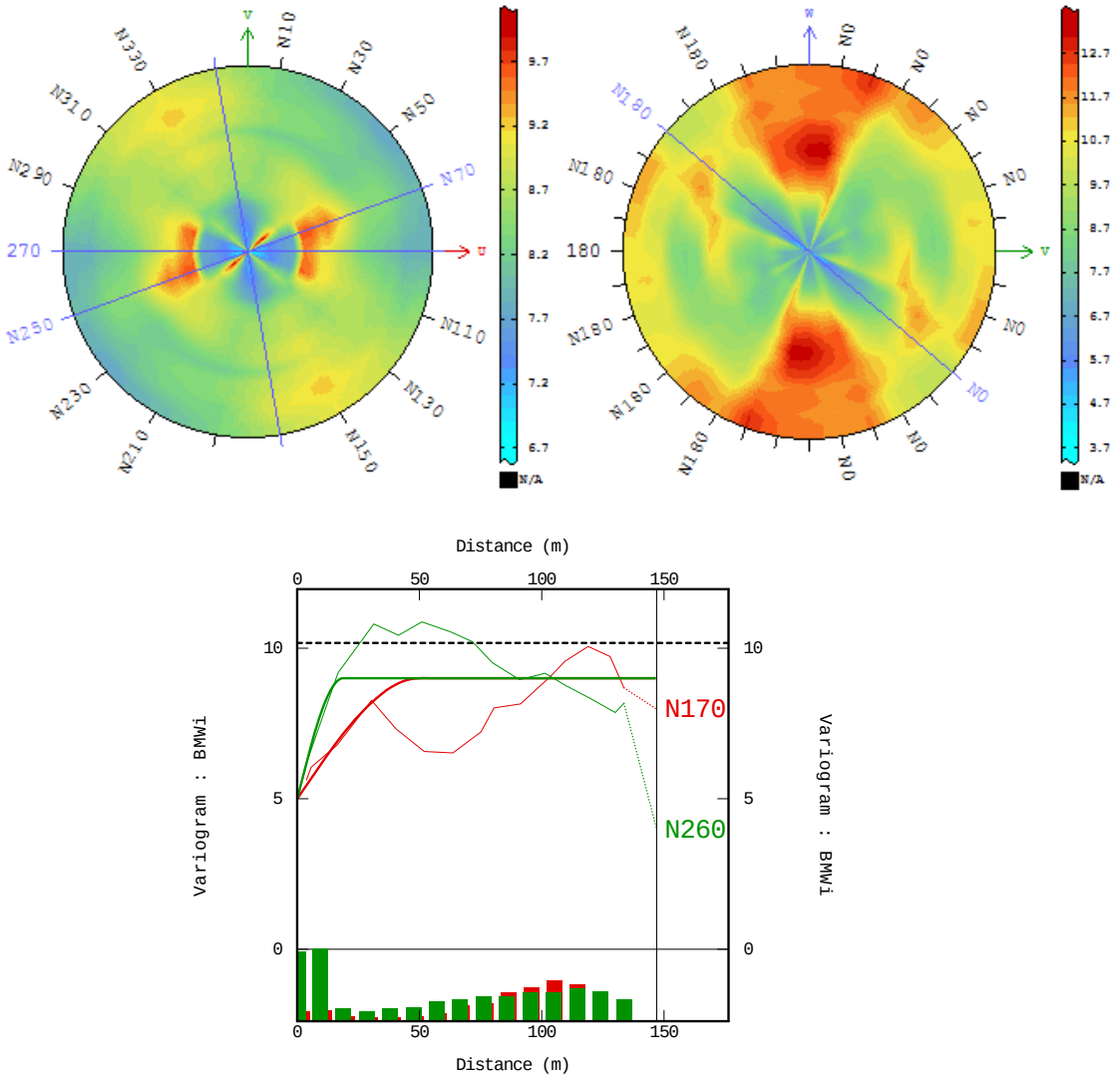

Figure 5.6 Variogram maps and experimental variogram for calculated BMWi values with azimuth top right and dip at top left.

Figure 5.6 shows two variogram maps, azimuth at right and dip at left with four variogram directions which represent the highest spatial continuity in the deposit for calculated BMWi. Azimuth plane showed three directions, N170, N250, N270, to demonstrate the variation. Dip plane showed the maximum continuity at 180/70. Azimuth N250 and N270 were ignored because

these directions are related to the drill hole direction. Therefore the BMWi spatial continuity is best represented by N170, dip 80/70.

Figure 5.7 displays two variogram maps for calculated A*b with azimuth at right and dip at left. As with the calculated BMWi, drill hole direction dominates in the anisotropy analysis, azimuth N260, dip 80/65. For that reason, this direction was not used as a modelling parameter. The anisotropy maps below also show a second direction, N170, dip 80/70 which represent the A*b anisotropy for La Colosa.

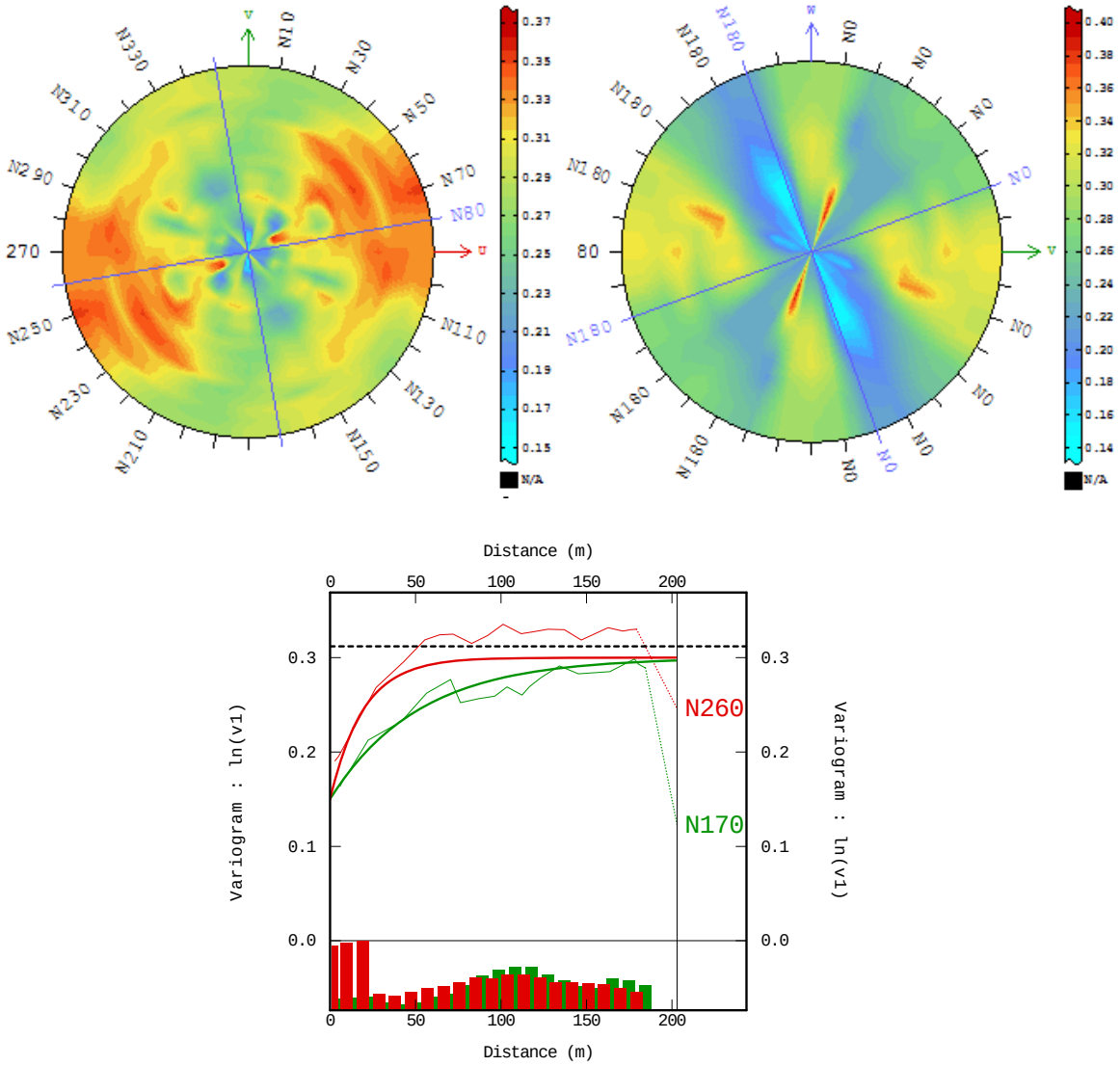

Figure 5.7 Variogram maps and experimental variogram for calculated A*b values with azimuth top right and dip at top left.

Figure 5.8 and 5.9 were developed to link the variography results in a geology context. The preferred variogram direction is closely related to fault corridors. Variography analysis showed that BMWi and A*b trend values (e.g. BMWi < 15 and A*b > 60) follow these fault zones (overall comminution preference direction N350/65E and faults corridors NS/70E).

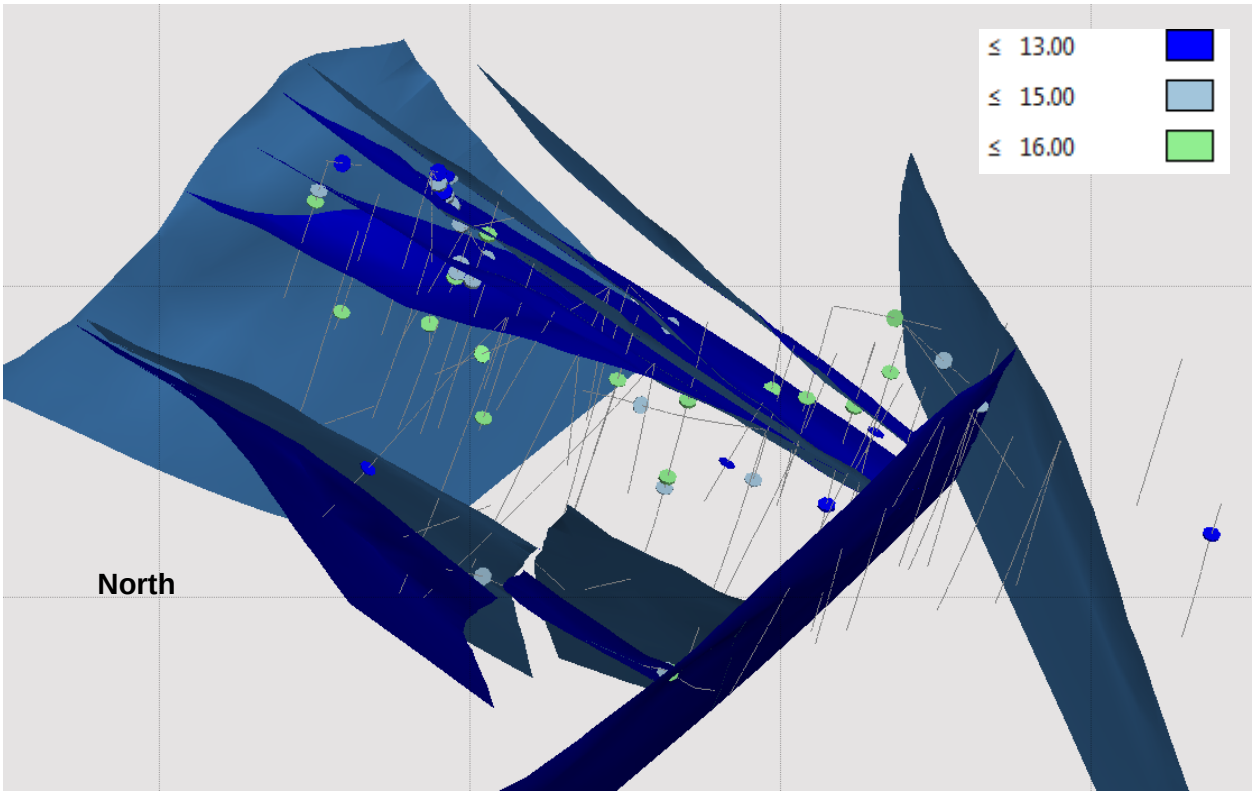

Figure 5.8 Fault corridors and BMWi < 15 values

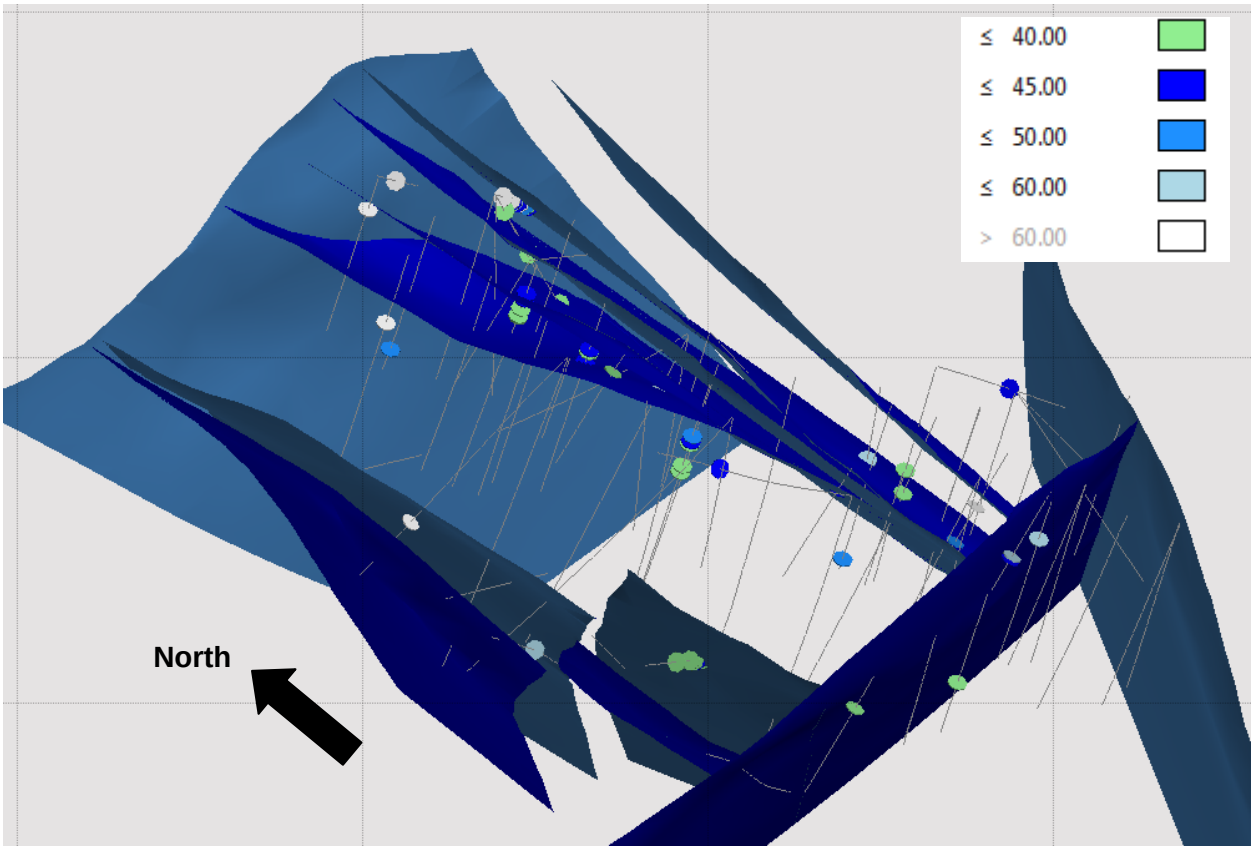

Figure 5.9 Fault corridors and A*b > 35 values

The variography analyses clearly show two preference directions which can distinguish zones of different hardness. The results from this analysis indicate that La Colosa has close relationships between comminution behaviour and faults. The zones of weakening generally are related to fault - contact zones or areas near to the surface indicating that the hardness variability is possibly being controlled by a structural or stratigraphic feature in the rock.

Once the anisotropy direction has been established, variogram results can be used to model the comminution parameters in a 3D space.

5.2 Wireframes

The traditional approach to modelling geological domains is drawing sectional interpretations of geological units connecting drill hole attributes from section to section to form a closed wireframe volume of the domain, resulting in an over smoothed subjective interpretation (Sinclair and Blackwell, 2002).

At La Colosa the spatial patterns of the calculated A*b and BMWi domains were estimated based on variography behaviour and structural controls. In order to map comminution variability into the La Colosa deposit seven A*b and BMWi wireframes domains were developed using isocurves techniques, variograms and structural controls. Table 5.1 show the La Colosa comminution domains developed in this study to differentiate different hardness ranges into the deposit.

Domain	A*b		BMWi	
	Range		Range	
1	Very Soft Crush	>127	Very Soft Grinding	< 10
2	Soft Crush	(67 - 127]	Soft Crush Grinding	(12 - 10]
3	Moderate Soft Crush	(56 - 67]	Moderate Soft Grinding	(14 - 12]
4	Medium Crush	(43 - 56]	Medium Grinding	(16 - 14]
5	Moderate hard Crush	(38 - 43]	Moderate hard Grinding	(18 - 16]
6	Hard Crush	(30 - 38]	Hard Grinding	(20 - 18]
7	Very hard Crush	< 30	Very hard Grinding	> 20

Table 5.1 La Colosa A*b and BMWi (kWh/t) domains

Seven A*b and BMWi wireframes domains were made following the same directions as those of the variograms and structural control. The soft and moderately soft crush boundaries are highly correlated with the logged saprolite zone and are controlled by fault corridors. In general, the crush hardness (i.e. 1/A*b) increases from east to west (Figure 5.10), from early diorites to intramineral diorites and hornfels, and from surface to depth. The same behaviour is shown by BMWi, which means, the grinding hardness also increases from east to west, except where soft areas are controlled by fault corridors. For BMWi most of the deposit is in the moderately hard grind envelope. The spatial locations of domains 1 to 7 are shown in Figure 5.11

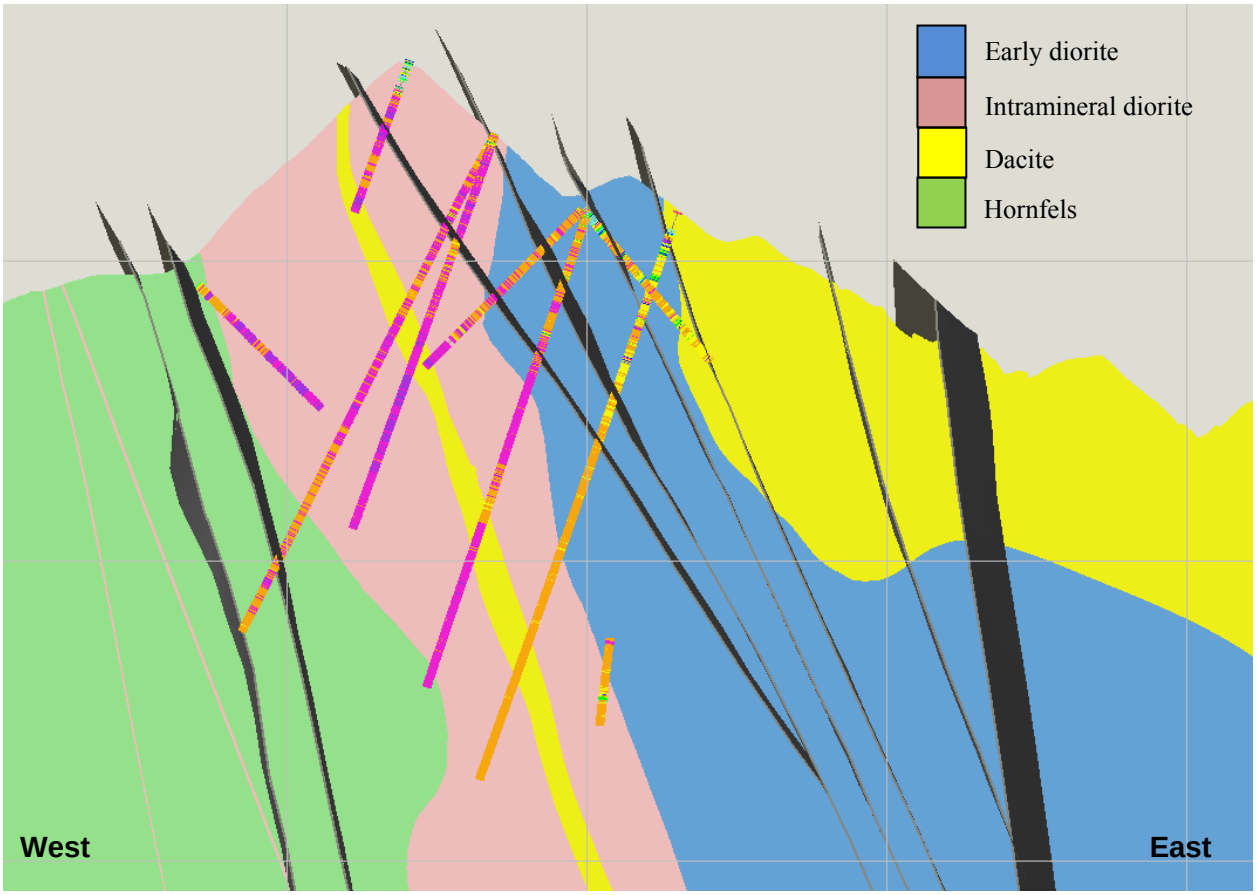

Figure 5.10 West- East section 4120N of BMWi estimated values. Drill hole colours match those shown in Table 5.1. (Section drawn using Leapfrog®)

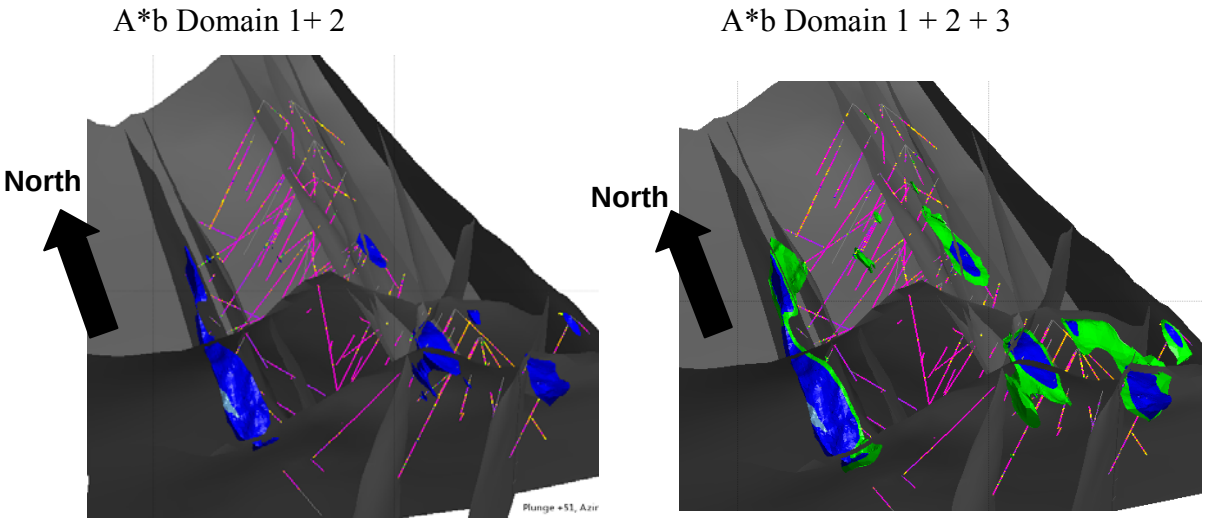

A*b Domain 1 + 2 + 3 + 4

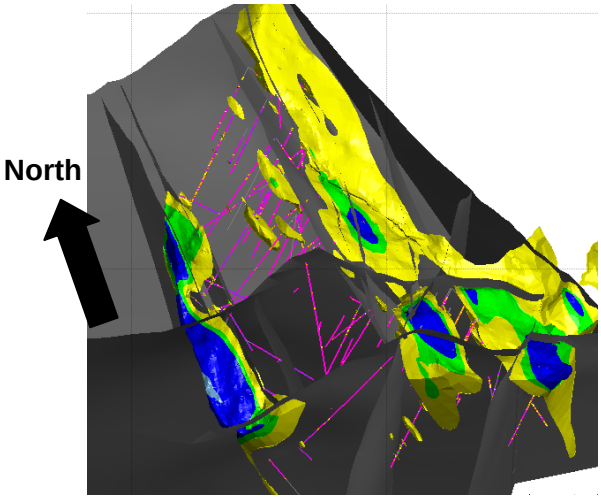

A*b Domain 1 + 2 + 3 + 4 + 5

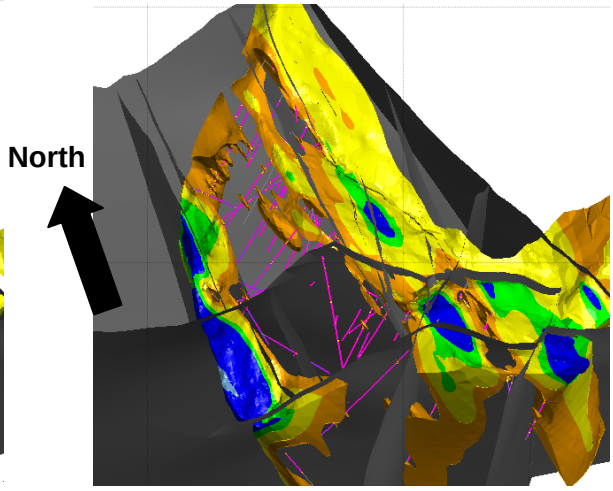

A*b Domain 1 + 2 + 3 + 4 + 5 + 6

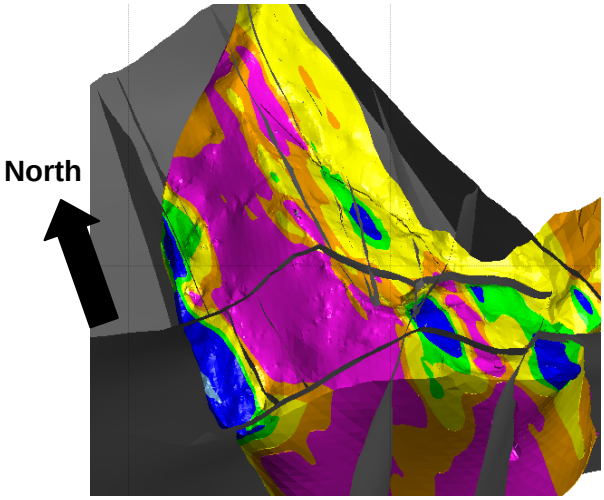

A*b Domain 1 + 2 + 3 + 4 + 5 + 6 + 7

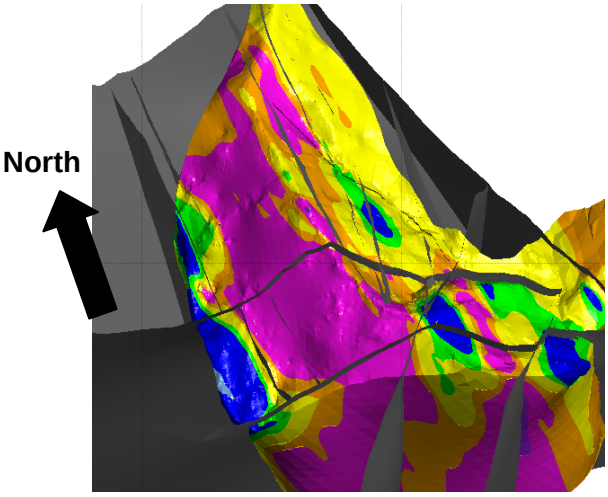

BMWi Domain 1 + 2 + 3

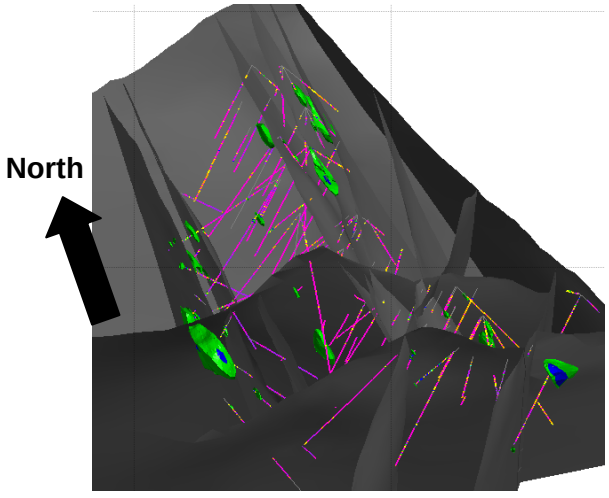

BMWi Domain 1 + 2 + 3 + 4

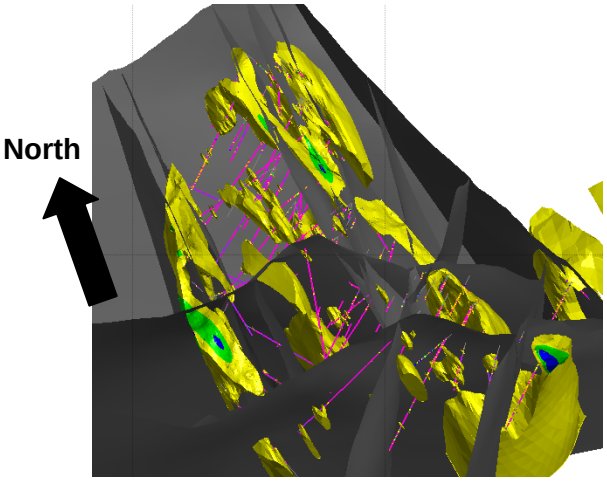

BMWi Domain 1 + 2 + 3 + 4 +5

BMWi Domain 1 + 2 + 3 + 4 + 5 + 6

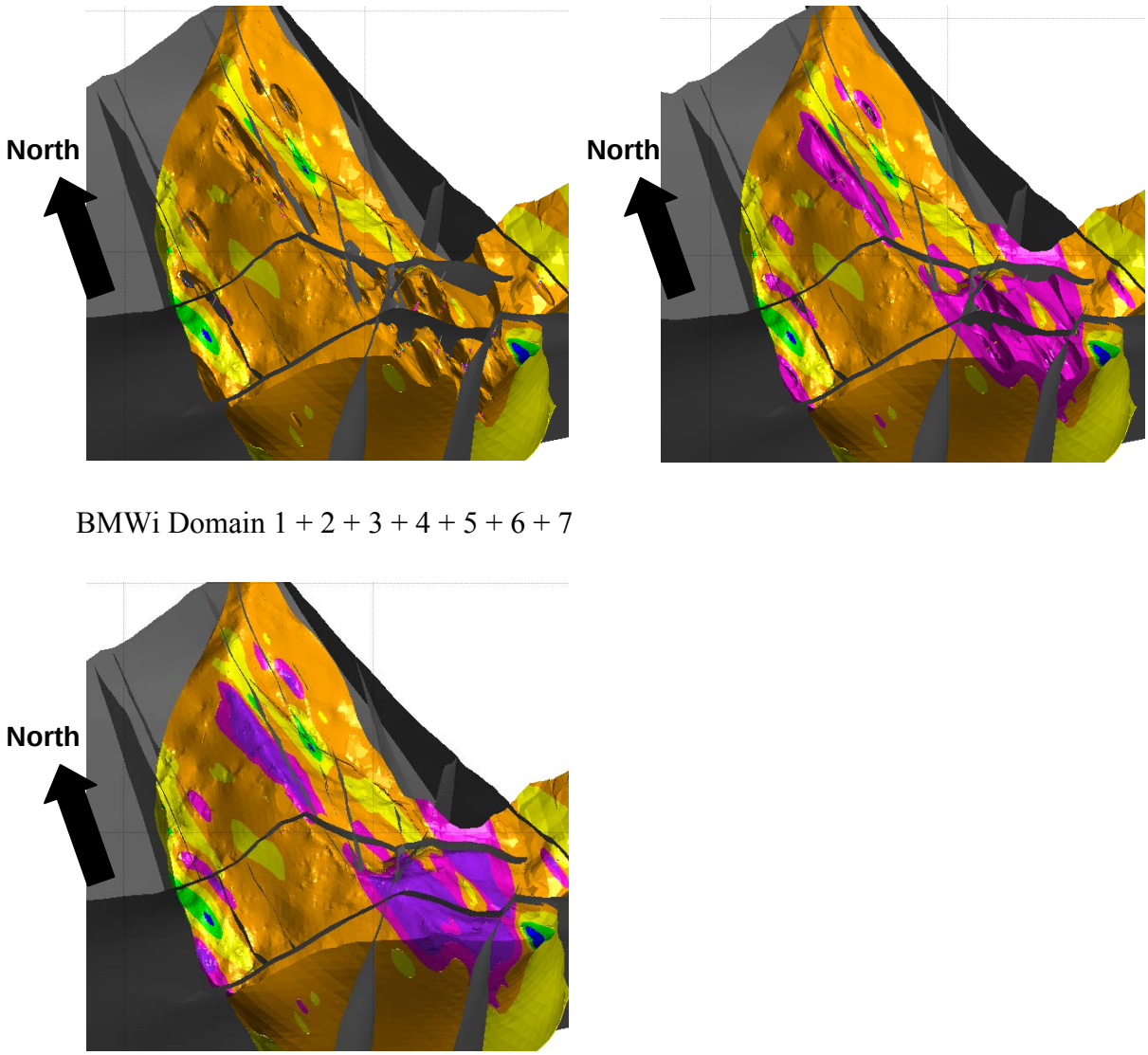

Figure 5.11 A*b and BMWi domain locations. Colours match those shown in Table 5.1. Volumes drawn using Leapfrog®.

5.2.1 Wireframes Validation

Validation is an essential step in order to provide confidence in each domain and show that it is well understood. The 3D models reflect the comminution variability of the La Colosa deposit. That means that each wireframe represents each comminution domain. In order to validate each domain the envelopes for each comminution variable were used with descriptive statistical techniques.

Table 5.2 shows the model confidence for a 3D geometallurgical model developed from 92 drill holes with a geometallurgy data set estimated from the calculated BMWi and A*b values. The mean values show that each wireframe covers the range present in each domain. The numbers

of samples indicate sufficient data to undertake an analysis of each envelope and the standard deviation indicates data dispersion in each domain.

FIELD	DOMAIN	RANGE	NSAMPLES	MINIMUM	MAXIMUM	MEAN	VARIANCE	STANDDEV	Variance Coefient
BMWi	1	<10)	1	8.01	8.01	8.01	0.00	0.00	0.00
BMWi	2	(12-10]	23	8.50	12.87	10.66	0.96	0.98	0.09
BMWi	3	(14-12]	191	6.13	18.88	12.70	4.59	2.14	0.36
BMWi	4	(16-14]	3166	5.83	29.58	15.17	2.53	1.59	0.17
BMWi	5	(18-16]	9411	6.67	33.91	16.96	2.01	1.42	0.12
BMWi	6	(20-18]	2166	7.10	34.78	18.81	5.42	2.33	0.29
BMWi	7	>20]	390	8.65	35.98	23.38	30.14	5.49	1.29

FIELD	DOMAIN	RANGE	NSAMPLES	MINIMUM	MAXIMUM	MEAN	VARIANCE	STANDDEV	Variance Coefient
Ab	1	>127	7	134.86	144.81	138.81	17.23	4.15	0.124
Ab	2	(67-127]	63	26.26	150.56	92.00	904.12	30.07	9.828
Ab	3	(56-67]	113	24.52	109.88	61.28	354.43	18.83	5.784
Ab	4	(43-56]	808	20.10	119.41	48.70	147.80	12.16	3.035
Ab	5	(38-43]	2221	20.12	80.61	39.95	35.62	5.97	0.892
Ab	6	(30-38]	10578	20.07	82.26	33.55	14.99	3.87	0.447
Ab	7	<30	1320	20.00	43.13	28.14	10.11	3.18	0.359

Table 5.2 Statistical analysis of BMWi and A*b geometallurgical domains for the La Colosa deposit.

5.3 Block Model

Block models offer a way of transferring the spatial model into the mining environment. They can carry information about hardness characteristics that support process models for mill throughput. Block models also provide the foundation for resource optimisation and mine planning activities.

Spatial block modelling for the domains developed in this study for La Colosa was done using the same block size that was used by site for the resource block model calculation (i.e. blocks 50 X 50 X 10 meters). A DATAMINE® application script was developed to fill each block with the mean value based on the wireframe domains (Table 5.2). Figures 5.12 and 5.13 show BMWi and A*b block models with fault corridors. The colours of each block are related to the Table 5.1 comminution domains.

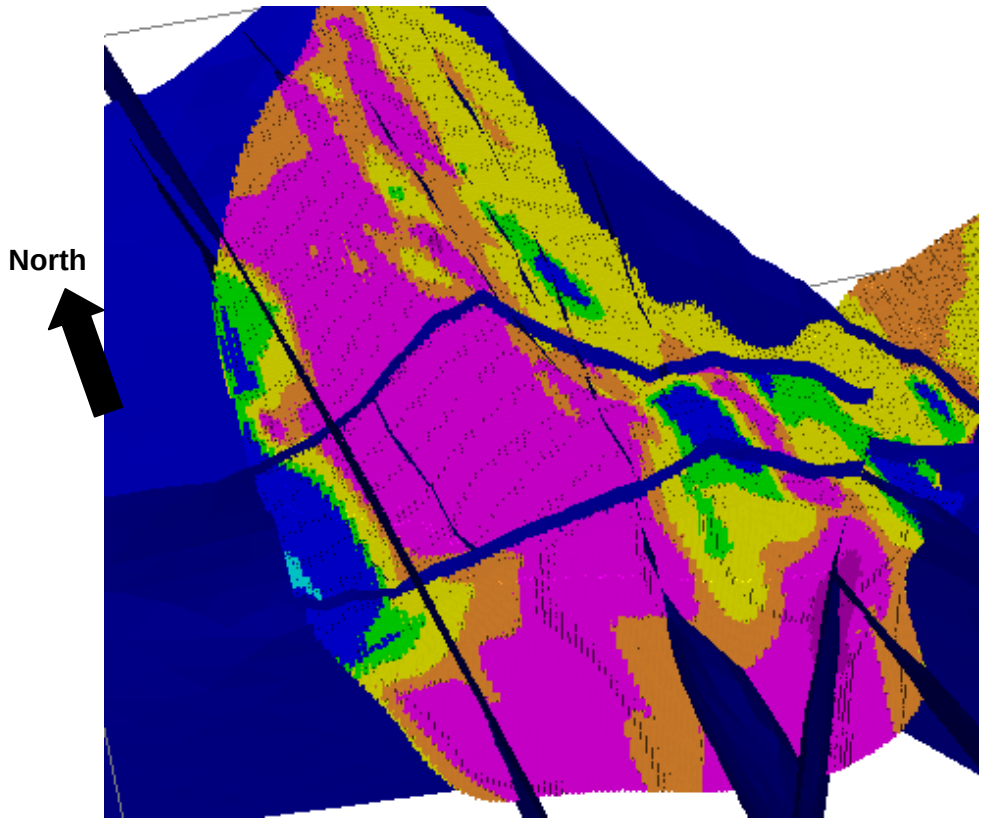

Figure 5.12 3D view of the block model showing A*b domains developed for the La Colosa deposit.

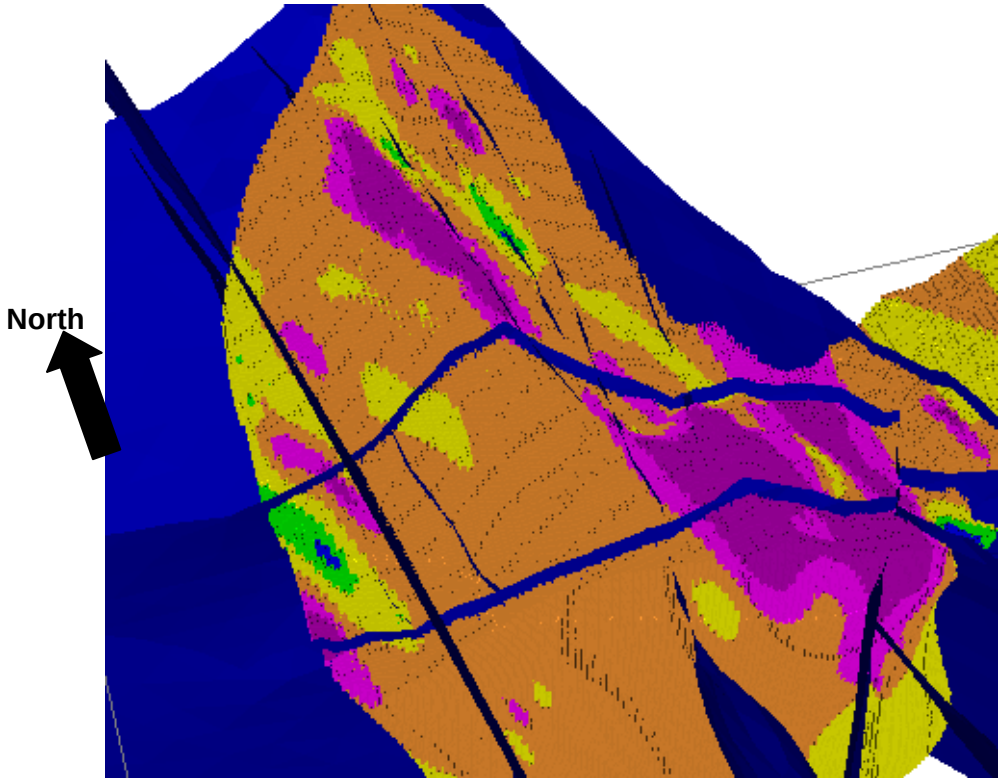

Figure 5.13 3D view of the block model showing BMWi domains developed for the La Colosa deposit.

Chapter 6: Research Conclusions

6 Introduction

The work developed in this thesis demonstrates the GeM method provides a good mechanism for mapping comminution variability at La Colosa, and provides a first pass geometallurgy prediction of key comminution parameters relevant to mine planning. This knowledge can be exploited in future mill design, mine planning and economic modelling of the resource as the project life cycle advances. Several factors are critical to achieving the results demonstrated in this thesis:

Data acquisition is one of the critical steps for any modelling process. Therefore, the development of measurement protocols is an indispensable requirement before starting to take routine measurements.

Secondly, there are different kinds of geological data that help to understand the geological behaviour. Logging data should be used in order to understand the overall lithology and alteration. Mineralogy estimated from assays and small scale physical tests (e.g. EQUOtip, sonic velocity, density) are indispensable parameters in order to estimate comminution indices.

Finally, 3D models offer a way of describing the spatial continuity which is an essential feature in order to estimate the spatial distribution of hardness characteristics. PCA, regression modelling and geostatistical techniques are useful tools in defining the spatial behaviour of variables.

6.1 Geometallurgy Results of La Colosa deposit

The aim of this geometallurgical study was to understand and map the inherent comminution variability across the La Colosa deposit. In order to find the answer to this aim this study followed the GeoMet methodology outlined in Keeney and Walters (2011).

The application of spatial domains to understand and map the variability across the La Colosa deposit shows that overall the rocks of La Colosa deposit are intermediate to hard in terms of crushing and grinding. The soft areas are related to structural corridors (trending 350),

weathering and the western contact between the intramineral diorites and hornfels. These conclusions provide critical information for mine/mill design and optimisation.

Chapter 7: Recommendations for Future Work

7 Introduction

This chapter provides recommendations for future work in three sections, the first focusing on recommendations for future work in specific areas of La Colosa, the second focusing on improving the geometallurgy methodology in order to obtain better models and the third involves integration of geometallurgical models at La Colosa (i.e. models for comminution, recovey and resources).

7.1 La Colosa Project

The La Colosa project area is subdivided into 6 different zones by structural controls. The focus of this research was zone 2 where the main porphyry gold deposit (La Colosa North) is located, therefore it is necessary to update the geometallurgy model so that it covers the whole of the La Colosa Start up pit.

7.2 Improving Geometallurgy Methodology

The following section presents some comments about how to improve the geometallurgy methodology of La Colosa in order to obtain more accurate models.

7.2.1 Data Collection and Geometallurgical Characterization

Incorporate new techniques and geological variables such as: spectral data, magnetic susceptibility values, texture analysis, veinlet density and point load testing so that geometallurgical characterization can produce more robust predictive models.

7.2.2 Class Based Analysis

In this study Principal Component Analysis was used in order to develop class based analysis. This technique takes into account the variability of the deposit in a non spatial way. But in order to improve classes it will be useful to try other kinds of statistical techniques such as Canonical Correlation Analysis (Hair et al, 1998). This technique is particularly useful in situations in which multiple output measures are available. Canonical correlation is considered to be the general model on which many other multivariate techniques are based because it can use both metric and nonmetric data for the dependent and/or independent variables.

7.2.3 Predictive Modelling

Results show two classes, 1 and 5, where predictive models were not reliable because of the small number of A*b and BMWi test values. As a result it is necessary to select more samples in these classes to obtain more robust estimations.

7.2.4 Domains, Wireframes and Block Modelling

There are many ways to develop domains, wireframes and block models. This thesis used methodology based on variograms in order to find the preference direction of A*b and BMWi. Then, based on these variograms and the isocurves technique, different domain envelopes were calculated. For future work it will be interesting to compare this technique with indicator krigging, 3D variogram maps and surface validation by Leapfrog® in order to find which methodology is more accurate.

7.3 Geometallurgy Model Integration

In order to understand orebody variability of the deposit it will be necessary to integrate comminution, recovery and resource models. This integration will likely give new domains that will be important for mine and mill design.

References

AngloGold Ashanti, 2011. Mineral resource and ore reserve report. Johannesburg, South Africa, 188 pp. (at www.aga-reports.com)

AngloGold Ashanti, 2009. Comminution samples. Ibague, Colombia, 10 pp. (Confidential report.)

AngloGold Ashanti, 2011. Comminution test work. Ibague, Colombia, 80 pp. (Confidential report)

Berry, R., Hunt, J. and McKnight, W., 2011. Estimating mineralogy in bulk samples. In Dominy SC (ed) First AusIMM International Geometallurgy Conference (GeoMet) 2011, 153-156.

Bye, A. and Newton, M., 2009 Integrated geometallurgy case studies – from core to cash flow. AMIRA P843 Geometallurgical Mapping and Mine Modelling. Technical Report 3, 24.1-24.18, Brisbane, Australia.

Bond F.C., 1952. The third theory of comminution. Trans SME/AIME, v. 193,

Bond, F. C., 1961. Crushing and Grinding Calculations, part 1. British Chemical Engineering, v.6, no. 6, pp.378-385.

Clark, A.H. and Arancibia, O.N., 1995. Occurrence, paragenesis and implications of magnetite-rich alteration-mineralization in calc-alkaline porphyry copper deposits: Kingston, QminExAssociates and Queen's University, Giant Ore Deposits. II. Giant Ore Deposits Workshop, 2nd, Kingston, Ontario, Canada.

Dagbert, M. and Bennett, C., 2006. Domaining for geomet modelling: a statistical/geostatistical approach. University of British Columbia Vancouver, B. C., Canada

Dobby, G., Bennett, C., Bulled, D. and Kosick, G., 2006. Geometallurgical Modeling The New Approach To Plant Design and Production Forecasting/Planning, and Mine/Mill Optimization, in SGS Minerals Services Metallurgical Expertise: A Collection of Technical Papers 1990-2006.

Dunham, S. and Vann J., 2007. Geometallurgy, geostatistics and project value — Does your block model tell You what you need to know?. Project Evaluation Conference, Melbourne, Australia.

Gustafson, L.B. and Hunt, J.P., 1975. The porphyry copper deposit at El Salvador, Chile: Economic Geology, v. 70, p. 857−912.

Hacker, B. R., and G. A. Abers, 2004. Subduction Factory 3: An Excel worksheet and macro for calculating the densities, seismic wave speeds, and H2O contents of minerals and rocks at pressure and temperature, Geochem. Geophys. Geosyst., 5, Q01005, doi:10.1029/2003GC000614.

Hair, J., Black, W., Tatham R.L. and Anderson R., 1998. Multivariate Data Analysis. 5th edition, Prentice Hall, New York 730 pp.

Hunt, J. (ed.), 2008. AMIRA P843 Geometallurgical Mapping and Mine Modelling. Technical Report 1.0, Australia, pp. 336.

IC Consulten, 2011. Structural geological study (PFS) - final report. Ibague, Colombia (Confidential report)

Isaaks, E. and Srivastava, R., 1989. An Introduction to applied geostatistics. OXFORD University press, New York, 561 pp.

Jahoda, R., 2012. La Colosa mineral resources report. Ibague, Colombia (Confidential report.)

Keeney, L., 2010. The Development of a Novel Method for Integrating Geometallurgical Mapping and Orebody Modelling. Unpubl. PhD thesis, JKMRC University of Queensland, Brisbane, Australia, 309 pp.

Keeney, L. and Walters S., 2011. Geometallurgical mapping and modelling of comminution performance at the Cadia East Porphyry Deposit. Ist International Geometallurgy Conference, Brisbane, Australia.

Kojovic, T., 2008. Overview of comminution tests for ore characterisation. AMIRA GeM Technical Report 1, 13.1-13.16, Australia.

Kojovic, T., 2007, JKMRC Rotary breakage tester. Operation, maintenance and parts manual, Section 9: Testing Procedure. Brisbane, Australia.

Lodder, C., et al. 2010. Discovery History of the La Colosa Gold Porphyry Deposit, Cajamarca, Colombia. Society of Economic Geologists, Inc. Special Publication 15, pp. 19–28.

Mavko G., Mukerji T. and Dvorkin J. 2009. The rock physics handbook: tools for seismic analysis of porous media: 2nd edition. Cambridge University Press, 511 pp.

Michaux, S. 2005. Mine to Mill: Technical Summary and Procedures. JKMRC Internal Report.

Michaux, S., 2006. Analysis of fines generation in blasting: Unpubl. PhD thesis, JKMRC University of Queensland, Brisbane, 440 p.

Michaux, S., 2013. Experimental protocol for the GeM Crushing Index.. AMIRA P843A Final Compendium of Results, Manual for comminution tests and tools, 16 pp. Brisbane, Australia

Michaux, S. and Kojovic, T., 2008. Comminution test work and modelling. AMIRA P843 Technical Report 1, 14.1-14.28, Australia.

Michaux, S. and Walters, P., 2011. Blasting in Geometallurgy. AMIRA P843a. 48 pp., Australia

Napier-Munn, T., Morrell, S., Morrison, R. and Kojovic, T., 1996. Mineral Comminution Circuits: Their Operation and Optimisation. JKMRC University of Queensland, Brisbane, Australia.

Netz, R. and Noel, W. 2007. The Archimedes codex. Cambridge University Press. London.

Schon, J.H., 2004. Physical properties of rocks: Fundametals and principles of petrophysics. Elsevier Amsterdam 583 pp.

Shillabeer, J. and Gypton, C., 2003. Highlighting Project Risk Following Completion of the Feasibility Study, in Mining Risk Management Conference. Sydney.

Sillitoe, R., 2007. Preliminary geological model for the colosa porphyry gold system, Bogota. Colombia (Confidential Report to AGA).

Sinclair, A. and Blackwell, G., 2002. Applied mineral inventory estimation. University of Cambridge. United Kingdom. 381 pp.

Valencia, V., 2012. Reporte de los resultados analíticos U-Pb del studio realizado en el Proyectó La Colosa, Colombia. Tucson, Arizona, USA (Confidential report to AGA).

Verwaal, W. and Mulder, A., 1993. Estimating rock strength with the equotip hardness tester: International Journal of Rock Mechanics and Mining Science and Geomechanics Abstracts, v. 30, no. 6.

Walters, S., 2008. Geometallurgical matrix building, sampling, measurement and testing strategies – Cadia East site deployment. AMIRA P843 Technical Report 1, 3.1-3.21, Australia.

Walters, S. and Keeney, L., 2008. Geometallurgical Modelling. AMIRA P843 Technical Report 1, 16.1-16.24, Australia.

Walters, P., 2012. Personal communication. JKMRC, University of Queensland, Brisbane, Australia